DIPLOMARBEIT

Assessment of isotopic signatures of ‚nuclear' and concomitant elements in environmental and human samples by ICP-MS

von
Karin König

Betreuer: Ao. Prof. Dr. Thomas Prohaska
Dr. Sergei Boulyga

Acknowledgements

Table of Content

Abstract

Nuclear contamination of humans and the environment is nowadays, over 20 years after the disastrous nuclear power plant (NPP) accident of Chernobyl and over 60 years after the first use of nuclear weapons in warefare, still an issue of great concern. In this thesis the attention was directed to keep track of nuclear activities by origin determination via isotopic signatures of three real-world problems.

First, urine and hair of an Austrian UN-soldier employed in Kosovo after NATO airstrike on Serbia and Montenegro in 1999 was analysed as a consequence of a possible uranium contamination. Urine samples were analysed with inductively coupled plasma quadrupole mass spectrometry (ICP-Q-MS) after UV digestion. The values were not high enough to detect a contamination. However, a high background level was observed in the blanks deriving from ubiquitous occuring natural U sources. Hair is more useful than urine for the assessment of contaminations with heavy metals dated back in time. Thus, hair material was directly analysed with laser ablation (LA)-ICP-Q-MS. Again, no contamination was discovered.

The second example was an investigation of thyroids obtained after operations on Belarusian residents of two different regions. Lead and uranium were determined in order to find out whether a contamination from the Chernobyl NPP accident can be observed or not. Concentrations and isotopic ratios were measured with a sector field (SF)-ICP-MS and a multiple collector (MC)-ICP-MS, respectively. The two regions could be distinguished by analyzing the concentration ranges. The thyroids revealed more Pb than U. The ratios $^{208}Pb/^{206}Pb$ and $^{207}Pb/^{206}Pb$ of the soil samples collected in the vicinity of Chernobyl were compared to values for different regions of former USSR from literature. They agreed well with an average of major lead production sites. The thyroids from the south of Belarus revealed values close to that obtained in the soil samples.

Third, investigations were performed aimed at development of a method for the measurement of micro-particles by the use of LA-MC-ICP-MS for nuclear safeguards purposes. Uranium oxide particles of certified isotopic composition on graphite and silicon backing were analysed. In addition, identical particles were introduced on a cellulose acetate (CA) filter. The ratios $^{235}U/^{238}U$, $^{236}U/^{235}U$ and $^{234}U/^{238}U$ could be measured even though the method was limited in all cases by the fixation of the particles on the particular underlay. The figures of merit and present limitations of the applied analytical technique are discussed in this work.

Zusammenfassung

Die nukleare Belastung von Menschen und Umwelt ist heutzutage, über 20 Jahre nach dem tragischen Unfall im Atomkraftwerk von Tschernobyl und über 60 Jahre nach dem ersten militärischen Einsatz von Kernwaffen, immer noch ein Thema von äußerster Wichtigkeit. In dieser Arbeit lag das Augenmerk auf der Verfolgung von nuklearen Aktivitäten in drei aktuellen Fragestellungen durch Herkunftsbestimmungen mittels Isotopensignaturen.

Zunächst wurden Urin und Haare eines österreichischen UNO-Soldaten, der nach dem Luftangriff der NATO auf Serbien und Montenegro 1999 im Kosovo war, nach einer möglichen Uranvergiftung untersucht. Urinproben wurden nach UV Aufschluß mit einem induktiv gekoppelten Plasma Quadrupol Massenspektrometer (ICP-Q-MS) analysiert. Die Werte waren nicht hoch genug, um eine Kontamination festzustellen. Jedoch wurde ein hoher Hintergrund in den Blanks gemessen, der von ubiquitären natürlichen Uranquellen stammt. Da Haare geeigneter für die Beurteilung von länger zurückliegenden Vergiftungen mit Schwermetallen sind, wurden diese mittels Laser Abtragungs (LA)-ICP-Q-MS untersucht. Auch in diesem Fall konnte keine Kontamination beobachtet werden.

Als zweites Anwendungsbeispiel wurde in Schilddrüsen aus Operationen an Weißrussen zweier unterschiedlicher Regionen Blei und Uran bestimmt, um herauszufinden, ob eine Belastung durch den Reaktorunfall von Tschernobyl festgestellt werden kann. Die Konzentrationen und Isotopenverhältnisse wurden mit einem Sektorfeld (SF)-ICP-MS bzw. einem Multikollektor (MC)-ICP-MS gemessen. Durch die Elementkonzentrationen konnten die Regionen unterschieden werden. Die Schilddrüsen enthielten mehr Blei als Uran. Die Verhältnisse $^{208}Pb/^{206}Pb$ und $^{207}Pb/^{206}Pb$ der in der Nähe von Tschernobyl erhaltenen Bodenproben wurden mit Literaturwerten verschiedener Regionen der ehemaligen UdSSR verglichen. Sie stimmten mit dem Mittelwert der Hauptproduktionsstätten von Blei gut überein. Die Schilddrüsen aus dem Süden von Weißrußland zeigten Werte nahe der Bodenproben.

Zuletzt zielte diese Arbeit auf der Entwicklung einer Methode für die Messung von Mikropartikeln mittels LA-MC-ICP-MS für die Überwachung der nuklearen Sicherheit. Es wurden dafür Uranoxidpartikel mit zertifizierter Isotopenzusammensetzung auf Graphit- bzw. Siliziumunterlagen untersucht. Außerdem wurden identische Partikel auf einen Zelluloseacetat(CA)-filter aufgebracht. Die Verhältnisse $^{235}U/^{238}U$, $^{236}U/^{235}U$ und $^{234}U/^{238}U$ konnten gemessen werden. Die Methode wurde jedoch durch die Befestigung der Teilchen auf der

jeweiligen Unterlage begrenzt. Bewertung und gegenwärtige Grenzen der angewendeten analytischen Technik werden in dieser Arbeit erörtert.

1　Introduction

1.1　General background

Nowadays increasing interest is directed to the determination of origin and pathways of different kinds of materials. Therefore analytical disciplines are developed in order to get e.g. information about food authenticity (a useful tool for prevention of fraudulent practice in food industry), to enable migration studies and to characterize cultural goods as well as to contribute to process control in industrial processes. Examples of very recently performed provenance studies comprise inter alia food authenticity [Benincasa et al. 2007, Crittenden et al. 2007, Swoboda et al. 2008], for which methods are reviewed by Peres et al. 2007, the reconstruction of migration patterns of fossil mammals [Hoppe and Koch 2007] and humans at the Nil Valley in the New Kingdom period [Buzon et al. 2007], both by means of strontium isotope measurements. Successful applications of Sr isotopes for the characterization of prehistoric human migrations were reported since the 1990s [Ezzo et al 1997, Sealy et al. 1991] and are reviewed by Bentley 2006.

Forensic sciences make use of the 'Locard principle', meaning there is no contact between two objects without exchange of material, which was framed by Edmont Locard, a French scientist and pioneer of forensics. Forensic science deals e.g. with the determination of origin of material court exhibits and unknown dead bodies with the aim to detect relations between events, locations and individuals involved in crimes. An approach to investigate the case of an unknown corpse found in Central-Eifel, Germany, by the means of forensic methods was documented by Rummel et al. 2007.

On the other hand public interest is also directed increasingly towards contamination monitoring, for instance with 'nuclear' elements. Particularly with regard to accidents of nuclear power plants, e.g. such as the accident at Chernobyl NPP in 1986, the use of depleted uranium (DU) ammunition and releases of radioactive materials into the environment during the nuclear fuel cycle, which consists of a number of process steps from fuel preparation, over its use during reactor operation to reprocessing and/or disposal of spent nuclear fuel.

The connection of forensic science and nuclear contamination monitoring leads to a new discipline since the beginning of the 1990s, 'nuclear forensics', which deals with crimes concerning nuclear materials using similar methods which are employed for the supervision of the Treaty on the Non-Proliferation of Nuclear Weapons (NPT). These methods serve as important means to detect undeclared nuclear activities as it is done by the International Atomic Energy Agency (IAEA) strengthening the nuclear safeguards and help solving cases of 'nuclear smuggling' (illicit trafficking of nuclear or other radioactive material), which became an increased matter of concern after the breakdown of the Soviet Union [Mayer et al. 2007].

Several cases have been reported in central European countries ever since, of which two are presented by Wallenius et al. 2006 from the Institute for Transuranium Elements (ITU) in Karlsruhe, Germany, one of the Joint Research Centres (JRC) of the European Commission dealing with nuclear research.

The investigation approaches used for the tasks listed above base on the analysis of certain measurable parameters, which are typical for the material of interest. These parameters (usually called 'signatures') are determined by fabrication processes (e.g. of food, cultural goods or nuclear materials) and by geographical origin of the material (its natural and technical environment).

Parameters include chemical composition (major and minor elemental composition) and impurities, age of the material, morphology and isotopic signatures of relevant isotopes.

The challenge is to find adequate (new) parameters, which are specific for a given problem and/or to discover a specific pattern of parameter (also by means of comparing with already available data), respectively. Such a pattern can be composed e.g. of several defined isotopic ratios from one or more elements of relevance for the given problem (the so called isotopic fingerprint). Isotopic analysis is propably one of the most powerful tools for designations of origin. But for these purposes the availability of reference materials is of particular importance.

In this work three real-world problems, which deal with contamination of nuclear elements in environmental and human samples, have been analysed by means of isotopic signatures. The analysed samples consisted only of small amounts of human tissues (thyroids, hair, urine) or inorganic particles (soil, uranium particles).

These problems are associated with the use of nuclear materials, especially in respect to the employment of nuclear weapons, which pose a threat to people both involved and uninvolved in military conflicts. It is also important to evaluate the consequences of accidents with nuclear facilities in order to prevent impairment of human health or the environment for possible future incidents. Therefore nuclear activities have to be tracked.

One method of choice for these purposes is isotopic analysis (partially on microscopic level) performed with inductively coupled plasma mass spectrometry. Inorganic mass spectrometry reveals a universal and very sensitive method for both determination of concentration and isotopic ratio measurements and it has been established in the last few years for the determination of radionuclides in environmental samples [Becker 2003, Becker 2005, Lariviere 2006].

1.2 Isotopes of interest for nuclear forensics and environmental contamination studies

Nuclear forensics focuse mainly on uranium and plutonium isotope measurements. However, impurities of the investigated material (e.g. calcium, iron, potassium) give additional information.

Signatures of uranium and plutonium provide information whether or not the material has an artificial source (e.g. nuclear fuel or particles from enrichment facilities) and allow making conclusions about the intended use. They enable to distinguish between weapon and reactor grade materials. The signatures of nuclear fuel can also recover the reactor type using this fuel normally. Further conclusions of the geographical origin can be drawn [Mayer et al. 2007].

Concerning Chernobyl NPP accident, which was the topic of many studies according to environmental contamination and its biological and ecological effects from 1986 to now [USSR State Committee on the Utilization of Atomic Energy 1986, Salbu et al. 1994, Kashparov et al. 1994, Likhtariov et al. 1995, Garger et al. 1997 (1998), Carbol et al. 2003, Møller and Mousseau 2006], basically three forms of (radioactive) release are of major importance: the fallout contained (I) radioactive (also called 'hot') particles, (II) caesium and (III) short lived radionuclides such as radioactive iodine (^{131}I).

The first can be divided in two subgroups, both found mainly whithin the close-in-zone (the 30 km exclusion zone): rather large 'ruthenium particles' (with a diameter of tens of µm) reveal a matrix of iron group elements including radioactive nuclides (mainly ^{103}Ru and ^{106}Ru) and smaller particles (with a diameter of several µm) consisting of uranium oxide

matrix of different impurity and a radionuclide composition close to irradiated fuel. Therefore the latter ones are also called hot fuel particles (HFP). Long-lived and non-volatile radionuclides like Pu and Sr-isotopes (^{239}Pu and ^{90}Sr) can be found mainly in HFPs.

By contrast caesium fallout (mainly ^{137}Cs) spanned relatively large districts and high levels of contamination were also found in remote areas.

Radioactive iodine with a total release of about 8.9 MCi ($3.3*10^8$ GBq) vanished within weeks from contaminated areas due to its short halflife.

Additional significant property of environmental contamination around Chernobyl NPP was caused by the occurrence of Pb and B in the fallout during the last stage of the accident. 5000 t of various materials, thereof 2400 t of lead and 40 t of boron carbide, were deposited on the reactor with the aid of helicopters from the 30th of April to the 10th of May, 1986 in order to stop radioactive release from the damaged unit 4 of Chernobyl NPP.

While in the first stage of the accident (on the 26th of April) dispersed fuel was released from the reactor caused by explosive processes, in the second stage (from the 26th of April to the 2nd of May) the release rate dropped. At the third stage the fallout rate increased again and mainly volatile components (especially ^{131}I) were released at the beginning of this stage. Temperatures rised due to heated fuel in the core caused by reactor after-heat. At the end of this stage (the 5th of May) they exceeded 2000 °C for about 3 days [Begichev et al. 1989] and therefore lead (with a melting point below 2000 °C) and other components of the deposited materials evaporized and contaminated the environment by means of transportation with the wind. As Pb is a very toxic element, high concentrations in the environment add another danger for people living in contaminated areas in addition to the exposure to radioactive substances of the fallout.

Isotopic signatures of Pb on the other hand provide a potent marker for the determination of its source and therefore help keeping track of nuclear contamination from Chernobyl accident although itself is not considered a 'nuclear' element.

Measurements performed in this work are limited to uranium (in 'hot' particles, soil and human samples) and lead (in soil and human samples).

1.2.1 Uranium

Uranium is naturally occurring in soil, rocks, water and air with a typical content of about 3 mg kg^{-1} in the earthcrust, up to 3 µg L^{-1} in seawater and up to 10^{-7} mg/m^3 in air (for details see table 1).

It is found in nature only chemically bound since uranium is a very reactive element. These compounds are quite mobile in the environment. Some of the compounds dissolve easily in water, and therefore are also present in plants and are transported via the food chain into animals and humans [U.S. department of health and human services 1999, Bleise et al. 2003].

Table 1. Typical concentrations of uranium in the environment [National Council on Radiation Protection and Measurements (NCRP) 1999, United Nations Scientific Committee on the effects of Atomic Radiation (UNSCEAR) 1993, World Health Organization (WHO) 2001]

Ocurrence	Concentration range
Soil	0.3 – 11.7 mg kg^{-1}
Air	$2.5*10^{-8}$ – 10^{-7} mg/m^3
Water	$3*10^{-3}$ – 2.1 µg L^{-1}

Natural sources of uranium (including uraninite also known as pitchblende, the most common ore to extract uranium) contain four isotopes: ^{234}U, ^{235}U, ^{236}U and ^{238}U, of which ^{238}U with 99.27% is the most abundant isotope. The abundances of naturally occurring U isotopes are given in table 2. ^{236}U is only rarely found in natural sources. The ratio ^{236}U/^{238}U in natural uranium ores was determined by acceleration mass spectrometry (AMS) to be about 10^{-10} [Zhao et al. 1994] or even smaller. The major part of ^{236}U is of anthropogenic origin and generated artificially in reactors out of ^{235}U by neutron capture. Therefore it is found in environmental samples due to release of uranium following nuclear activities (for instance after accidents of power plants). Thus ^{236}U has a great potential for the use for nuclear safeguards, since the ratio ^{236}U to certain Pu isotopes gives information about the type of source (e.g. hot cell facility) [Donohue 1998].

Table 2. Abundances and halflifes of natural occuring uranium isotopes [abundances from Rosman and Taylor 1998, halflifes from Bleise et al. 2003]

Isotope	Abundance (mass%)	Halflife (a)
^{238}U	99.2745 (106)	$4.47*10^9$
^{235}U	0.7200 (51)	$7.04*10^8$
^{234}U	0.0055 (2)	$2.46*10^5$

Natural and artificial uranium isotopes are radioactive and undergo decay series with many more or less stable intermediates until a stable isotope is formed. During these decay chains radiation is emitted (mainly as α-particles). To distinguish between ^{238}U and ^{235}U decay series

they are called in respect to their long lived members of practical importance radium and actinium decay series, respectively. In both cases the stable end product is lead (^{206}Pb for radium and ^{207}Pb for actinium decay).

^{235}U undergoes a nuclear fission reaction in nuclear reactors. During the reaction a neutron collides with the ^{235}U atom and leads to nuclear fission that releases energy finally used to produce electricity (in nuclear power plants) or explosion (in nuclear weapons). Additional neutrons deriving from the fission are then able to split other ^{235}U atoms releasing further heat and neutrons leading to a controlled or uncontrolled chain reaction.

At first uranium ore has to be chemically enriched by separation and extraction in order to produce nuclear fuel with about 0.1 – 1% pure uranium content. Afterwards it usually undergoes an isotopic enrichment due to its ^{235}U content from the natural level of 0.72% to over 2% referred to as low enriched uranium (LEU). Weapon grade material (for nuclear weapons) in contrast consists of highly enriched uranium (HEU) with about 90% ^{235}U [Donohue 1998, Lieser 1997].

Higher concentrations of U in comparison to the natural level are found after accidents with nuclear power plants (Chernobyl) and the use of DU ammunition for example.

Measuring isotopic ratios of uranium in particle as well as in bulk samples (with plutonium analysis) is used in nuclear forensics [Donohue 1998, Wallenius et al. 2006] and contamination studies of the environment (for instance related to the fallout of Chernobyl NPP) [Carbol et al. 2003] or public health (contamination with DU) [Bleise et al. 2003] as well as in geochronical sciences (e.g. U/Th dating) [Alcaraz-Pelegrina and Martinez-Aguirre 2007].

1.2.2 *Plutonium*

Most plutonium is generated in nuclear power plants out of ^{238}U by capturing one neutron (1) deriving from the fission of ^{235}U. Thereby ^{239}U is generated and γ-radiation is emitted, ^{239}U decays finally by double β-emission via ^{239}Np to ^{239}Pu.

$$^{238}\text{U} + {}^{1}\text{n} \rightarrow {}^{239}\text{U} \rightarrow {}^{239}\text{Np} \rightarrow {}^{239}\text{Pu} \tag{1}$$
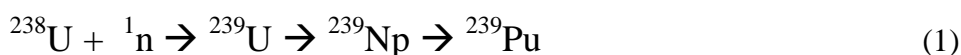
^{238}Pu on the other hand is generated via decay of ^{238}Np, which, in turn, derives from three neutron capture reactions: ^{235}U leads to ^{236}U, ^{236}U to ^{237}U and, after decay to ^{237}Np, finally to ^{238}Np.

Other Pu isotopes such as ^{240}Pu and ^{241}Pu are created by further neutron absorption of ^{239}Pu [Binder 1999].

When ^{239}Pu is released, it is artificially introduced into the actinium decay series (^{239}Pu → ^{235}U) emitting α-particles. The isotopes ^{238}Pu, ^{239}Pu, ^{240}Pu, ^{241}Pu and ^{242}Pu are mainly found in irradiated nuclear fuel. Pu also occurs naturally in very small amounts. Natural Pu is found as ^{239}Pu in uranium ores like Canadian and Congolese pitchblende for example. An increased amount was also discovered in Gabun, West Africa, where natural induced nuclear fission reactions took place two million years ago [Binder 1999]. In addition it was found in 1971 that ^{244}Pu was a primeordial element during mass spectrometric analysis of a sample of bastnaesite (a Precambrian mineral) from California [Hoffman et al. 1971].

Artificial contaminations with Pu were observed after several nuclear weapon tests and the Chernobyl NPP accident, so that nowadays it is widespread over the northern hemisphere. The global distribution of Pu isotopes was described by Kelley et al. in 1999 by means of measuring soil samples from different locations around the world. Pu from natural as well as artificial sources deposits in the human body in small amounts, mainly in the liver and the skeleton, where it is retained persistently [Taylor 1995].

The ratio of ^{240}Pu/^{239}Pu is of major importance for determining the source of Pu containing material. Weapon-grade material consists of over 90% ^{239}Pu and about 0.5% ^{240}Pu resulting in a very low ratio between 0.02 and 0.06. Global atmospheric fallout on the other hand reveals an isotopic signature of approximately 0.18 ^{240}Pu/^{239}Pu [Perelygin and Chuburkov 1997, Agarande et al. 2003, Zheng and Yamada 2006].

1.2.3 Lead

Natural lead is usually found in ores - most common in galena (lead sulphide, PbS), but also inter alia in anglesite (lead sulphate, $PbSO_4$), minim (lead oxide, Pb_3O_4), cerussite (lead carbonate, $PbCO_3$) - with zinc, silver and copper, metallic Pb is rather rare.

Lead has four stable isotopes with abundances of approximately 1.4% (^{204}Pb), 24.1% (^{206}Pb), 22.1% (^{207}Pb) and 52.4% (^{208}Pb), respectively [Rosman and Taylor 1998]. The last three ones are the heaviest stable isotopes and their abundances vary in nature because they are final products of the decay chains of radium (^{238}U → ^{206}Pb), actinium (^{239}Pu/^{235}U → ^{207}Pb) and thorium series (^{232}Th → ^{208}Pb). They are used in geochronological sciences [Gerdes and Zeh 2006, Juul-Pedersen et al. 2007, Jung and Hellbrand 2007]. Intermediate nuclides of decay chains such as ^{210}Pb are found in geological studies [Yamada and Aono 2006].

The major part of lead in the environment is distributed by human activities. Due to its favourable attributes like malleability and the low melting point together with its availability and the simplicity of its extraction, it was already used in ancient times: Ancient Egyptians, Greeks and Romans produced vessels, built water pipes and fabricated building materials with the help of metallic lead. Also lead compounds had a wide range of applications [Neuburger 1921].

During industrial revolution the extraction of lead increased significantly. In 1924 tetra-ethyl lead (as antiknock agent) was added to the fuel of four-stroke engines for the first time, which soon led to a maximum of anthropogenic lead contamination of the environment in 1976. Nowadays tetra-ethyl lead has been forbidden as gasoline additive in most countries since the 1970s, a measure immediately causing an observable decrease [Horn et al. 1987].

The isotopic signatures of natural lead sources depend on the one hand on the age of the rock and on the other hand on the original concentrations of mother nuclides of the according decay series (^{235}U, ^{238}U or ^{232}Th). For this reason, and since lead isotopes have a small relative mass difference leading to only little fractionation, the signature is site-specific. However, origin determination by means of isotopic signatures of indigenous lead sources is not an easy task, since natural lead represents only about 1% of the total amount in the troposphere.

Nowadays industrial/anthropogenic Pb is ubiquitous, contamination of the environment is still related to the greatest part to fuel and can currently be used as suitable marker of geographical origin rather than natural lead. Its isotopic composition refers to the location, where the raw material was mined. Pb signatures are still widely used in environmental studies for the determination of atmospheric contamination [Miralles et al. 2006, Preciado et al. 2007, Brännval et al. 2000]. However, the global trade with lead and its compounds and even more the worldwide contamination of atmo-, pedo- and hydrosphere will increasingly restrict these possibilities in future [Rummel et al. 2007].

Higher concentrations of lead from man-made origin at certain locations are also caused by the previously mentioned Chernobyl NPP accident, where lead and other materials were used to eliminate further release of radioactive substances from the damaged reactor.

Metallic lead is a toxic substance, but since it has a low bioavailability, there is only little risk of intoxication. Lead poisoning is rather caused by soluble organic (like tetra-ethyl lead) and inorganic compounds, which can be considered as very hazardous. The toxicity of lead ions in the human body are based on their ability to displace other metals such as calcium, iron and zinc, which have - in contrast to lead - important biological functions (for instance enzymes can be inhibited in that manner). In principal every organ can be effected of lead poisoning, while most sensitive targets are the developing nervous system, hematological and cardiovascular systems and kidneys [U.S. department of health and human services 2007].

1.2.4 Boron

Both natural occuring isotopes of boron, ^{10}B and ^{11}B with abundances of 19.9 and 80.1%, respectively, are stable [Rosman and Taylor 1998].

Natural solute sources of boron have a large range of variations in their isotopic ratio ^{11}B/^{10}B as a result of isotope fractionation due to their large relative mass difference. In contrast to that natural sodium borate minerals, the raw material for the production of bleaching agents (used in detergents and cleaning products), which is the main application of boron compounds in industry, exhibit a narrow range in its isotopic composition.

After the use of detergents soluble boron compounds are transferred into the waste water and remain as contaminants in the aquatic environment. Hence this fact can be used to reveal anthropogenic contamination of the environment via isotopic analysis [Barth 1998].

Boron was used besides lithium isotopes by Hogan and Blum 2003 as groundwater tracers.

Other uses of boron compounds include inter alia fertilisers, insecticides, corrosion inhibitors for cooling systems and the deployment in nuclear industry, where boric acid solutions or boron-containing control rods are used to control nuclear reactions by absorption of neutrons. They are absorbed by the isotope ^{10}B, which is also employed in the form of boron carbide. The end products of the neutron capture reaction are lithium and α-particles [Taylor and Goldhaber 1935]. Therefore sources of boron involved in nuclear processes can reveal isotopic signatures reduced in ^{10}B (except for a ^{10}B enriched boron, being an even more efficient neutron absorber, was used) and elevated ^{7}Li concentrations. Neutron absorbtion with ^{10}B is also used in medicine for cancer treatment [Salt et al. 2004].

A large amount of boron (in form of boron carbide) was used after Chernobyl NPP disaster and since boron has generally non-reactive properties, there is a potential of using its isotopic signature for determining environmental contaminations due to that incidence.

1.3 Environmental contamination with nuclear and related materials

Environmental contamination with nuclear elements very often deals with radioactive particles. Such particles are generated mainly during the burning of uranium-containing materials.

Violent explosions during Chernobyl accident are assumed to have initiated several mechanisms associating radionuclides with particles: the condensation of volatiles on particle surface after the release, interaction with aerosol particulates during atmospheric transport and the release of fuel matrix or clusters. In such fuel particles volatiles are reduced relative to refractory elements depending on the prevalent temperature and activity ratios reflect reactor fuel burn-up [Salbu et al. 1994]. Wind-driven resuspension of particles took place mainly in the 30-km-exclusion zone.

Although description of models of hot particle formation exist [Kashparov 1994], the principal process causing the dispersion of nuclear fuel during Chernobyl accident still remains obscure.

DU on the other hand is dispersed in the evironment as a consequence of aerosol generation after the impact of DU containing projectiles and a subsequent resuspension in soil and water.

'Hot' particles are also formed wherever radionuclides are handled like for e.g. in enrichment facilities for the production of nuclear fuel or nuclear weapons.

Assessment of 'hot' particles is important for both environmental monitoring, in order to scale contamination and thus determine the radiobiological significance, and nuclear forensics, for the characterization of means of evidence.

1.3.1 Contamination with depleted uranium

Depleted uranium is a by-product of enrichment processes of natural uranium and reprocessing of spent nuclear fuel. DU consists mainly of ^{238}U and has only about one third of the natural ^{235}U abundance (0.2 - 0.3% vs. 0.7% in natural uranium). Areas of application are found for civilian, but mainly for military purposes. Civilian usage includes the coloring of glassware and dental ceramics (until the middle of the 20th century), employment as chemical catalyst, for counterbalance weights and ballast and radiation shielding in hospitals, since DU,

although itself is weakly radioactive, provides a suitable protection against gamma radiation [Betti 2003].

The use of DU ammunition in local conflicts leads to a contamination with DU in certain areas, which is a good example for the introduction of very specific non-natural isotopic signatures by human activities.

In several conflicts the use of DU ammunition was recognized, like in Gulf War (Iraq and Kuwait, 1990), which was the first reported wide-scale use of DU in warfare (321 t of DU used), in Bosnia-Herzegovina 1995 (approximately 3 t of DU) or NATO air strike on Serbia and Montenegro in 1999 (112 locations mainly in Kosovo), where about 10 t of DU were employed [Bleise et al. 2003] and more recently the conflicts of Afghanistan and Iraq [Bleise et al. 2003, McLaughlin et al. 2005, Milačić et al. 2004].

Further examples of local contaminations with actinides of specific non-natural isotopic composition are the collision of an US Air Force bomber mounted with thermonuclear bombs with a fuel tanker aircraft (Pu and U containing particles were released) in Spain (Palomares) in 1966, a similar accident in Greenland (Thule) in 1968 [Lind et al. 2007, Pöllänen et al. 2006] and the crash of a civil airplane ballasted with DU as counterweight in the Netherlands (Amsterdam, 1992) [Uijt de Haag et al. 2000, Arbuthnot et al. 1999].

DU is a toxic and hazardous substance, on the one hand, because uranium causes chemical effects in the body as a heavy metal, and on the other hand due to its remaining radioactivity as an α-emitter. The radiotoxicity of natural uranium exceeds the one from DU by 60%, since ^{235}U (which is reduced in DU) has a shorter halflife than ^{238}U . Unsaid, a shorter halflife goes along with a higher specific activity. The health risk due to external exposure to natural uranium is low, since it produces only small numbers of α-particles, which are not able to pass through solid materials like human skin unlike β and γ-radiation released by nuclides deriving from uranium decay. On the other side, α-emitters once ingested are significantly more dangerous than bettas or gammas irradiating inner tissues and organs.

As enriched uranium contains not only more ^{235}U, but is also increased in ^{234}U (the uranium isotope with the shortest half-life), it is more radioactive than natural uranium. If high amounts get into the body by drinking water or food different types of diseases can be observed as consequence (bone and liver cancer and blood diseases such as leukemia for example) [U.S. department of health and human services, 1999].

Although DU is less radioactive than natural or enriched U, it presents a greater danger to people considering its high concentration. A DU penetrator for example weighs 280 g, of which 99.25% are made of pure metallic DU [Bleise et al. 2003]. During combat activities fragments of such a penetrator remain in wounds or aerosols are generated after the impact of DU rounds on hard surfaces. Normally 10 - 30% of the DU is then converted to an aerosol. These aerosols immediatly burn forming DU dust particles with a diameter of less than 10 µm of low-soluble uranium oxide, which can be inhaled easily and contaminate the environment sustainably [Roth et al. 2001].

External exposure to DU affecting the skin by beta and gamma components (resulting in very low doses) mainly occurs during combat activities. Soldiers in vehicles shielded with DU armor have the highest risk, since they are exposed for longer time periods.

The main pathways of DU penetrating the human body are ingestion (mainly by drinking water), inhalation (aerosols are also generated by fires) and via embedded fragments or contaminated wounds (during combat activities). DU is incorporated either as uranium metal (from fragments) or uranium oxides (major oxides are U_3O_8, UO_2 and UO_3).

According to their solubility U compounds are divided into fast, medium and slow soluble substances. The speed of solubility decides whether compounds can be absorbed in the human blood stream, carried and retained in body tissues and organs before being excreted. The soluble fraction is considered to be responsible for the chemical toxicity of uranium. 2 - 5% of ingested (soluble) uranium is absorbed into the blood from the intestines and the rest is eliminated within a short time. The insoluble fraction (uranium oxides), which is rather associated with radiation effects, is less absorbed - only about 0.2% and thereof just 10% deposits in tissues and organs (kidney, bones) [Bleise et al. 2003].

Several studies about environmental and human contamination with uranium by ingestion [Orloff et al. 2004], inhalation [Parrish et al. 2008] and embedded fragments [McDiarmid et al. 2000] from different regions have been published by now.

In this work urine and hair of an UN-soldier, who was deployed in Kosovo, was analysed due to a DU contamination. The quantification of uranium in urine is the standard test for the determination of possible uranium contaminations deriving from exposure to increased amounts [U.S. department of health and human services 1999] for it is assumed that U excretion in urine is proportional to the U level in the human body [Roth et al. 2001]. Hence

urine analysis is widely used in literature for this purpose [Oeh et al. 2007, Orloff et al. 2004, Roth et al. 2001].

1.3.2 *Particle analysis for nuclear safeguards*

The forensic study of a corpse found in Central Eifel [Rummel et al. 2007] emphasized the importance of particle analysis: In the lung tissue of the dead person micro-particles (with a size of <5 µm) were found, which proved to consist of DU. It is very likely that they derive from aerosols generated after the impact of penetrators on hard surfaces. The DU together with desert-specific minerals also present suggests a prior stay in Iraq, for which no evidence was produced during routine investigation of tissues.

Nowadays the threat of nuclear terrorism and violations of the Non-Proliferation Treaty is a matter of public concern. Therefore powerful tools must be prepared to the aid of antagonizing organizations. The ITWG (International Technical Working Group on Nuclear Smuggling) provides international collaboration on nuclear forensics by exchange of experience, discussing of analytical methods, initializing round robins in order to challenge participating laboratories and so on [Mayer et al. 2007].

The IAEA concerns about the observance of the NPT. This is fulfilled by inspections of nuclear fuel reprocessing and enrichment facilities of the signatory States, where both nuclear and environmental sampling is performed. The analysis of the carefully taken swipe (from inside and around nuclear facilities) and other samples (soil, vegetation, water, sediment and biota from distances up to 20 km) is performed in IAEA laboratories and the Network of Analytical Laboratories (NWAL) in several Member states [Donohue 1998].

Two general types of analysis are employed: the measurement of dissoluted samples (referred to as bulk analysis) and the chemical or isotopic analysis on microscopic level, which is represented in particle analysis.

Bulk analysis of environmental samples is often not sufficient, since it reveals only an average of the given isotopic composition, which can be composed of different sources, while more specific isotopic information is obtained from particles (without interference of non-relevant bulk).

In this study 'hot' particles of different degrees of enrichment provided by the IAEA were analysed for their isotopic composition of uranium. These particles consist mainly of UO_2 and have a diameter of about 1 µm with an absolute amount of U not much higher than 10 pg.

The formation of uranium oxide particles is typical for enrichment facilities. They show a specific signature of their isotopic composition [Donohue, 1998]. The degree of enrichment in certain uranium and plutonium isotopes reveals whether or not materials, which can be used for the production of nuclear weapons, have been handled in the vicinity of the inspected facility.

1.3.3 Human contamination with lead after Chernobyl nuclear power plant accident

Detailed information regarding the radioactive fallout content of Chernobyl NPP accident can be found in literature [Begichev et al. 1989, Kaspharov et al. 2003], in particular because of the health risks posed by radiation.

Only emergency workers engaged in the measures taken on the first day of the accident suffered from radiation sickness with deterministic effects, 95% of the workers exposed to doses higher than 6 Gy died immediately [UNSCEAR 2000].

The consideration of health effects on cleanup workers ('liquidators') and even more on the population of the most contaminated areas (located in Belarus, Russia and Ukraine) on the other hand is a rather intricate task - radiation doses have been lower, but persistent for an extended period. The occurrence of cancer is considered to be caused by external or internal dose of radiation, but as many types of carcinoma have a long minimum latency period and along with that can be caused by a variety of different factors, it's hard to prove if every particular case can be ascribed to the NPP disaster.

Mainly two types of cancer having a shorter latency and are known to be radiosensitive are to date associated with the accident: leukemia and thyroid cancer, while others are under suspicion [Hatch et al. 2005].

While reliable cohort studies for radio-induced leukemia after Chernobyl accident exist, an increased risk for thyroid cancer of liquidators is only suggested [Ivanov et al. 1997], maybe because the internal doses of ^{131}I and other short-lived radionuclides from the early emergency workers are more difficult to estimate.

The thyroid gland in children is more sensible to radiation and therefore an increased risk of thyroid cancer in contaminated areas was observed. 10 years after the accident for example a 30 times higher rate of pediatric thyroid cancers occurred in Belarus [Williams 2002].

A review about cancer related to Chernobyl disaster was published by Hatch et al. 2005.

In many studies elements specifically occurring in nuclear facilities are investigated in bioaccumulators (such as lichens, mosses and pine trees) due to their concentrations and isotopic signatures [Boulyga et al. 2003, Buchman et al. 2003].

The idea in this work was to determine Pb isotopic ratios in pathologic thyroid samples from residents of different regions of Belarus that showed elevated levels of lead and to find out whether these signatures relate to Chernobyl accident. Lead from Chernobyl was derived from the materials dumped onto the damaged reactor in order to absorb neutrons.

1.4 Methods applied for analysis of micrometer sized particles in environmental samples

The analysis of micrometer sized particles in environmental samples is a great challenge, since there's need of sophisticated methods working on a microscopic level. The challenge is to estimate isotopic ratios in small samples with low concentrations such as microparticles or small amounts of biological tissues.

A micro-particle with a diameter of 1 µm for e.g. is a very small object, which is hard to find within the sample. In other samples such as human body fluids or hair the desired analyte has very often a low overall concentration, for instance the total U concentration in the human body is only about 56 µg in unexposed individuals [Fisenne et al. 1988].

Another challenge is the fact that small sample amounts, either to avoid a health risk when radioactive material is handled or because only little material is available like single hair strands or biopsy samples, are difficult to manipulate, and, in addition to that, they may reveal a low overall chemical recovery due to matrix effects.

Also the heterogeneous spatial distribution of isotopes in 'hot' particles can not be determined by simple bulk analysis. It is demanded of the method to be able to analyse different isotopic ratios along the sample surface.

Usually a combination of several analytical methods is required to overcome these problems such as the application of SEM or FT technique for the location of particles and mass spectrometric techniques for the analysis of isotopic ratios.

1.4.1 Methods for isotopic analysis of radionuclides

Conventional radiochemical methods like α-spectrometry are based on the measurement of activities of radioisotopes. They require careful chemical separation of the analyte (via extraction or chromatography), which is delicate and time-consuming. If samples of high radioactivity are handled, it is preferable to use rather small sample amounts and a fast analytical method in order to minimize radioactive contamination of laboratory environment and irradiation dose on operators. On the other hand radiochemical methods fail to measure long-lived radionuclides at very low levels, because such nuclides have a low specific activity and therefore very long measurement time is required, which can take from days up to several weeks. Nowadays radiochemical methods, having been dominant techniques in long-lived radionuclide analysis for decades, are increasingly replaced by inorganic mass spectrometry [Becker 2005]. However, in the analysis of short-lived radionuclides they still achieve lower detection limits than for e.g. ICP-MS [Solatie 2002].

The advantages of mass spectrometry for isotopic analysis are excellent sensitivity, good precision and accuracy [Becker 2005]. Different ion sources and mass analyzers are employed for radionuclide measurements. The most commonly used ion sources for this field of application include thermal (for TIMS), secondary (SIMS) and inductively coupled plasma ionization (ICP-MS).

Analytical methods used for nuclear safeguards are described by Donohue 2002, general practice in nuclear forensics by Wallenius 2006.

1.4.1.1 Thermal ionization mass spectrometry

Ionization in TIMS analysis is accomplished by heating a filament on which the sample was deposited. Larger ion signals can be detected with multiple Faraday-cup detectors, while minor isotopes or small samples require an ion-counting system with increased sensitivity. TIMS is widely used for the determination of Pu and U isotopes in micrometer-sized particles, particularly for nuclear safeguards after location of the particles with the fission track (FT) technique. Routinely 10-20 particles are measured for each sample [Donohue 1998]. FT-TIMS is a selective method and provides highly precise isotopic ratios of major and minor isotopes, but it has no multielement capability, since the ionization potential of the desired analyte must be >7 eV and it requires time-consuming sample preparation steps [Becker 2005].

1.4.1.2   Secondary ion mass spectrometry

SIMS is applied in nuclear forensics to characterize and identify particles and reveal isotopic ratios of plutonium and uranium [Tamborini et al. 1998, Betti et al. 1999].

Particles are transferred to an organic solvent, which is then dried on a graphite planchet. The planchet is put into the SIMS sample holder and a primary ion beam (consisting of O_2^+ ions for U and Pu measurements) between 10 and 17 keV is directed towards the sample in a high vacuum chamber. Only charged secondary ions (neutral species are lost) emitted from the sample (in case of an O_2^+ beam positively charged ions will be maintained) are separated according to their mass-to-charge ratio in a mass analyzer (which can be a quadrupole, sector field or time of flight device).

SIMS can be operated in microscopic and microprobe mode. In microscopic mode a defocused primary ion beam (5-300 µm) is used for investigating a large surface with an imaging detection system producing spatially resolved images for each isotope. Microprobe mode with a focused primary ion beam (<10 µm) on the other hand is applied for small defined spots or for rastering a smaller area of the sample (detecting inclusions in bulk material). Ions are usually counted by an electron multiplier [Betti 2005].

A large numbers of particles can be located in microscope mode within a field of view. Ion images of the desired isotopes are formed (each isotope is recorded for a given time period), of which isotopic ratios are obtained (e.g. $^{235}U/^{238}U$). Information about minor isotopes (e.g. ^{234}U and ^{236}U) are received during microprobe mode [Donohue 1998].

Limitations of SIMS include the need for rather high uranium concentrations, the occurrence of isotopic fractionation during various stages of the analysis, spectral interferences and the high sensitivity to matrix effects.

1.4.1.3   Multiple collector inductively coupled plasma mass spectrometry

Although TIMS and SIMS are state-of-the-art concerning sensitivity and selectivity, new and accurate methods for the nuclear safeguards must be developed achieving high sensitivity together with high sample throughput.

ICP-MS is a universal, rapid and extremely sensitive analytical method for isotope analysis of long-lived radionuclides. The use of ICP-MS for the measurement of radionuclides in environmental samples was reviewed by Becker 2005 and Lariviere et al. 2006, the principle is described in more detail in chapter 2.2.

ICP-MS in general is advantageous due to its relative low costs compared to SIMS and usually easier sample preparation compared to TIMS resulting in a high sample throughput.

ICP-MS is able to measure ratios of minor to major isotopes (such as ^{234}U/^{238}U or ^{236}U/^{238}U), which is of interest for nuclear forensics and the determination of environmental contamination. Very low ratios of ^{236}U/^{238}U in environmental samples originating from a location 200 km to the North of Chernobyl NPP was successfully performed with ICP-SF-MS [Boulyga and Heumann 2006].

However, today routine applications of ICP-MS in nuclear forensics consist of bulk analysis including concentration (with IDMS) and isotopic ratio measurements of U and Pu as well as multi-element analysis for the determination of chemical impurities [Wallenius et al. 2006].

The use of ICP-MS in particle analysis was limited due to the fact that conventional sample preparation procedures were rather complicated and prone to cross contamination in contrast to the ones applied to bulk analysis. Particles from Palomares accident were located with other methods (SEM) for example and afterwards digested and dissolved in suitable media before measuring the solution with a sector field ICP-MS [Pöllänen et al. 2006]. Nonetheless analysis of the entire particle after dissolution doesn't reveal a possible heterogeneous spatial distribution of isotopes within the particle.

In this work a method was investigated using a laser ablation system for the location and sample introduction of particles immobilised on a cellulose acetate filter as well as on graphite and silicon wafer to overcome previously mentioned limitations.

LA-ICP-MS for direct isotopic analysis on solid samples was already used for the differentiation of DU and naturally occurring U using a quadrupole based instrument [Seltzer 2003] and for the analysis of U-oxide particles with a SF device with single ion detection [Becker et al. 2008]. LA coupled to ICP-SF-MS with multiple ion counters for the determination of uranium and fission products isotopic ratios in radioactive microsamples was performed by Boulyga and Prohaska 2008.

1.4.2 *Methods applied for particle localization*

As previously mentioned most methods need to combine two systems in order to cope with analytical difficulties when microsamples are analysed. Common methods for particle localization are SEM and FT. ICP-MS was coupled to a LA system for a new approach. The

great advantage of LA-ICP-MS is the possibility of a rapid and sensitive direct isotopic analysis of microparticles with simple sample preparation steps.

The principle of LA is described in chapter 2.2.2.2, while SEM and FT are briefly presented here.

1.4.2.1 Scanning electron microscopy with X-ray fluorescence spectroscopy

At first the dispersed sample is fixed on an aluminium specimen stub and afterwards lightly coated with carbon. The electrically conducting adhesive ensures that the particles stick on their place. Afterwards the stub is put into the electron microscope where it is exposed to X-ray radiation. All chemical elements except for the 3 lightest ones can be excited.

Two types of detectors are applied: while the EDX (energy dispersive X-ray spectroscopy) capability is routinely used to differentiate particles containing for instance Pu and U from the sample matrix, the more expensive WDX (wavelength dispersive X-ray spectroscopy) device has a higher resolution resulting in more precise and detailed measurements. The employment of WDX on the other hand is restricted, because only one element can be measured at a time with low efficiency of X-ray collection. If the screening (particle searching) with EDX shows interesting spots, they can be analysed with WDX in addition. Data thus obtained reveals elemental composition and microstructure of particles, which can provide information about the production process of nuclear materials, but SEM/XRF cannot estimate isotopic ratios. Hence it is usually employed in preparation to further analysis, especially for particle location [Ciurapinski et al. 2000, Donohue 2002, Wallenius 2006].

1.4.2.2 Fission track technique

In FT analysis particles are located by fission tracks produced after the impact of thermal neutrons. With this technique fissile nuclides like Pu and U can be detected at very low levels after they were irradiated in a nuclear reactor causing damage to a fission fragment detector like Lexan (polycarbonate plastic) [Lee et al. 2007].

The located particles are then electrodeposited onto a rhenium filament, overcoated with platinum and measured by TIMS.

Disadvantages are the need of a nuclear reactor with a neutron irradiation facility and the time-consuming sample preparation steps.

2 Instrumental

2.1 Reagents and Standards

Water was treated by reverse osmosis, laboratory reagent grade water system purification (F+L GmbH, Vienna, Austria) and single subboiling distillation in an ultrapure quartz apparatus (Milestone-MLS GmbH, Leutkirch, Germany). 37% hydrochloric acid p.a. grade (Merck KGaA, Darmstadt, Germany) was purifed by single, 65% nitric acid p.a. grade (Merck KGaA, Darmstadt, Germany) by double subboiling distillation (Milestone-MLS GmbH, Leutkirch, Germany). Other reagents were of analytical, ultrapure, suprapure or equivalent quality: 31% ultrapure H_2O_2 (Merck KGaA, Darmstadt, Germany), 48% ultrapure HF (Merck KGaA, Darmstadt, Germany), 70% suprapure $HClO_4$ (Merck KGaA, Darmstadt, Germany), methanol of p.a. grade (Thermo Fisher Scientific Inc., Waltham, USA), acetone of p.a. grade (Merck KGaA, Darmstadt, Germany), 28% double distilled NH_4OH (Sigma Aldrich, St. Louis, USA) and 99.5% suprapure $H_2C_2O_4.2H_2O$ (Merck KGaA, Darmstadt, Germany).

The following reagents were used in addition for experiments with a hydride generation sample introduction system: $NaBH_4$ ReagentPlus® (Sigma Aldrich, St. Louis, USA), NaOH purum pellets (Acros Organics, Geel, Belgium) and $K_3[Fe(CN)_6]$ ReagentPlus® (Sigma Aldrich, St. Louis, USA).

Dilution of sample solutions and standards was performed with 1% (w/w) HNO_3 unless otherwise mentioned. 1% (w/w) nitric acid was prepared with subboiled deionized water and double subboiled concentrated HNO_3.

0.05 M ammonium oxalate solution for U/matrix separation procedure was prepared by mixing NH_4OH and $H_2C_2O_4.2H_2O$ with subboiled deionized water.

Solutions for hydride generation experiments were prepared with subboiled water.

A solution of 11 ng g^{-1} indium standard was prepared gravimetrically from a 1000 mg L^{-1} stock solution (ICP standard, CertiPUR®, Merck KGaA, Darmstadt, Germany) and used as internal normalisation standard for the determination of U concentration in urine, a 10 ng g^{-1} iridium standard out of a 1000 mg L^{-1} stock solution (ICP standard, CertiPUR®, Merck KGaA, Darmstadt, Germany) was used for Pb quantification. A 110 ng g^{-1} solution of Thallium from a 1000 mg L^{-1} stock solution (ICP standard, CertiPUR®, Merck KGaA,

Darmstadt, Germany) was employed as internal standard for Pb isotope ratio measurements. U concentration measurements were calibrated with gravimetrically (using a semi-micro balance, BP 210D, Sartorius AG, Göttingen, Germany) prepared uranium standards (Sigma Aldrich, St. Louis, USA).

IAEA-375 (soil from a farm in Brjansk, Russia) is a certified reference material (International Atomic Energy Agency, Vienna, Austria) for the activities of ^{134}Cs, ^{137}Cs, ^{129}I, ^{40}K, ^{226}Ra, ^{106}Ru, ^{125}Sb, ^{90}Sr, ^{232}Th, ^{238}U, ^{241}Am, ^{238}Pu, $^{239+240}$Pu, ^{228}Th and ^{234}U, which were determined by a round robin in 1990.

IRMM 184 (Institute for Reference Materials and Measurements, Geel, Belgium) and CRM U-500 (New Brunswick Laboratory, Argonne, USA) were used as certified reference materials for the determination of isotopic ratios of U.

The certified reference material SRM 281 (NIST, Gaithersburg, USA) was applied for the determination of isotopic signatures of Pb.

Commodities (polyethylene flasks, tubes, pipette tips) for sample preparation and measurement procedures were treated for purification in a three step washing procedure in a clean room of class 100 000: first they were soaked in 10% (w/w), then in 1% (w/w) nitric acid and afterwards rinsed with deionized water.

2.2 Inductively coupled plasma mass spectrometry

In this section the technique of ICP-MS is described, method parameters of the particular measurements can be found in the respective chapters (3 and 4).

The analytical technique of ICP-MS is well described in literature [Montaser 1998, Hill 1999, Nelms 2005] and was used in this work for quantification of trace elements and to obtain isotope ratios. Quantitative analyses were performed with ICP-Q-MS devices (ELAN DRC II and ELAN DRC-e, both Perkin Elmer, Ontario, Canada) and with a high resolution (HR) ICP-SF-MS with a single collector (ELEMENT2, Thermo Electron GmbH, Bremen, Germany) by the use of already established methods. A MC-ICP-SF-MS (Nu Plasma HR, Nu instruments, Wrexham, UK) was employed for the determination of isotope ratios.

Table 3 summarizes important attributes of the used instruments (ICP-Q-MS, ICP-SF-MS, MC-ICP-SF-MS) and the possible fields of application as well as their benefits and limitations.

Table 3. Attributes, applications, benefits and limitations of 3 different ICP-MS instruments [values from Montaser 1998].

	ICP-Q-MS ELAN DRCII	ICP-SF-MS ELEMENT2	MC-ICP-SF-MS Nu Plasma HR
Example			
Resolution (R)	Low	Fixed values for low, medium and high (>10 000) R, adjustable via entrance and exit slits [Thermo Electron GmbH 2004]	Adjustable via 3 sets of slits (source, collector and alpha slits) high and pseudo high R possible [Nu Instruments 2005b]
Sensitivity [cps/µg g^{-1}]	~10^8	10^9 (low R) 10^8 (medium R) 10^7 (high R)	
Backgroundlevel [cps]	2 – 50	<0.1	
Isotope ratio precision (relative standard deviation)	<0.5%	0.05 – 0.5%	down to 0.003%
Advantages	Robust, high throughput, cost, rel. small instrument size, fast mass scanning;	High resolution capability, high sensitivity, extremely low background levels leading to low detection limits, flat top peaks in low resolution	Ultrahigh precision for isotope ratio measurements by removing source stability as limitation factor;
Disadvantages	Spectral interferences, limitations measuring 'difficult' elements and complex matrices due to low resolution (limitations can be partially solved with a dynamic reaction cell), rounded peak shapes;	Slower mass scanning for multielemental analysis, lower precision for isotopic ratios than MC-ICP-MS;	cost, large instrument size;
Application	Routine and multielement analysis, (isotopic analysis)	Quantitation of isotopes prone to spectral interferences/ in complex matrices, isotopic analysis	Isotopic analysis with highest precision, elemental concentration with isotope dilution technique

In a novel approach for analysis of U isotopes in 'hot' particles the ICP-MS instrument was coupled to a laser ablation system (UP193 Solid-State, New Wave, Fremont, USA), therefore

a method had to be developed. Since that was the main instrumental part of this work, the following description of ICP-MS will focus on the Nu Plasma HR.

2.2.1 Principle

An ICP-MS device consists of a sample introduction system, an ion source (ICP), an interface region, an ion focusing system (ion optics), a mass analyzer and a detection system.

The structure of a double focusing sector field ICP-MS with Nier Johnson geometry (Nu Plasma HR) from ion source over ion optics to the mass analyzer (consisting of an electrostatic and a magnetic sector device) and detection system is shown in figure 1.
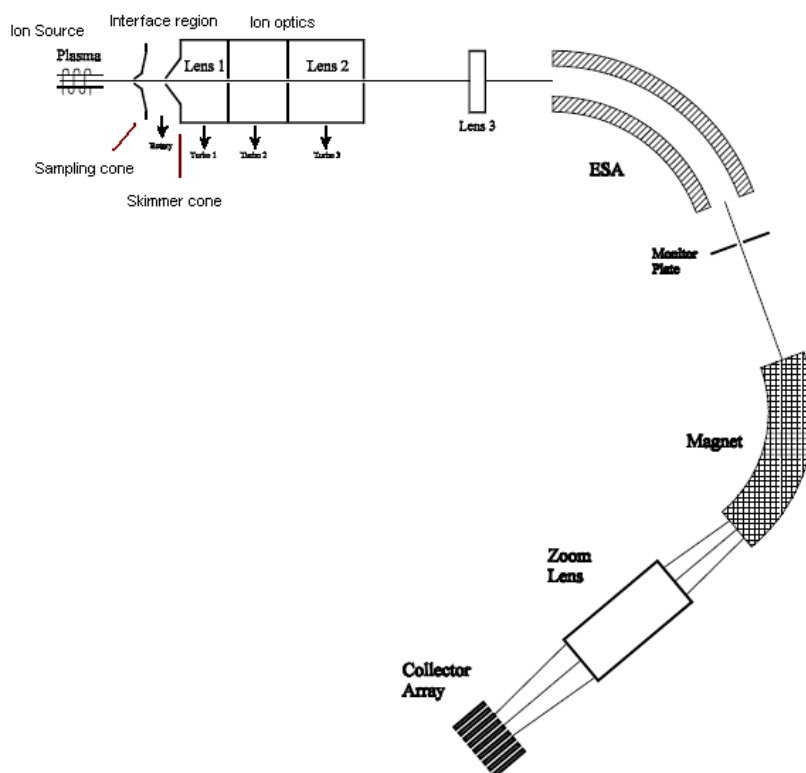
Figure 1. Scheme of the Nu Plasma HR, ESA = electrostatic sector analyser [slightly modified from Nu Industries 2005a].

The sample enters the ion source via sample introduction system in form of a fine droplet-aerosol, it is dried, vaporized, atomized and finally ionized in the plasma torch. In the interface, the region defined by the position of sampling and skimmer cons, ICP generated ions are transported from the torch at atmospheric pressure, to the highly evacuated mass analyzer. The ion optics are a series of electrostatic lenses used to focus and accelerate the ion beam into the mass separation device, where the ions are separated by their mass-to-charge ratio (m/z) and finally registered by an appropriate detection system.

2.2.2 Sample introduction

Samples can be introduced either in gaseous, liquid or solid form. Since thereby an excellent measurement accuracy and precision is achieved due to the ease of sample handling and dilution as well as of calibration for quantification, for liquid sample introduction the most commonly used systems are offered, based on the same principles: A nebulizer is employed to generate an aerosol and a spray chamber assures that only fine droplets will reach the plasma. The sample liquid is peristaltically pumped into the nebulizer (or a self-aspirating device is used), where it is dispersed into an aerosol by the help of the nebulizer gas flow (pneumatic nebulizer). Other common types of liquid sample introduction systems are ultrasonic and thermospray nebulizer. In addition aerosol desolvation devices reduce droplet size and solvent loading, leading to improved detection limits and reduced interferences caused by the matrix of the solvent.

Gaseous sample introduction reveals the highest transport efficiency (nearly 100%), matrix interferences are eliminated to a great content by separation of analyte vapour from the sample solution and no further desolvation and vaporization is needed. The main challenge remains to convert the analyte to a gaseous state [Montaser 1998].

The direct introduction of solids into the ICP reduces sample preparation time and therefore the possibility of cross contaminations from other samples and reagents. Molecular spectral interferences specially occurring during analysis of solutions (deriving from the solvent) are not present. However, interferences deriving from the matrix are still present, since a matrix separation is not possible with solid samples.

A great disadvantage is the limitation of quantification capability due to the lack of primary standards [Montaser 1998].

Methods include direct sample insertion, electrothermal vaporization and arc and spark ablation.

In this work each one of the three types of sample introduction systems, liquid, solid and gaseous, were employed together with the Nu Plasma HR.

2.2.2.1 Desolvating nebulizer system

Sample solutions were introduced to the ICP with a desolvating nebulizer system, the DSN 100 (Nu Instruments, Wrexham, UK) and a self-aspirating PFA 100 nebulizer (Elemental Scientific Inc. Omaha, USA).
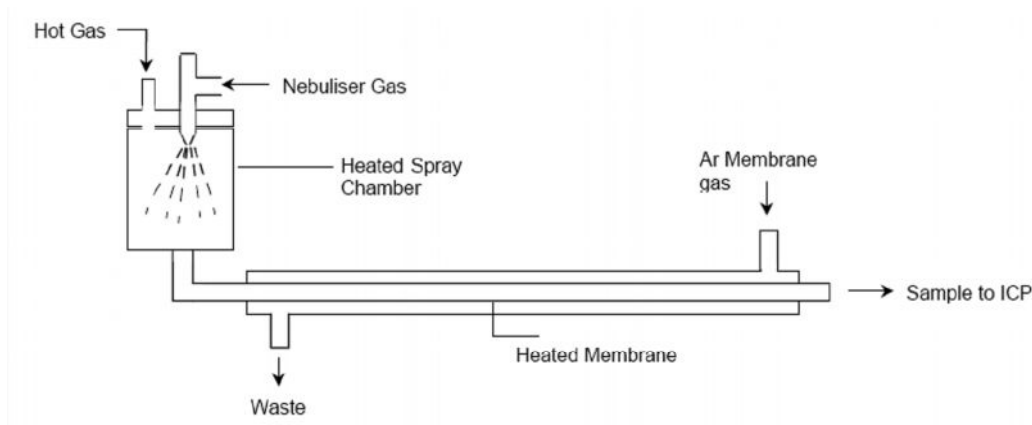
Figure 2. Scheme of the DSN 100 [Nu Instruments 2005].

Desolvation in the DSN 100 is accomplished by a membrane separator, the principle is shown in figure 2: A fine aerosol is introduced into the heated spray chamber, where it is vaporized and carried to the membrane. The solvent is separated from the sample by passing the membrane and finally carried away by the membrane gas flow, while the sample is transferred to the ICP. The hot gas flow (preheated gas) was installed to avoid condensation of the sample aerosol.

2.2.2.2 Laser ablation

The technique of laser ablation (LA) is able to sample various materials and does not require a conducting surface in comparison to old arc/spark systems [Hill 1999].

A laser beam of defined energy is pointed to the sample (located in an ablation cell) leading to sputtering and vaporization processes of the impacted surface and finally the released material is carried to the ion source in a gas flow (usually Ar or He).

Different types of laser are employed in ICP-MS, most commonly the Nd:YAG (yttrium aluminium garment) operating at a wavelengths of 213 or 266 nm, furthermore the ruby (694 nm) and the excimer gas laser ArF (193 nm). Shorter UV wavelengths are better absorbed by most materials.

Figure 3.   The UP193 Solid-State laser ablation system [New Wave research 2005].

The ablation of 'hot' particles was performed with the UP193 Solid-State (figure 3), operating in the deep UV (193 nm) at very short pulse widths. Sufficiently small spot sizes can be chosen (spot size ranges from 2 µm to 110 µm), being advantageous for the analysis of small-sized particles.

2.2.2.3 Hydride generation

Some elements (such as As, Bi, Ge, Sb, Se, Sn, Te and Pb) can be converted to gaseous forms (volatile hydrides) and therefore separated from their non-hydride forming matrix by using a hydride generator (HG) as sample introduction system for ICP-MS.

The desired reaction is achieved by the use of a suitable acid and oxidant matrix for the sample solution. Dependent on the element different concentrations and types of oxidants and acids provide an optimal conversion. The emerging gas is then separated from the liquid matrix via a gas liquid separator (GLS). Separation is obtained for example when the solution containing the gaseous hydrides passes a teflon membrane over which additional plasma gas flows horizontally. A scheme of such a GLS can be seen in figure 4.
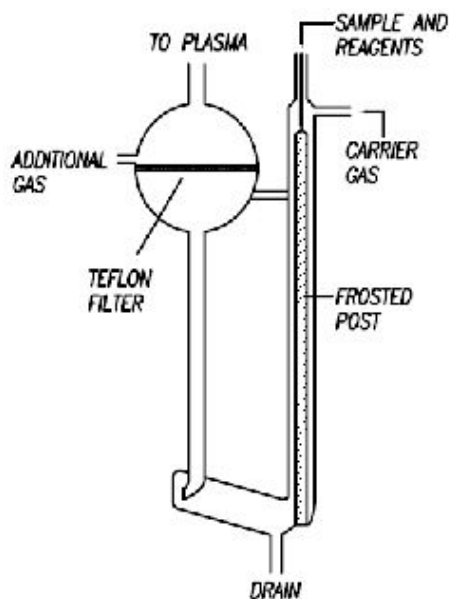
Figure 4.   Principle of a GLS [Cetac 2007].

A commercially available HG is composed of reagent vessels for acid and reductant (usually NaBH$_4$), tubings and connections, solution mixing blocks and coils and, of course, a GLS. In addition a pump for sample solution, reagents and waste flow is needed.

2.2.3 Ion source, interface region and ion optics

These three parts are responsible for generation, focusing and acceleration of ions.

The ion source, inductively coupled plasma, is formed by a stream of gas (mostly Ar) flowing through a plasma torch consisting of 3 concentric quartz tubes, which are encircled by an induction coil (the load coil, usually made of copper) connected to a radiofrequency (RF) generator. The RF current induces an electromagnetic field, which initiates a current in the Ar gas stream. The interaction of ionized Ar with the electromagnetic field provides an energy transfer into the ICP.

The ions are generated at atmospheric pressure, but the mass analyzer requires a vacuum of better than $5*10^{-5}$ mbar [Montaser 1998]. Therefore the ions are directed through the interface region. Sampling and skimmer cones encompass the interface region to the ion source and the analyzer side, respectively. They are often made of nickel and have a small ofrice (about 1 mm). The pressure is reduced in the interface region to about 2 mbar by the means of a rotary pump.

Behind the sampling cone (the sampler) a free jet of conical structure is formed (supersonic expansion) into the high vacuum region (depending on the mass analyzer from about 10^{-5} –

10^{-9} mbar). The area between the base of this cone and the sampler is called zone of silence. The skimmer cone is placed within that region.

Ions are then extracted from neutral species and photons to improve performance and focused by a series of electrostatic lenses.

2.2.4 Magnetic sectorfield mass analyzer

The Nu plasma HR is a double focusing sector field ICP-MS device with a forward Nier Johnson geometry, meaning energy focussing of the ions is achieved by an electrostatic analyzer (ESA) and separation due to the mass-to-charge ratio of the ions by a magnet sector analyzer (MSA).

Double focusing sector field instruments can be either operated in a forward or a reverse geometry. In the forward geometry the ESA is placed ahead of the MSA. The Nier Johnson geometry as used in the Nu Plasma HR consists of a 90° ESA, a long intermediate drift length and a 60° MSA curved in the same direction. Forward configuration offers the possibility of applying a multiple collector for detection, since the MSA spatially separates different masses of the same kinetic energy. Multiple detection improves the precision of isotope ratio measurements, since temporal fluctuations in the ion beam do not influence the analysis when the detection of the desired isotopes is performed simultaneously. Reverse geometry on the other hand has the advantage of improved abundance sensitivity (a measure of the tailing from a larger into a smaller peak) by a factor of up to 100 [Montaser 1998].
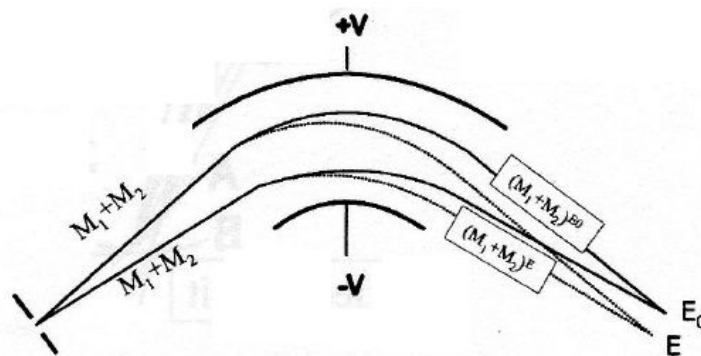
Figure 5.   Ion deflection in the electrical field [Boulyga 2007a].

Ions are separated by both magnetic and electrostatic field in a double focusing SF-MS.

An ESA device consists of two curved plates with a certain voltage (500 to 1000 V) applied between them (figure 5). The outer plate is positive, the inner plate negative and the center line is at ground [Montaser 1998].

In an electrical field the centrifugal force of an ion (2), which reflects its kinetic energy ($m*v^2/2$) must be balanced with an electrostatic force expressed by equation 3 in order to focus ions of the same translational energy in a defined curve from the entrance through the exit slit (4).

This is achieved for a given ESA geometry (defined radius and distance of the plates) by the applied voltage leading to a potential difference between the plates.

$$F_{cent} = mv^2/r \qquad (2)$$

F_{cent}... centrifugal force [newton]
m… mass of the ion [atomic mass unit, amu]
v… velocity of the ion [m/s]
r… radius of the circular path of the ion [m]

$$F_{el} = zeE/d \qquad (3)$$

F_{el}… electrostatic force [newton]
z... number of electrons
e… electron charge [$1.602177*10^{-19}$ coulomb]
E... potential difference between the two plates [volt]
d… distance of the plates [m]

$$mv^2/2 = rzeE/2d \qquad (4)$$

An MSA consists of a curved flight tube located in the gap between the poles of an electromagnet [Montaser 1998]. A scheme can be found in figure 6.
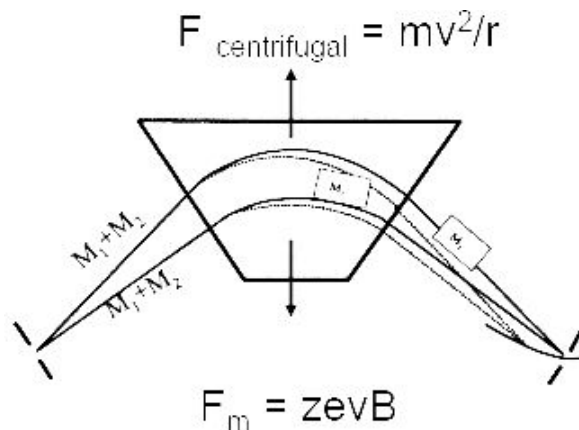
Figure 6.   Principle of ion separation in the magnetic field [Boulyga 2007a].

The magnetic field is perpendicular to the flight direction of the ions. The magnetic force depends on the charge of the species (z*e), the strength of the magnetic field (B) and the velocity (5).

$$F_m = zevB \qquad (5)$$

F_m… magnetic force [newton]
B… magnetic field [tesla]

Again this force must be balanced with the centrifugal force (2) in order to achieve focusing:

$$mv^2/r = zevB \qquad (6)$$

The velocity in a single focusing magnetic sector is determined by the accelerating voltage applied to the electrostatic slit located in front of the MSA (7).

$$mv_{final}^2/2 = E_{initial} + zeU \qquad (7)$$

U... accelerating voltage [volt]

When equation 7 is substituted in equation 6, the following mass-to-charge ratio (for e = constant, it is also referred to as m/z) is achieved:

$$m/ze = r^2B^2/2U \qquad (8)$$

If all ions have the same initial energy each ion has a unique trajectory depending on its mass-to-charge ratio, and can therefore be focused (led through the exit slit) by changing the strength of the magnetic field.

In single focusing magnetic sectors ion energies vary due to the difference in initial kinetic energy of the sample molecules and atoms in the ion source. Another point is the type of ion source, 'soft ionization' such as applied in TIMS leads to minor energy spread for instance [Montaser 1998]. Wide differences in ion energy lead to peak broadening and low resolution, since ions of the same momentum (m*v), but of different masses are selected together. This problem is mastered by double focusing.

Since ions deriving from the ESA of a (forward) double focusing sector field device are focused due to their kinetic energy, the velocity is thus controlled and the ion beam can be separated spatially afterwards by the magnetic field according the mass-to-charge ratio of the species only.

Other common mass analyzers used with ICP-ion source are quadrupole, time of flight and ion trap MS.

2.2.5 Detection

The detection system produces a computer-usable number out of an incident ion beam.

Single collector instruments generally use two stage secondary electron multipliers which can be operated in two different operating modes: the pulse and the analog mode. The first is used, when intensities are below about 100 000 cps (depending on the instrumentation), because it reveals best relative standard deviation of the signals and low detection limits. For higher signals the pulse mode is no longer operable, but measurement can be performed with analog mode. Dual detection systems can deal with a wide range of signal intensities arriving

at the detector. High currents are detected in the analog mode of a secondary electron multiplier, the signal is extracted either at the end or partway down the multiplier chain. Low signals are detected by the normal pulse counting output. A rapid changeover is possible with this arrangement [Montaser 1998].

Faraday cup collectors are employed for analog detection of ion currents in MC-instruments. They consist of a metal electrode surrounded by a cage. When positively charged ions strike the electrode, the are neutralized by electrons from ground through the resistor, causing a drop in the potential, which is recorded after amplification. Faraday cups are very robust and reveal good linearity. Detection limits are by the factor of 10^3 higher than those obtained by SEV detectors. They can measure currents down to 10^{-15} A (10^4 cps), overlapping the upper range of the ion-counting system [Montaser 1998].
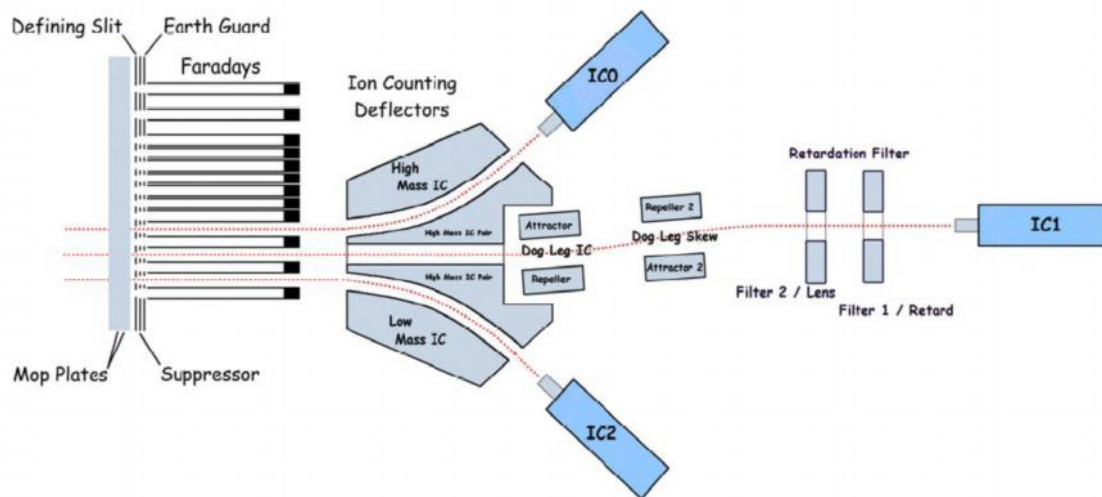
Figure 7.   Schematic of the collector system from Nu Plasma HR [Nu Instruments 2005a].

In addition to 12 Faraday cups three ion-counting multipliers ('ion counters', ICs) are installed in the Nu Plasma HR (figure 7). The multipliers are discrete dynodes, pulse counting models. Dynodes are surfaces at high voltages, which are able to multiply electron impacts by the release of secondary electrons, finally leading to an electron cascade. The multiplication factor is typically in the order of 10^8. Discrete dynodes make use of a resistor chain to provide the appropriate potentials [Montaser 1998].

The period known as the multiplier dead time, is the time for which an ion counting system is unable to count incoming ions after the impact of a previous ion [Nelms et al. 2001]. Corrections are applied, but dead time presets an upper limit to the count rate remaining in the linear mode of detection.

3 Forensic uranium and lead isotope measurements in biological tissues

3.1 Uranium analysis in urine and hair samples

3.1.1 Sample preparation

Three urine samples of a Kosovo soldier were prepared due to Schramel et al. 1997: 1 mL urine was mixed in quartz eprouvettes (equipped with teflon caps) with 250 µl concentrated HNO_3, 2.75 mL subboiled water and 1 mL 31% hydrogen peroxide. Digestion was performed with a Metrohm UV-1000 (Methrom, Switzerland) for 40 min under water cooling (<90 °C). They were let cool off and filled into plastic tubes. Finally 500 µl of an internal standard (11 ng g^{-1} Indium) was added. Three method blanks were obtained in the same way.

Samples and blanks were stored in the fridge until ICP-Q-MS measurements for quantification purposes of U took place. A freezer is recommended for long-term storage.

No further dilution was necessary prior to analysis.

Two recent hair samples from the soldier and two collected from the sleeping bag used during Kosovo deployment together with 6 reference hair strands from laboratory staff were affixed on glass micro slides with commercially available glue and put into the laser ablation chamber for measurement with ICP-Q-MS.

3.1.2 Measurement procedures

In this work measurement was performed with a quadrupole ICP-MS device (ELAN DRC II). See table 4 for the operational parameters applied. Three isotopes were analyzed: ^{115}In, ^{235}U and ^{238}U.

An 11 ng mL^{-1} Indium standard solution was added to the blank (1% (w/w) nitric acid), the standards and samples to a final concentration of 1 ng mL^{-1}. Indium has the advantage that the only possible interferents (Sn and MoO) can be corrected mathematically via ^{118}Sn by the Elan software.

Quantification was obtained by the employment of five calibration standards with a U concentration of 1, 5, 10, 25 and 50 ng mL^{-1}, respectively. The relative intensities of the calibration standards were used for linear calibration after blank correction.

Table 4. Parameters for ICP-Q-MS (ELAN DRC II) measurement of U in urine.

RF power	1300 W
Gas flow rate	1.8 mL min^{-1}
Auxilary gas flow rate	0.98 mL min^{-1}
Cool gas flow rate	13.7 mL min^{-1}
Detection mode	Dual
Auto lens	Off
Scanning mode	Peak hopping
Number of Sweeps	40
Number of Readings	1
Number of Replicates	10
Measurement time	~ 4 min

Alternatively to urine, a possible U contamination can be determined by the analysis of hair or nail samples. The use of hair as study object for the detection of contamination has several advantages in comparison to urine: it is stable and robust and its composition does not change over time, storage and handling is simpler and it has the ability to reflect the total body intake over an extended period [Sela et al., 2007].

The hair was analyzed by ICP-Q-MS (ELAN DRC-e) operated in DRC mode using oxygen as DRC gas combined with a laser ablation system (UP193 Solid-State). See table 5 for the operational parameters. Two uranium isotopes (^{235}U and ^{238}U) were measured to determine a possible U contamination. Sulfur, an abundant matrix element of hair, was used as internal standard (measured as SO on mass 48 due to reaction with the cell gas) to correct variations in ablation efficiency and plasma.

Each hair was ablated on two or three independent areas by the use of line scans. Every line was scanned twice: the first for the hair surface with larger laser spot size and lower energy output and the second for the interior with smaller spot size and higher energy output.
Blank values (gas blank) were obtained by taking the average of the first ten readings. Intensities were normalized to the internal standard after blank correction.

Table 5. Parameters for the determination of U in hair by LA-ICP-Q-MS (ELAN DRC-e and UP193 Solid-State).

ICP-MS	
RF power	1300 W
Gas flow rate	1.2 mL min^{-1}
Auxilary gas flow rate	0.85 mL min^{-1}
Cool gas flow rate	14 mL min^{-1}
Cell gas (O$_2$) flow rate	0.55 mL min^{-1}
Detection mode	Dual
Auto lense	On
Scanning mode	Peak hopping
Number of Sweeps	1
Number of Readings	150
Number of Replicates	1
Measurement time	~ 2 min
Laser ablation	
Wavelength	193 nm
Method	Line scan
Repetition frequency	10 Hz
Spot size line 1	75 µm
Spot size line 2	25 µm
Laser energy line 1	20%
Laser energy line 2	40%
Scan speed	100 µm s^{-1}

3.1.3 Results and discussion

The exact concentrations of the standards and the blank corrected ratio of the uranium signal to the indium signal was used to obtain a linear calibration curve (see figure 8) for both ^{235}U and ^{238}U for the U determination in urine.

The calibration of ^{238}U could only be performed as 3 point calibration, because the signal for this isotope was negative for the two highest standards for an unknown reason. However, values of the measured samples were found at the lower concentration side of the calibration curve.
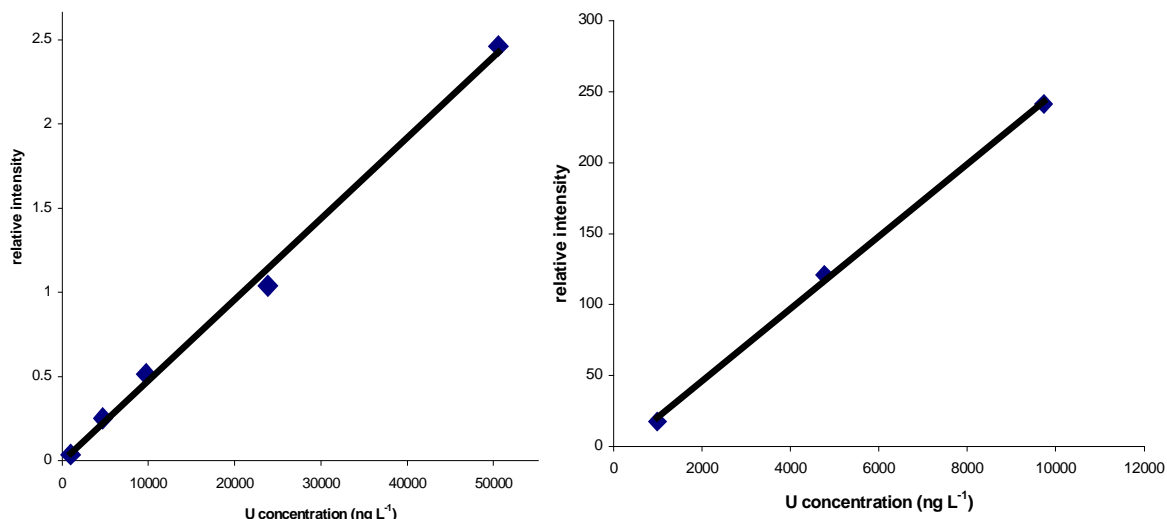
Figure 8. Linear calibration curves for a) ^{235}U and b) ^{238}U, respectively.

Two of the method blanks revealed a higher signal than the samples themselves. Therefore the background level could not be subtracted when calculating the concentrations.

The concentrations of the three samples (GS 1, GS 2 and GS 3) were estimated via ^{238}U, since the intensities of ^{235}U were relatively low and the measurement revealed a significant uncertainty. The limit of detection (LOD) was calculated by the use of the 1% nitric acid as blank to be 864.1 ng L^{-1}. Measured samples and method blanks were all below the LOD.

The normal concentration of uranium in urine in not contaminated individuals was estimated to be in the range from 1 and 40 ng L^{-1} [Beyer et al. 1993, Dang et al. 1992, Medley et al. 1995], therefore the achieved detection limit was too high to achieve reliable results.

It should be stated that determining the concentration of U in urine is only of limited use for the detection of contamination anyway, because most of the uranium leaves the body within a few days, and therefore the method can only determine exposure to U that happened recently or derives from a long period intake of contaminated drinking water or food. Elevated levels of natural uranium in urine from long-term exposed individuals for example could be detected up to 10 months after the last intake of contaminated groundwater [Orloff et al. 2004].

It was also observed that Gulf War veterans with retained metal shrapnel fragments revealed elevated uranium levels in urine 7 years after the first exposure [McDiarmid et al. 2000]. However, if high amounts of DU (or other sources of U) enter the body at once via inhalation or ingestion the highest concentration of uranium in urine can be found within a few days

(two thirds of the total amount of absorbed U is excreted within 24 h) after contamination [Taylor and Taylor 1997].

Hair was also analysed in order to make sure that the possibility of a DU contamination can be eliminated. Both U isotopes (^{235}U and ^{238}U) were not detectable with the applied method in any of the hair samples, neither from uncontaminated laboratory staff nor from the hair of the soldier.

3.2 Lead and uranium analysis in thyroid samples

3.2.1 Sample preparation

Dried thyroid samples, obtained from persons who underwent surgery in hospitals in Minsk, Belarus, were used for trace elemental analysis after molecular, cellular and biological studies had been conducted previousely [Boulyga et al. 2000].

These samples were analysed together with dried thyroid tissues from persons living in rural areas in the south of Belarus (Homel) and thyroids from cancer patients for this study.

The preparation of a total of 86 samples was carried out by microwave assisted digestion (MLS1200 mega, Milestone-MLS GmbH, Leutkirch, Germany) using the time and power program presented in table 6.

Table 6. Program of the high performance microwave digestion unit.

Step	Time (hms)	Power (W)
1	00:05:00	250
2	00:05:00	400
3	00:10:00	600
4	00:05:00	250

Between 9 and 112 mg (depending on availability) of each thyroid sample was weighed into a digestion bomb and 3 mL concentrated HNO_3 with 0.5 mL 31% H_2O_2 were added. Afterwards the bombs were put into the microwave. Method blanks were obtained using the same digestion procedure prior to each sample digestion.

After digestion blank and sample solutions were filled up to a final weight of about 10 g with subboiled H_2O.

400 µl iridium standard solution (10 ng g^{-1}) was added to 0.2 mL of the digestion solution and finally the tubes were filled up to 4 mL for the determination of Pb and U concentrations.

2 mL of the digested solutions were spiked with 0.2 mL thallium standard (110 ng g^{-1}) and subsequently measured by MC-ICP-SF-MS in order to obtain isotope ratios.

Three soil samples were collected in the vicinity of Chernobyl, Ukraine (KRA, RAD and MAS). They were taken from the upper 0-1 cm soil layer using a special coring device. The samples were homogenized and ashed in 1996.

Another soil sample (IAEA–375), which is a certified reference material from the IAEA, was used in this work together with KRA, RAD and MAS to obtain isotope ratios of lead as reference to thyroid samples.

Possibly interfering organic matter can be removed by ashing samples in furnaces, a measure just taken for IAEA-375 being only dried and homogenized before. For this purpose 3 crucibles were glowed to weight constancy by putting them into a muffle oven (Medlin Naber GesmbH, Vienna, Austria) at 550 °C with subsequent cooling at room temperature in an desiccator. The procedure was repeated until a constant weight was achieved: the first time the crucibles were heated for four hours and cooled over night, the second time heating and cooling were reduced to one hour each.

5 g of IAEA-375 was subdivided into the crucibles, ashed for four hours and afterwards cooled over night. About 12% weight loss was observed.

The samples were digested with a high performance microwave digestion unit (MLS1200 mega). The digestion procedure was optimized before due to the method suggested by Milestone 1996, where HF is used for solubilization of silicates by complex formation (see equation 9 for the reaction of hydrofloric acid with SiO_2) and $HClO_4$ for organic compounds.

$$SiO_2 + 6\ HF \rightarrow H_2SiF_6 + 2\ H_2O \hspace{3cm} (9)$$

4 mL 48% hydrofluoric acid and 1 mL 70% perchloric acid were pipetted into digestion bombs for the blanks and afterwards put into the microwave. The same time and power program was employed as for the thyroid sample digestions (table 6).

After the digestion the solutions were transferred into PFA- vessels and the digestion bombs were rinsed with 1% nitric acid. The solutions were then evaporated for removal of the hydrofluoric acid by placing them on a hot plate until there was only about 1 mL left, which was filled up to a weight of 10 g with 8 M HNO_3.

About 0.3 g of each sample (dry ashed IAEA-375, KRA, RAD, MAS) was weighed into a digestion bomb and 4.8 mL 48% hydrofluoric acid and 1.2 mL 70% perchloric acid were added. After digestion with the same program as was applied for the blanks, the procedure was repeated two times and the solutions of the 3 digestions were pooled. Finally about 1 g of each sample was digested in total.

The solutions were again concentrated and since there were solid particles left about 3 mL aqua regia (3:1, subboiled HCl and double subboiled HNO_3) was added to the solutions and the samples were placed on the hot plate again (at first for about 2 h covered, then further evaporation uncovered at 100 °C). Finally the remaining liquid was again filled up with 8 M HNO_3 to a weight of 10 g (there were still particles left in the IAEA standard). This concentration of nitric acid was chosen, because it is considered to be optimal for Sr/matrix separation, which was performed with the same samples in another work.

The determination of the Pb concentration and isotope ratios was performed with 1:50 diluted samples (with subboiled water) and after screening, KRA was further diluted 1:3 (to a total dilution of 1:150). 400 µl iridium standard solution (10 ng g^{-1}) was added to 0.2 mL of the diluted sample solution and finally the tubes were filled up to 4 mL for the determination of the Pb and U concentrations.

2 mL of the 1:50 (and 1:150, respectively) diluted sample solutions were spiked with 0.2 mL thallium standard solution (110 ng g^{-1}) and subsequently measured by MC-ICP-SF-MS in order to obtain isotope ratios.

3.2.2 Measurement procedure for lead and uranium quantitation

U and Pb concentrations were measured in 4 soil samples. 86 thyroid samples were quantified for Pb. Measurements were performed with a SF-ICP-MS device with reversed geometry and single collector detection (ELEMENT2) in a low resolution mode. Sample introduction was accomplished by a cooled spray chamber PC3 and a PFA nebulizer (both from Elemental Scientific Inc., USA). A microwave digestion blank was also measured for each sample in order to detect possible contaminations deriving from the sample preparation process.

^{206}Pb, ^{207}Pb and ^{208}Pb isotopes were analysed for lead quantification, ^{193}Ir was used as internal standard. Operational parameters can be found in table 7.

A six point external calibration was performed with gravimetrically prepared standards. Internal normalization was obtained with 1 ng g^{-1} Ir in the measured solutions. Element concentrations in calibration standards covered the concentration range of corresponding elements in diluted samples. 1% (w/w) nitric acid was used for the determination of the blank value.

The relative intensity of the blank value was then subtracted from the one obtained from each standard and sample and the concentration was calculated via linear calibration performed by

the instrumental software. After the calibration standards and between the samples a 1 ng g^{-1} standard solution was measured for quality control.

Table 7. Operational parameters (ELEMENT2) for the determination of Pb and U concentration.

RF power	1300 W
Gas flow rate	0.90 mL min^{-1}
Auxiliary gas flow rate	0.90 mL min^{-1}
Cool gas flow rate	15.80 mL min^{-1}
Extraction lens potential	2000 V
Sample uptake rate	~ 100 µL min^{-1} (self aspirating mode)
Detection mode	Dual
Scanning mode	Peak hopping
Number of runs	6
Number of passes	10
Measurement time	3 min

^{238}U, ^{235}U, ^{234}U, ^{236}U and ^{193}Ir were recorded for uranium quantification. Measurement and calculation of the results were performed as described for Pb.

3.2.3 Measurement procedure for lead isotopic analysis

As soon as the first samples were digested, they were screened together with their corresponding blanks to prepare the adequate dilutions for subsequent isotopic measurement. Screening and isotopic analysis were performed with the Nu Plasma HR MC-ICP-MS. Sample introduction was accomplished by a desolvating nebulizer (DSN 100).

Table 8. Faraday cup arrangement for the determination of Pb isotopes with MC-ICP-SF-MS (Nu Plasma HR).

Cup	L5	L4	L3	L2	L1	Ax	H1	H2	H3	H4	H5	H6
Analyte			^{203}Tl	^{204}Pb	^{205}Tl	^{206}Pb	^{207}Pb	^{208}Pb				

The measurement was optimized for the signal of ^{206}Pb by introducing a 10 ng g^{-1} Pb standard solution. 10 ng g^{-1} SRM 981 spiked with a Tl standard to a final concentration of 10 ng g^{-1} Tl was measured as certified reference material for quality control of the performed analysis.

The isotopes ^{204}Pb, ^{206}Pb, ^{207}Pb, ^{208}Pb, ^{203}Tl and ^{205}Tl were directed into 6 faraday cups (L3 – H2) for detection (table 8), measurement parameters are summarized in table 9.

Table 9. Operational parameters for Pb isotope measurement with MC-ICP-MS (Nu Plasma HR).

ICP-MS	
RF power	1300 W
Auxiliary gas (Ar) flow rate	0.95 mL min^{-1}
Cooling gas (Ar) flow rate	13.0 mL min^{-1}
Zoom optics parameter	
Quad 1	10.0 V
Quad 2	18.4 V
Lin 1	0 V
Lin 2	0 V
Lin Corr	0 V
Cubic	0 V
Q15 corr	0 V
Q16 corr	0 V
Analysis mode	Batch run
Sampling mode	6 blocks of 10 measurements
Measurement time	~ 13 min
Wash time	3 min
Transfer time	2 min
DSN	
Nebulizer gas (Ar) pressure	30.3 Psi
Hot gas flow (Ar)	0.37 mL min^{-1}
Membrane gas flow (Ar)	3.12 mL min^{-1}
Spray chamber temperature	112 °C
Membrane temperature	120 °C

Background analysis for blank correction was determined by measuring 1% (w/w) nitric acid via 'measure zero' method (magnet set point on axial mass 206) for 100 s. An average value was then substracted from the following sample measurements in addition to the digestion blanks.

The ratios ^{208}Pb/^{204}Pb, ^{207}Pb/^{204}Pb, ^{206}Pb/^{204}Pb, ^{208}Pb/^{206}Pb, ^{207}Pb/^{206}Pb and ^{205}Tl/^{203}Tl were recorded.

Correction for mass bias was achieved by the measured and accepted value for the ratio ^{205}Tl/^{203}Tl and therewith the bias factor for the desired Pb ratios could be calculated via the exponential law (10).

$$R_t/R_m = \exp(F * m_1/m_2) \tag{10}$$

R_t... true or corrected ratio
R_m... measured ratio
F... correction factor
m_1/m_2... masses of interest

3.2.3.1 Experiments with hydride generation sample introduction system

Digested thyroids reveal a complex matrix. When introducing the sample solution by conventional liquid sample introduction systems, impurities (especially calcium) are taken along and soil the cones during measurement leading to a reduction of sensitivity and stability. Therefore the procedure had to be stopped every 15 samples for cleaning purposes, which is in fact not a desirable operational condition. To overcome this problem and in addition to impede possible interferences caused by the matrix elements, HG-sample introduction was investigated.

The first step for plumbane (PbH_4) generation is to oxidize lead to +IV state, which is then mixed with a reductant ($NaBH_4$) to be transformed to PbH_4.

While no serious complications occur when trying to determine some species (e.g. Bi), the hydride formation of lead causes more or less severe difficulties: a narrow pH interval is recommended, the oxidant (kind, concentration and reaction time) has critical effects on the success of the reaction and the chemical yield of plumbane is rather low. In real samples a lot of mechanisms are involved with the process with either inhibiting or catalysing effect [Petrov et al. 2006].

A couple of publications can be found, but each with another method for lead hydride generation with different kinds of acids and oxidants [Petrov et al. 2006, Chen et al. 2002, Cankur et al 2005, Tysen et al. 2000].
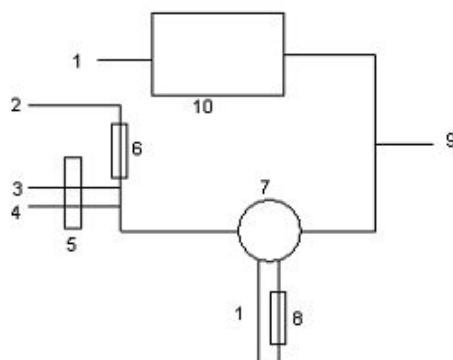
Figure 9. Schematic diagram of the sample introduction system: 1 Ar gas supply 2 sample container 3 acid container 4 reductant container 5 reagents pump 6 sample pump 7 GLS (zyclonic chamber) 8 drain pump 9 plasma torch 10 DSN (desolvating nebulizer).

Experiments with different acids and oxidants were performed, in order to find an optimal procedure for measuring lead isotopes within a complex matrix. Therefore a Pb standard solution mixed with the oxidizing reagent and acid to a final concentration of 10 ng g^{-1} lead was used to define the performance of the actual setup. Fresh sodium borohydride solution was prepared daily. Solid $NaBH_4$ was dissolved in 0.1 M NaOH for a better stability.

A schematic diagram of the sample introduction system with the hydride generator (HGX-100, Cetac Technologies, Omaha, USA) is given in figure 9.

Table 10.   Parameters of the HG sample introduction system (HGX-100) for the first experiment.

Parameter	concentration/flow rate
Acid (HNO$_3$)	0.1 M
Acid flow rate	0.7 mL min^{-1}
Oxidizing agent (H$_2$O$_2$)	0.28 M in sample mix
Sample flow rate	0.2 mL min^{-1}
Reductant (NaBH$_4$)	1.5% (w/v) in 0.1 M NaOH
Reductant flow rate	0.7 mL min^{-1}

A mixture of H$_2$O$_2$ and HNO$_3$ served as oxidant/acid matrix of the sample due to Petrov et al. 2006 for the first experiment. The concentrations of acid, oxidant and reductant were selected as shown in table 10 together with the corresponding flow rates (these are approximate values). With the same setup except for a lack of hydrogen peroxide a 10 ng g^{-1} bismuth standard solution was measured, as well.

The second approach was performed with ferricyanide (K$_3$[Fe(CN)$_6$]), which was described in several publications to be favorable for lead oxidation [Chen et al. 2002, Cankur et al. 2005, Tysen et al. 2000].

The sample mix consisted of the before mentioned lead standard, potassium hexacyanoferrite, HCl and oxalic acid. The last reagent is said to reduce possible interferences by masking disturbing ions [Cankur et al. 2005]. Parameters of the second experiment can be found in table 11.

Table 11.   Parameters for HG (HGX-100) for the second approach.

Parameter	Concentration
Acid (HCl)	2% in the sample mix
Oxidizing agent (K$_3$[Fe(CN)$_6$])	2% in the sample mix
Oxalic acid	0.4% in the sample mix
Reductant (NaBH$_4$)	4% (w/v) in 0.1 M NaOH

3.2.4 Results and Discussion

3.2.4.1 Concentrations of lead and uranium

The concentrations of Pb in thyroids varied significantly depending on the region and they were also distinguishable from the cancerous samples (figure 10). The thyroids from Minsk showed the lowest concentrations, which is an interesting point for Minsk is the capital of

Belarus and therefore a large city with over 1.5 millions of inhabitants. Usually the lead exposure in cites is increased compared to rural areas, giving a first hint for the occurrence of a possible contamination.

The concentrations of Minsk thyroids were in the range from 0.204 to 2.836 µg g^{-1} with an average of 0.606 µg g^{-1}, Homel samples were between 0.300 and 2.358 µg g^{-1} with an average of 0.890 µg g^{-1}. Cancerous thyroids revealed an elevated lead concentration from 0.212 to 2.514 µg g^{-1} with an average of 1.262 µg g^{-1}.
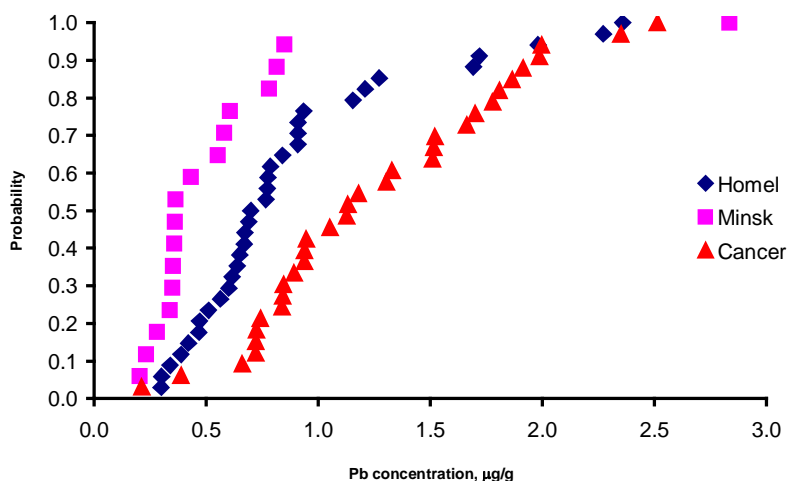
Figure 10.   Comparison of Pb concentrations of thyroid samples of two different regions and of cancer patients.
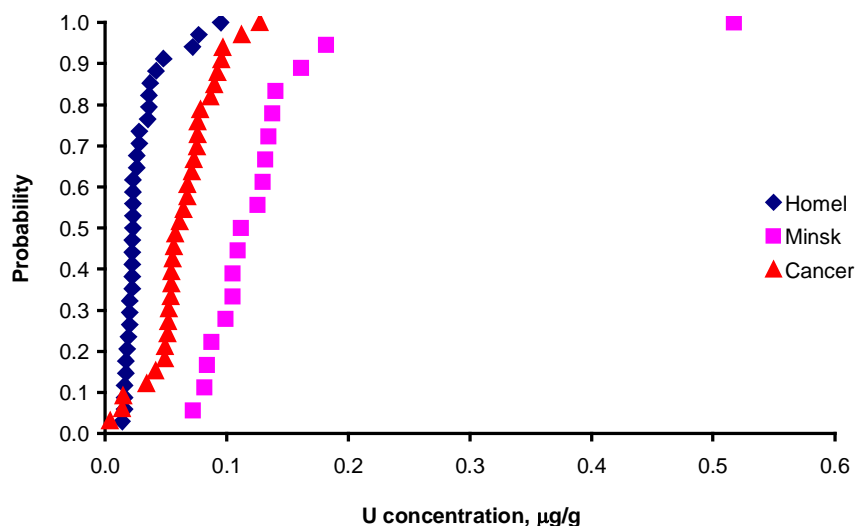
Figure 11.   Comparison of U concentrations of thyroid samples of two different regions and of cancer patients.

Although ^{235}U, ^{236}U and ^{234}U were also measured, uranium was quantified via the intensities of ^{238}U, because the intensities of the minor isotopes were relatively low and had significant measurement uncertainty. U concentrations (figure 11) were lower than the ones observed

from lead and could also be related to their according region. In this case Minsk values were the highest, they varied from 0.072 to 0.517 µg g^{-1} (average of 0.140 µg g^{-1}), Homel samples showed U concentrations from 0.014 to 0.095 µg g^{-1} (average 0.030 µg g^{-1}). Cancerous samples were found to lie between 0.004 and 0.127 µg g^{-1} (average 0.064 µg g^{-1}). A summary of the results is listed in table 12, the concentration for each sample can be found in the appendix (chapter 7.3.1).

Since the concentrations of Pb were significantly higher, Pb exhibits more reliable results in isotopic analysis than U.

Table 12.   Summary of the quantification of Pb and U in thyroids.

	Concentration range Pb (µg g^{-1})	Average Pb (µg g^{-1})	Median Pb (µg g^{-1})	Concentration range U (µg g^{-1})	Average U (µg g^{-1})	Median U (µg g^{-1})
Minsk (N=18)	0.204 - 2.836	0.606	0.364	0.072 - 0.517	0.140	0.118
Homel (N=34)	0.300 - 2.358	0.890	0.733	0.014 - 0.095	0.030	0.023
Cancerous (N=33)	0.212 - 2.514	1.262	1.132	0.004 - 0.127	0.064	0.061

The concentrations of U and Pb in the soil samples are listed in table 13. The results vary strongly from 10.437 to 54.874 µg g^{-1} Pb and 0.104 to 4.510 µg g^{-1} U. Uranium concentrations are in the range of normal soil, which lies between 0.3 – 11.7 µg g^{-1} [UNSCEAR 1993].

Here both elements reveal concentrations high enough for isotopic analysis.

Table 13.   Pb and U concentrations in soil samples. Measurement uncertainty is expressed as 95% confidence interval.

	Pb concentration (µg g^{-1})	U concentration (µg g^{-1})
IAEA	24.767 +/- 0.106	4.510 +/- 0.094
KRA	54.874 +/- 0.397	0.104 +/- 0.003
RAD	19.243 +/- 0.074	0.885 +/- 0.004
MAS	10.437 +/- 0.151	0.333 +/- 0.009

3.2.4.2   Isotopic analysis

In the first experiment with the HG-system even after changes in acid concentration and flow rates no significant detector response could be registered. For this reason the HG-system was tested with a Bi standard solution, which worked adequately (without further optimization a sensitivity for ^{209}Bi of about 200 V/µg g^{-1} was achieved).

A possible reason could be that the lead was oxidized incompletely or the plumbane decomposed in the reaction coil before it reached the GLS. A stronger oxidizing reagent was also tested (5% (v/v) perchloric acid in the sample mix instead of H_2O_2) unsuccessfully.

In the second experiment at first a different concentration for the reductant solution was chosen (1% (w/v) in 0.2% (w/w) NaOH solution), which proved to be unstable. The concentration was then changed according to the first experiment. A weak signal for lead was registered. After adapting the reductant to the final concentration of 4% (w/v) the signal increased (also the shortening of the sample loop and the increase of the flow rates had a favorable effect), the sensitivity reached a value of about 3 V/µg g^{-1} for ^{208}Pb at the highest in comparison to at least 200 V/µg g^{-1} with the DSN. In literature a similar efficiency of lead hydride generation was achieved with a quadrupole instrument coupled to a hydride generation sample introduction system (with account to the differences in sensitivities for lead detection provided by a quadrupole and a sector-field ICP-MS) [Chen et al. 2002].

It was proven that the HG systems works with Pb, but the sensitivity was too low for the measurement of Pb isotopic ratios.

Therefore analysis was finally performed by liquid introduction via the DSN. The results of the soil samples for the ratios ^{208}Pb/^{206}Pb, ^{207}Pb/^{206}Pb and ^{206}Pb/^{204}Pb are listed in table 14 together with literature values of samples collected in different parts of former Soviet Union. Here the average of the analysed samples is presented, while in figure 12, where the ratio ^{208}Pb/^{206}Pb is plotted against ^{207}Pb/^{206}Pb, each of the two measurements of KRA, RAD and MAS is shown. Although this figure demonstrates a scatter of the sample values because of matrix effects, the values are close to the average of major lead production sites of former Soviet Union (Tetyukhe, Nerchinsk, Salair and Sadon), which indicates that Pb used in Chernobyl could be composed of different sources from the USSR. The other literature values are from cities, where lead mainly derives from fuel. This lead represents cumulative contamination which had been produced during several decades of using gasoline with lead additions (as well as other industrial emissions). The isotopic composition is assumed therefore to reflect an 'average' isotopic composition of Russian lead production cites used during several decades of industrialisation.

The given value in Table 14 (Pb production) reflects the average of lead isotopic composition of lead production sites used only recently (mainly Kazakhstan's ores).

Table 14. Absolute isotopic ratios of $^{208}Pb/^{206}Pb$ and $^{207}Pb/^{206}Pb$ of measured samples and literature values of other regions of former Soviet Union. The uncertainties are expressed as one standard deviation. [c] 95% confidence interval [b] average of major lead productions sites of former Soviet Union (Tetyukhe, Nerchinsk, Salair and Sadon).

Sample	$^{208}Pb/^{206}Pb$	$^{207}Pb/^{206}Pb$	$^{206}Pb/^{204}Pb$	Reference
KRA	2.084 +/- 0.007	0.844 +/- 0.003	18.53 +/- 0.01	
RAD	2.084 +/- 0.008	0.849 +/- 0.003	18.48 +/- 0.01	
MAS	2.080 +/- 0.007	0.851 +/- 0.003	18.36 +/- 0.01	
Moscow	2.102 +/- 0.006	0.860 +/- 0.001	18.01 +/- 0.16	Mukai et al. 2001
Moscow	2.104 +/- 0.003[a]	0.862 +/- 0.001[a]	18.13 +/- 0.02[a]	Bollhöfer and Rosman 2002
Moscow	2.111 +/- 0.001[a]	0.871 +/- 0.001[a]	17.87 +/- 0.02[a]	Bollhöfer and Rosman 2001
Vilnius	2.097 +/- 0.001[a]	0.864 +/- 0.001[a]	17.97 +/- 0.02[a]	Bollhöfer and Rosman 2001
Kharkov	2.098 +/- 0.008[a]	0.859 +/- 0.001[a]	18.08 – 18.20	Bollhöfer and Rosman 2001
Pb production[b]	2.079 +/- 0.067	0.854 +/- 0.014		Mukai et al. 2001

Table 14 presents absolute isotope ratios of lead. The results for the thyroids together with the soil samples are plotted in figure 13. Here, in contrast to figure 12, relative (delta) values for the ratios $^{208}Pb/^{206}Pb$ and $^{207}Pb/^{206}Pb$ are presented corresponding to the deviations of the isotopic ratios of the samples to the ratios of the standard reference material SRM 981. The ratios obtained from thyroids of Homel inhabitants show lead isotope ratios which are closer to the lead isotopic composition observed in soil samples contaminated by Chernobyl fallout and they can be distinguished to the ones observed for Minsk and cancerous samples (in figure 13 referred to as tumor). As soon as thyroid samples of Homel inhabitants originate from a relatively large area, they can represent in general a mixed isotopic signatures of industrial (pre-accident) contamination and 'Chernobyl lead'.

In the thyroids of Minsk inhabitants a wide variation of both concentration and isotopic composition of lead was observed. This is probably due to different sources of lead in the organs of particular persons. Importantly, the isotopic composition of tissues from Homel area was found to be more close to 'Chernobyl lead' than the isotopic composition of Minsk tissues.

It is difficult to make a conclusion about the sources of lead found in cancer tissues because of the lack of background information about the previous in-vivo and in-vitro treatment of these tissues (e.g. chemicals and procedures of chemotherapy and applied medicines).

The entire data can be found in the appendix (chapter 7.3.2 and 7.3.3).
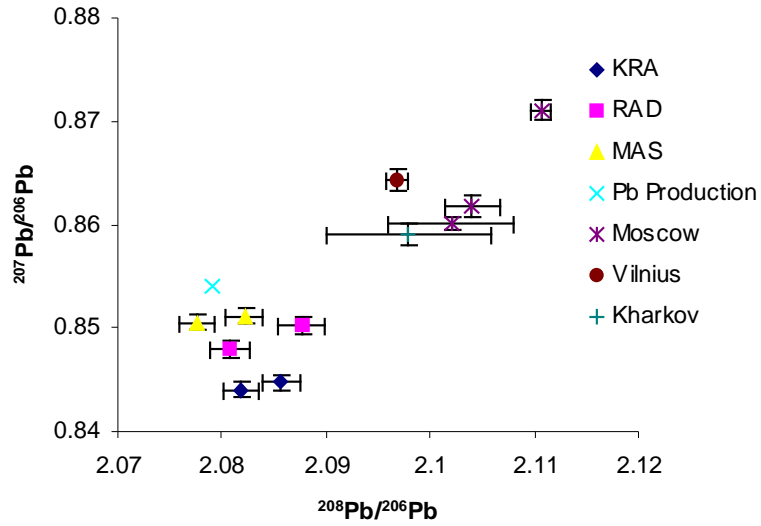
Figure 12. The ratios ^{208}Pb/^{206}Pb versus ^{207}Pb/^{206}Pb for soil samples collected in different parts of the former Soviet Union. KRA, RAD and MAS were measured in this work, the other values are from the literature.
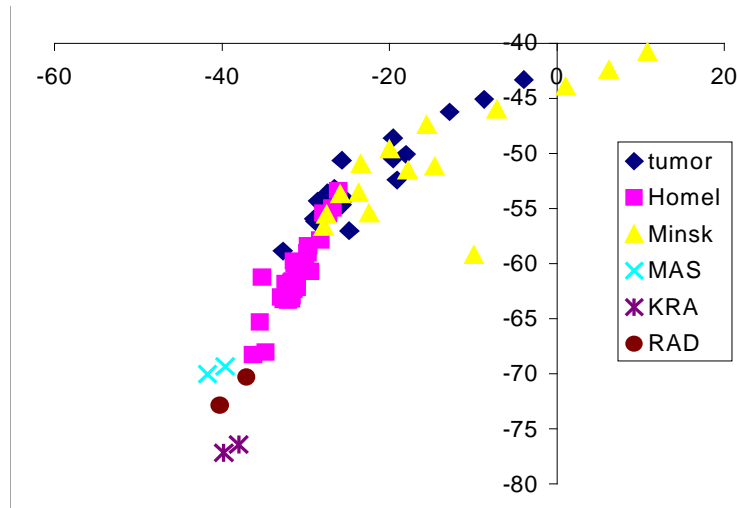
Figure 13. Deviations of the isotopic ratios ^{208}Pb/^{206}Pb versus ^{207}Pb/^{206}Pb of thyroids and soil samples from the corresponding ratios obtained from SRM 981 (delta values).

4 Uranium isotopic analysis in micro particles

4.1 'Hot' particles

Particles with 2 and 10% enrichment with ^{235}U fixed on carbon and silcon planchets, respectively, were provided by the IAEA. These samples were prepared in IAEA's Safeguards Analytical Laboratory (SAL) in Seibersdorf, Austria, according to Erdmann et al. 2000: certified standard reference uranium oxide (U_3O_8) powder (in this case SRM U020 and SRM U100), which is certified with respect to ^{234}U, ^{235}U, ^{236}U and ^{238}U abundance (for details see table 15), was dissolved in HNO_3 and added to a mixture of 50% MilliQ-water and 50% isopropanol (analytical grade). Different concentrations of U standard affects the mean diameter of the final aerosol particles, so a concentration of 62.5 mg L^{-1} U in the 50:50 mixture of water and isopropanol was chosen to achieve 1 µm sized particles. An aerosol generator produced droplets of this hydro-alcoholic uranyl-nitrate solutions and let the solvent vaporize. The formed particles passed a drying column and a series of three furnaces. After this calcination process (uranylnitrate is transferred to uranium oxide) the particles were cooled and finally collected on a Nucleopore filter. They can be transferred to various substrates afterwards, like high purity carbon planchets for SIMS analysis. For this purpose particles are simply dissoluted in an ultrasonic bath and the suspension is then dispersed on a graphite planchet. Finally the sample is sputtered with a graphite layer.

A comprehensive description of the production of particles for the nuclear safeguards together with details of the calculation of the according concentration depending on the particle diameter can be found in the work of Stetzer 2001.

Table 15.   Values for the isotopic ratios of the certified reference materials (CRMs) applied in this work.

CRM	$^{235}U/^{238}U$	$^{234}U/^{238}U$	$^{236}U/^{235}U$
U-100	1.14*E-1	7.54*E-4	3.72*E-3
U-020	2.07*E-2	1.77*E-4	5.28*E-3

Particles on the IAEA samples were located by SEM.

In addition to the IAEA samples particles were introduced on cellulose acetate (CA) filters. Therefore particles (with the same enrichment as the ones on the silicon/carbon planchets) were released from two nuclear membrane filters provided by SAL. The filters were dissolved in methanol by the use of an ultra sonic bath for about ten minutes. 0.05 mL of the solution was pipetted onto a CA filter. The filter was dried at room temperature and then put into a

petri dish for about 30 min, where a transparent film peeled off from the filter in an acetone vapor. The particles were now fixed on that film.

In addition a 'blank' (a fresh filter treated in the same way as particle filters after drying the methanol) was obtained.
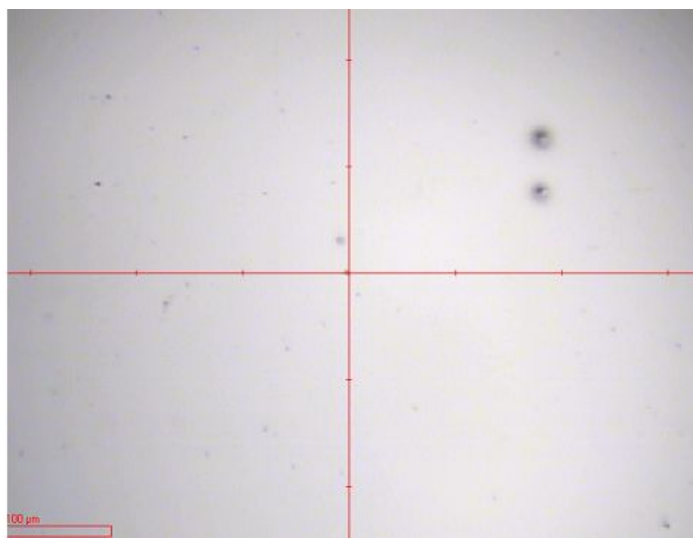
Figure 14. Image of a silicon wafer with U containing particles.

Images of the silicon wafer surface and the CA filter are given in figure 14 and 15, respectively.
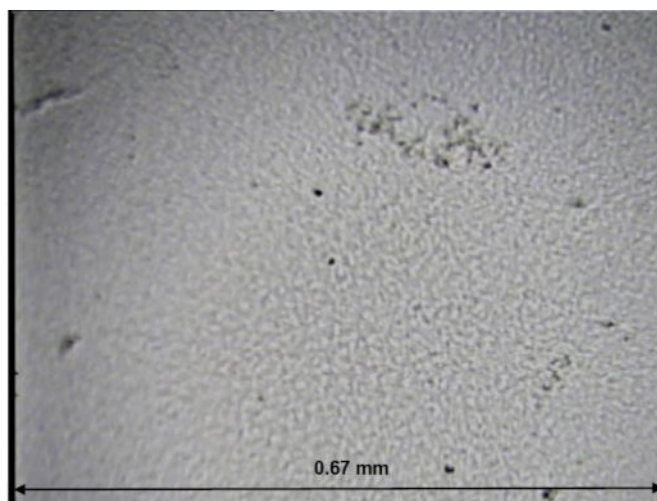
Figure 15. Picture of the film surface produced by acetone vaporizing of a CA filter containing U particles.

4.2 Measurement procedure

Particles affixed on graphite and silicon planchets as well as on cellulose acetate filters were analysed with a high resolution double focusing sector field MC-ICP-MS device (Nu Plasma HR) coupled to a laser ablation system (UP193 Solid-State) and a high-efficiency solution introduction system (DSN 100). The laser ablation system and the DSN were connected to the

ICP-MS via a 'Y'-type fitting to ensure that the gas flow (Ar) from both systems is mixed before entering the ICP.

The MC-ICP-MS instrument was equipped with a U/Pb collector block, primarily used for the simultaneous determination of U and Pb isotopes in geochronical sciences [Simonetti et al. 2005].

The ratios of $^{235}U/^{238}U$, $^{236}U/^{235}U$, $^{234}U/^{238}U$ were obtained in different experiments by the employment of two ion counting multipliers (IC0 and IC2/ IC0 and IC1) and two ion counters together with one faraday cup (L2, IC0 and IC1), respectively. The last arrangement is only possible, if sensitivity for the isotope detected by a faraday cup (^{238}U) is high enough. The experimental set-up is shown in figure 16.
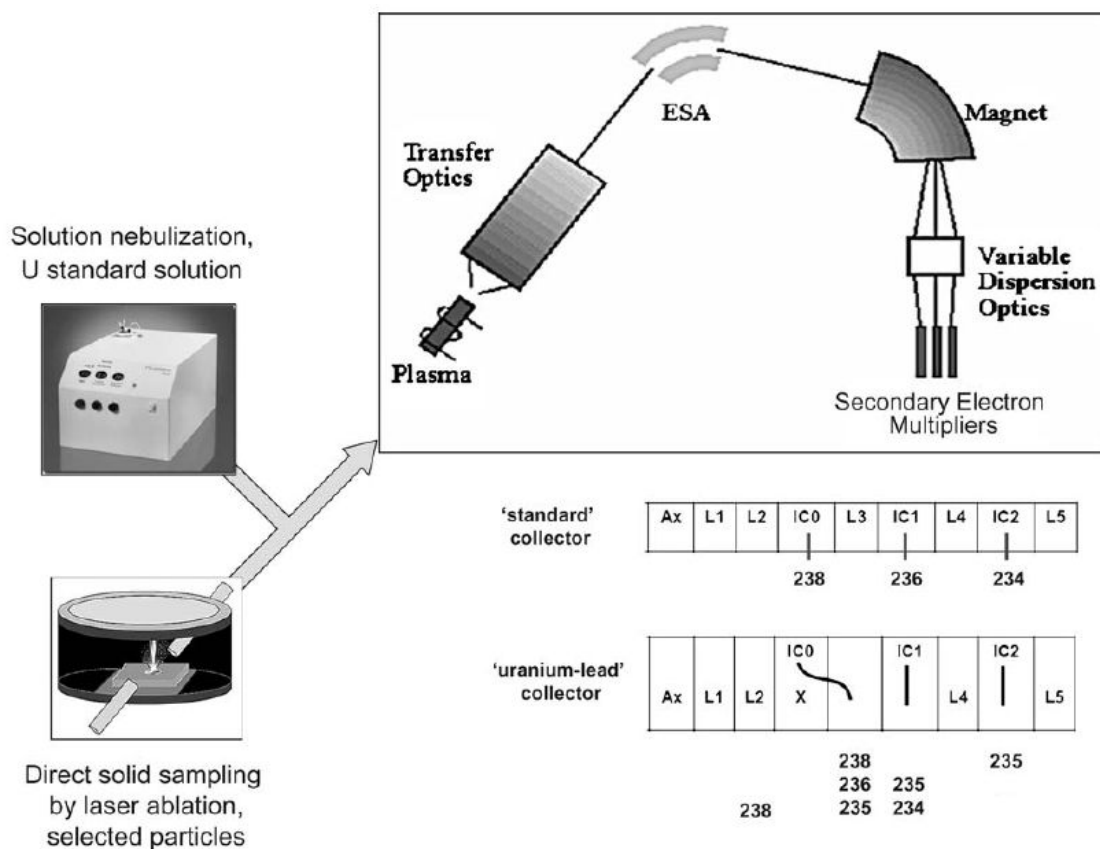
Figure 16. Schematic diagramm of the test arrangement of LA-MC-ICP-MS (UP193 Solid-State, Nu Plasma HR) for particle analysis [slightly modified from Boulyga and Prohaska 2008].

Before ^{238}U was detected by a faraday cup in the last set up, an experiment was performed with reduced sensitivity, since the intensity of ^{238}U proved to be too high in comparison to other isotopes in previous measurements. Reduction was achieved by changing the voltage of the central deflector (Cent Def) to –460.0 V. The central deflector voltage is responsible for the direction of the ion beam into the high mass IC in the U/Pb collector block.

Optimized parameters for the ICP-MS instrumentation were accomplished by nebulization of a U standard solution with natural isotope composition (and 50% enrichment due to [235]U, respectively) into the DSN by the use of a self-aspirating nebulizer. A compilation of optimized ICP-MS-, DSN- and LA-parameters can be found in table 16.

Table 16. Optimized parameters for U isotope measurements (single spot analysis) of 'hot' particles by LA-MC-ICP-MS.

ICP-MS	
RF power	1300 W
Auxiliary gas (Ar) flow rate	0.95 mL min^{-1}
Cooling gas (Ar) flow rate	13.0 mL min^{-1}
Mixed gas flow rate	0.8 mL min^{-1}
Analysis mode	Time resolved
Zoom optics parameter	
Quad 1	46.9 V
Quad 2	-90.9 V
Lin 1	0 V
Lin 2	0 V
Lin Corr	0 V
Cubic	0 V
Q15 corr	0 V
Q16 corr	0 V
Voltages applied to the multiplier collectors	
Low mass IC	-296.0 V
High mass IC	-304.0 V
Dog leg IC	250.0 V
Dog leg skew	0.0 V
Cent Def	-510.0 V
Laser ablation system	
Carrier gas (Ar) flow	0.7 mL min^{-1}
Laser wavelength	193 nm
Laser irradiance	0.02 J/cm^2
Method	Single spot
Repetition frequency	5 Hz
Laser energy	20%
Spot size	20 µm
DSN	
Nebulizer gas (Ar) pressure	25.0 Psi
Hot gas flow (Ar)	0.30 mL min^{-1}
Membrane gas flow (Ar)	2.16 mL min^{-1}
Spray chamber temperature	113 °C
Membrane temperature	119 °C

A blank (1% (w/w) nitric acid) and a standard solution (0.2 ng g^{-1} U500 and 5 ng g^{-1} IRMM 184, respectively) introduced by the DSN was measured (each one for 10 min) prior to analysis of the solid samples for calibration purposes. A correction factor was then calculated

for both compensation of mass bias effects and the different ion registration efficiencies of the ion counters (gains). 1% nitric acid was used as washing solution after the calibration. During solid sample analysis there was no solution uptake via DSN.

Particles from the IAEA graphite planchet were located by the use of a software (Particles Relocation between SEM and other instruments (TIMS, SIMS, optical microscope), program created by Uri Admon 2000, modified and designed by Andrzej Ciurapinski, 2005) designed to convert SEM achieved co-ordinates to other systems, since they could not be seen on the optical microscope from the LA-system.

On the IAEA silicon wafer particles could be spotted without further localization. LA-single spot analysis was performed for 56 individual particles to obtain $^{235}U/^{238}U$ ratio and 53 particles for $^{236}U/^{235}U$ ratio by the employment of two ion counters. In addition 40 particles were analysed simultaneously for $^{234}U/^{238}U$ and $^{235}U/^{238}U$ with two ion counters and one faraday cup for detection.

Apart from single spot analysis also raster scanning was tested on silicon wafer and CA filter with the intension to develop a semi-automatic procedure. The final settings for raster scanning applied to the LA-system are compiled in table 17.

Table 17.   Optimized settings for the LA-system (New Wave) during raster scan analysis.

Method	Raster scanning
Repetition frequency	5 Hz
Laser energy	20%
Spot size	50 µm
Scan speed	5 µm s^{-1}
Raster spacing	50.0 µm

4.3 Results and discussion

4.3.1 Single spot analysis

The measurement time for each particle varied between about 30 s to several minutes. Particles on the graphite planchet could not be spotted with the laser ablation system, therefore they had to be located by the translated SEM coordinates determined by the IAEA. Ablation was performed with 50 µm spotsize instead of the 20 µm applied in later analysis on the silicon wafer.

In the first experiment the measurement of 30 particles of 10% enrichment revealed an average isotopic ratio $^{235}U/^{238}U$ of 0.123 and in the second experiment (26 particles analysed) 0.151. The certified value for U-100 is 0.114. Results of the measurements of particles on the

graphite planchet are summarized in table 18 and figure 17 shows the measured ratios in comparison to the certified value for the first experiment.

Deviation of the certified value was calculated as % bias = ((measured value – certified value)/certified value)*100.

Precision and accuracy were rather poor. The average value turned out to be significantly higher than the certified value.

Table 18.   Isotopic ratios obtained from CRM U-100 via laser ablation of the graphite planchet.

Experiment Nr.	Certified value $^{235}U/^{238}U$	Measured value $^{235}U/^{238}U$	Precision (RSD %)	Accuracy (%)
1 (N=30)	1.14 E-1	1.23 E-1	18.8	8.08
2 (N=26)	1.14 E-1	1.51 E-1	37.6	32.5
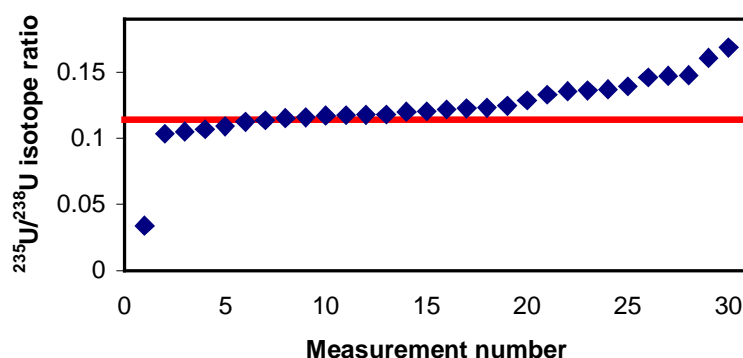
Figure 17.   Measured 235U/238U ratios for particles on the graphite planchet in the first experiment. The red line indicates the certified value of U-100.

The course of one single measurement on a carbon backing is illustrated in figure 18, it underlindes the poor precision obtained for isotopic ratio measurements and demonstrates that ratios are higher at the beginning of the ablation process.

The highest count rate per particle achieved on graphite was about 10^6.

Possible problems with graphite backing are the formation of carbon cluster ions with masses up to actinide range, the formation of non-volatile carbides which reduce the sensitivity by ~100 folds and clogging of the interface of the mass spectrometer.

Figure 19 shows an image of the silicium wafer with ablation spots surrounded by some dust and uranium particles.
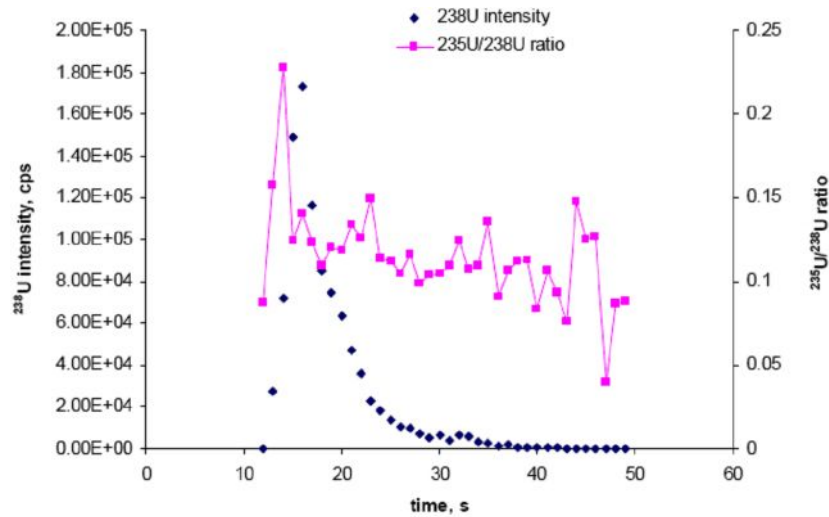
Figure 18. Intensity of ^{238}U and $^{235}U/^{238}U$ ratio versus ablation time from a particle on the carbon planchet.
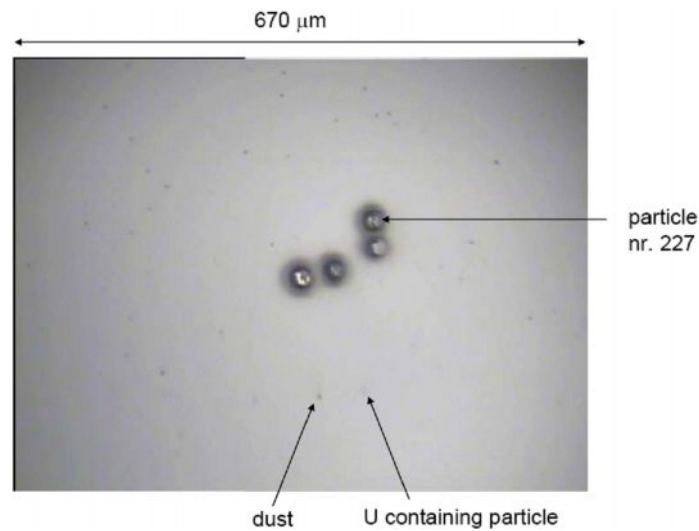
Figure 19. Image of four ablation spots on a silicon backing. Particle nr. 227 (located by translated SEM coordinates) is highlighted, also dust and other particles can be recognized.

On the silicon wafer the count rate per particle (up to $2.4*10^7$) was at least 10 times higher than the one observed on the graphite target, leading to an absolute sensitivity of about 10^{-3} counts per atom (one pure uranium oxide particle with a diameter of 1 µm weighs about 4 pg and consists of approximately 10^{10} atoms). The measured ratio U^{235}/U^{238} was also more precise, as it is shown in figure 20 for the measurement of one particle, but the ratio was still higher at the beginning of the ablation process.
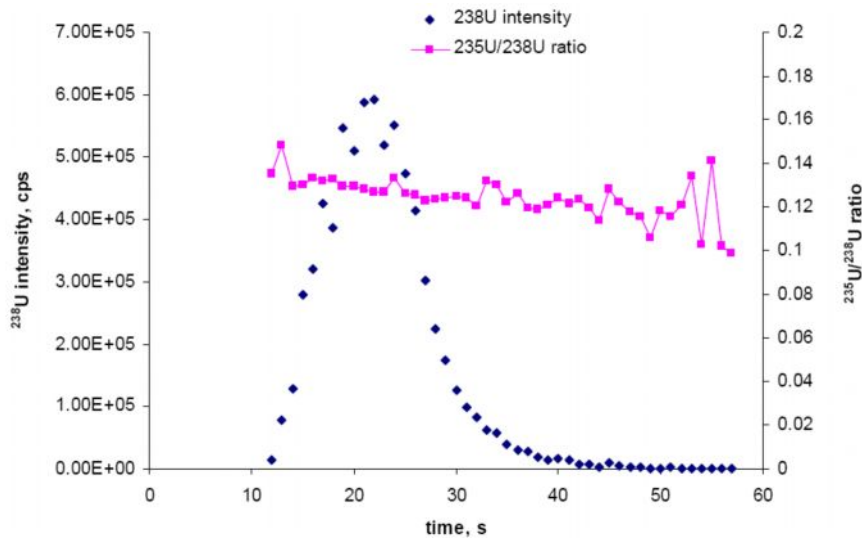
Figure 20. Intensity of ^{238}U and ^{235}U/^{238}U ratio versus ablation time from a particle on the silicon planchet.

In some cases the analysis of one particle took up to several minutes, probably because some of the uranium oxide was mixed with the Si melt during ablation, therefore a longer time was needed to remove all the U of one particle. An example was the ablation of particle nr. 227b, the course of the measurement is represented in figure 21.
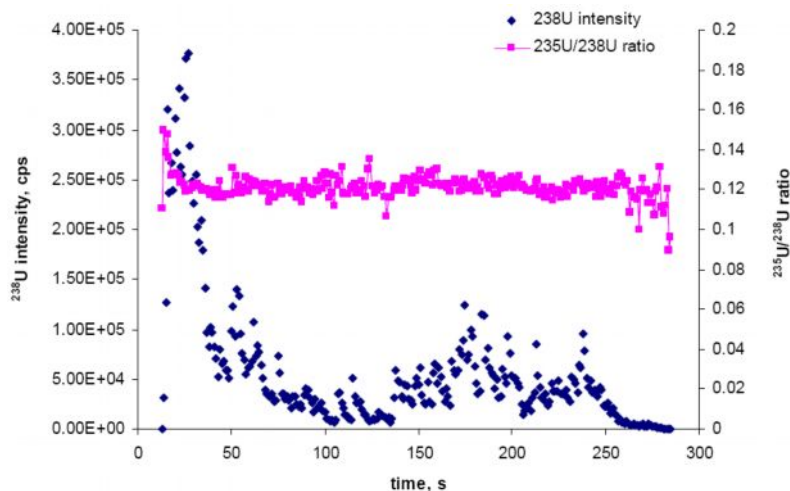
Figure 21. Intensity of ^{238}U and ^{235}U/^{238}U ratio versus ablation time from particle nr. 227b on the silicon planchet.

During the optimization of the laser parameter different spot sizes and also different values for laser energy were tested. Thereby it was observed that the laser beam profile was not homogeneous, so that an ablation spot with reduced energy (15% instead of 20% output) also revealed a smaller spot size (figure 22).

Spot sizes smaller than 20 µm had the effect to remove particles from the ablated area.
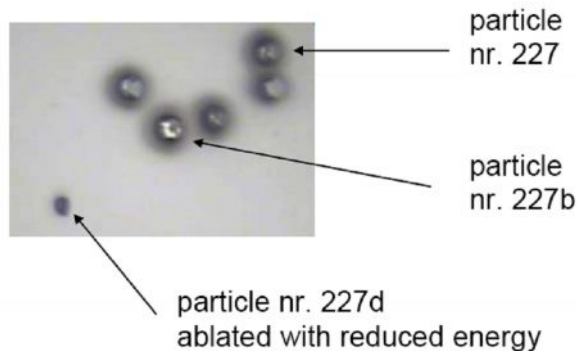
Figure 22.   Ablation spots produced by laser beams with 20% and 15% output, respectively.

The measured $^{235}U/^{238}U$ ratios of 56 individual particles on the silicon wafer in comparison to the certified values of U-100 and U-020 are plotted in figure 23, revealing a poor accuracy for the performed measurements. During the measurements spikes in the isotopic ratios occurred at the same time with spikes in intensity (figure 24). The probable reason is an overload of the ion counter IC0 with $^{238}U^+$ ions deriving from the aerosol after the ablation of a larger particle.
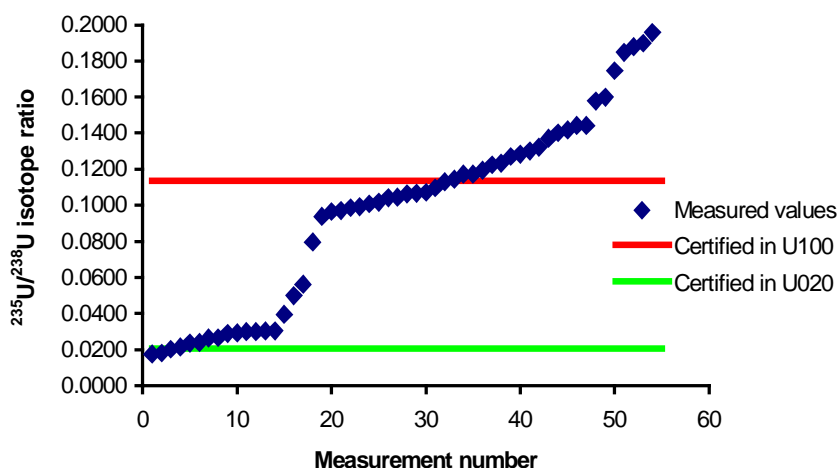
Figure 23.   Measured $^{235}U/^{238}U$ ratios for particles on the silicon wafer in comparison to the certified values.
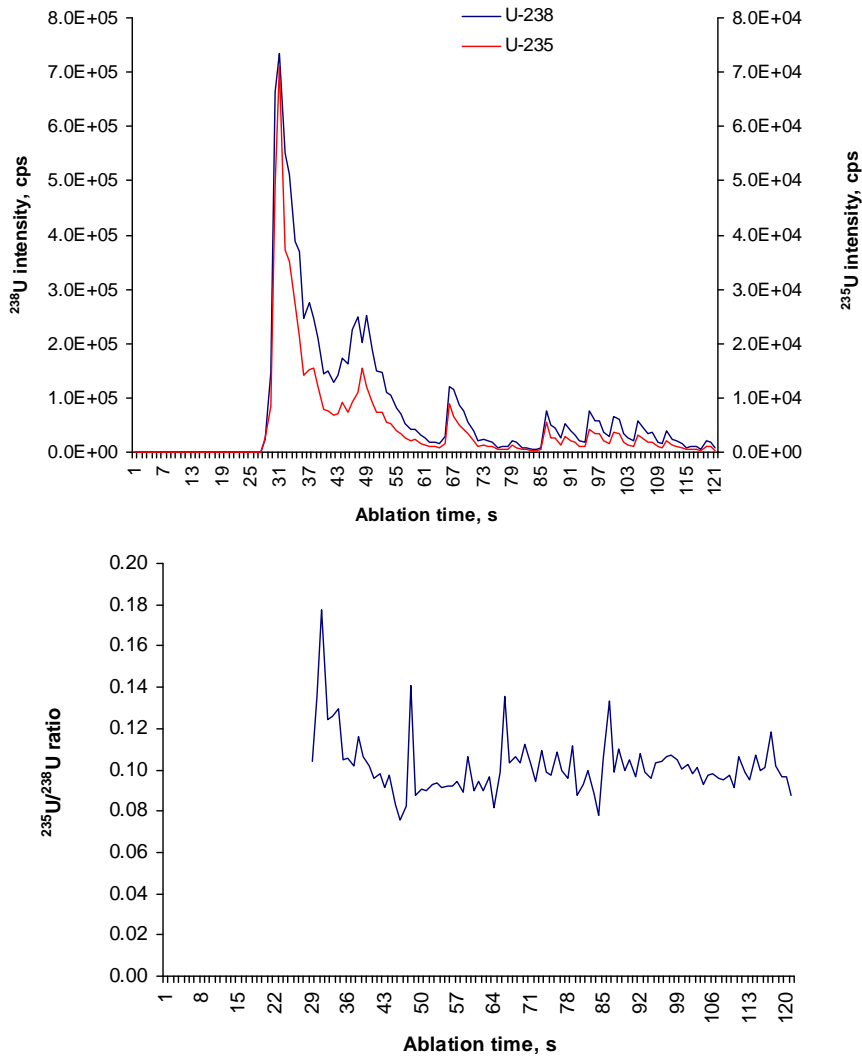
Figure 24. Spikes in a) the intensity of the measured isotopes ^{238}U and ^{235}U and b) the ratio ^{235}U/^{238}U during the measurement of a particle on the silicon wafer.

The main problem was that particles were not affixed sufficiently and therefore they were ablated as 'packages', which led very often to a saturation of the ion counter measuring the higher abundant isotope. 10-12% of the particles could not be measured due to this problem.

The measurement of the ratio ^{236}U/^{235}U was performed on 53 particles on the silicon wafer. Figure 25 demonstrates that the ratios were significantly too high (especially in the case of the particles certified with 2% enrichment).
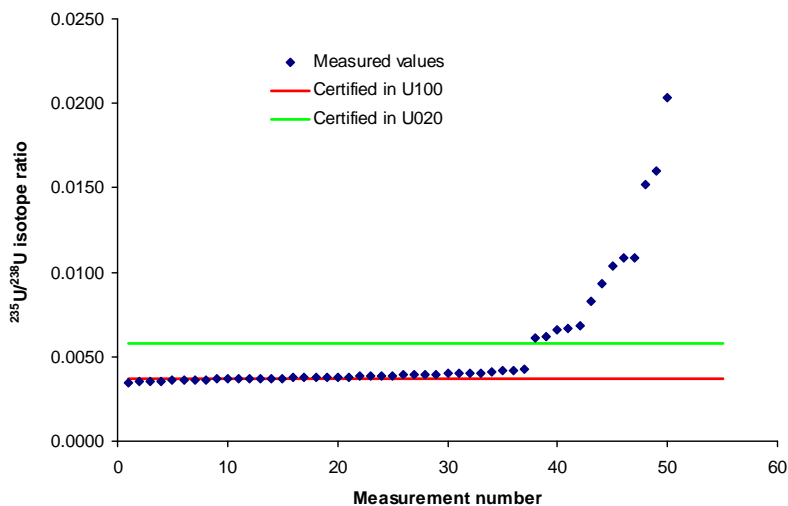
Figure 25. Measured ^{236}U/^{235}U ratios for particles on the silicon wafer in comparison to the certified values.

The highest count rate per particle was $2.2*10^6$, the average $5.2*10^5$.

Spikes of the measured ratio and the isotope intensities could be observed also during this analysis, particularly when the whole particle was ablated within a short period (an example is given in figure 26). It is possible to calculate the isotopic ratios neglecting the spiked areas, but then a loss of sensitivity and precision is the consequence.
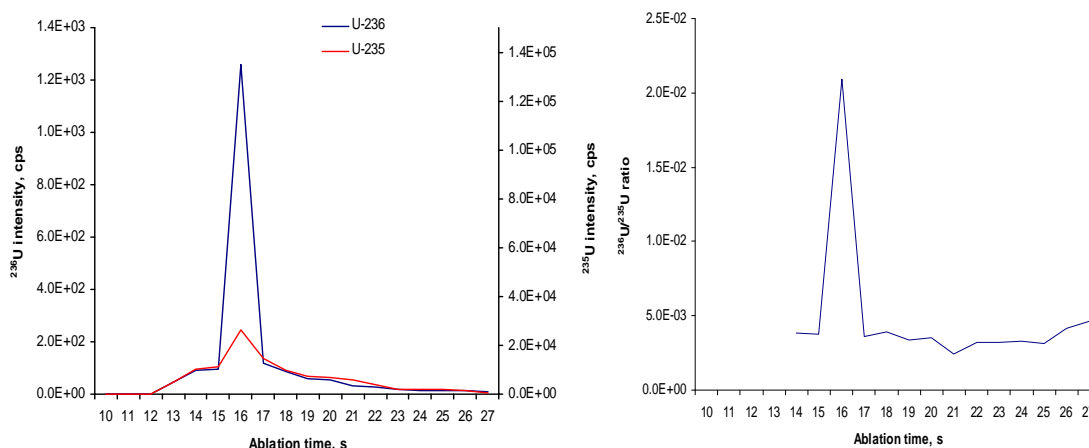
Figure 26. Spikes in a) the intensity of the measured isotopes ^{236}U and ^{235}U and b) the ratio ^{236}U/^{235}U during the measurement of a particle on the silicon wafer.

Within the ^{235}U/^{238}U ratio measurements the main problem was that the sensitivity of ^{238}U proved to be too high in comparison to the minor isotope. Therefore it was tried to reduce the sensitivity by changing the voltage of the central deflector. This was unsuccessful, since the signal thus obtained turned out to be unstable.

In another approach the high abundant isotope ^{238}U was directed into the faraday cup L2. This setting has the additional advantage that not only ^{235}U (detected with IC0), but also ^{234}U

(detected with IC1) can be measured simultanously and therefore both ratios $^{235}U/^{238}U$ and $^{234}U/^{238}U$ are obtained.

The measurements resulted in lower isotopic ratios than the certified values for both ratios (figure 27). Lower ratios were obtained, because when a particle was ablated within a short time and the impact of $^{235}U^+$ and $^{234}U^+$ species on the ion counters is too high, it leads to a detector saturation, while the less sensitive faraday cup is still able to handle the $^{238}U^+$ ions. Again, significant spikes in the ratios were observed. This time a great drop of the according ratio (figure 28) and a sharp peak of the ^{238}U intensity measured by the faraday cup were the consequence. About 15% of the measurements showed similar behaviour.
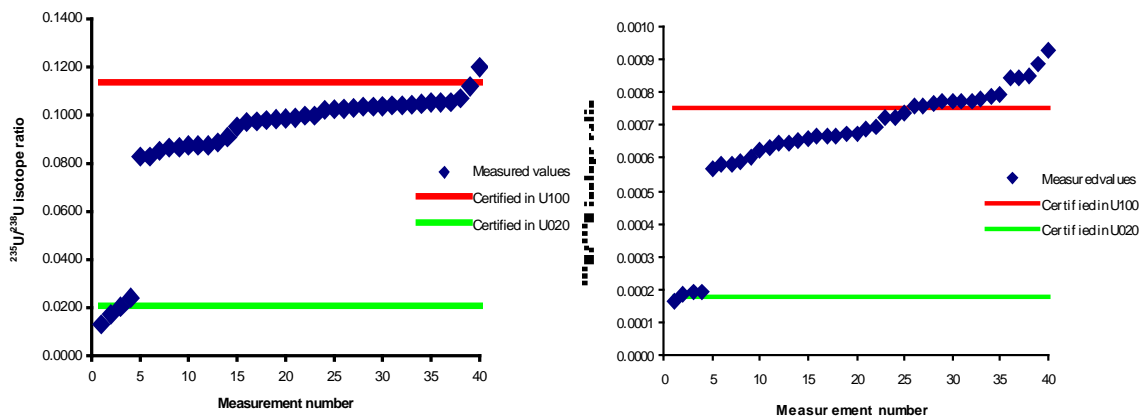
Figure 27.   Measured a) $^{235}U/^{238}U$ and b) $^{234}U/^{238}U$ ratios for particles on the silicon wafer in comparison to the certified values. In this setting ^{238}U was detected by the faraday cup L2.
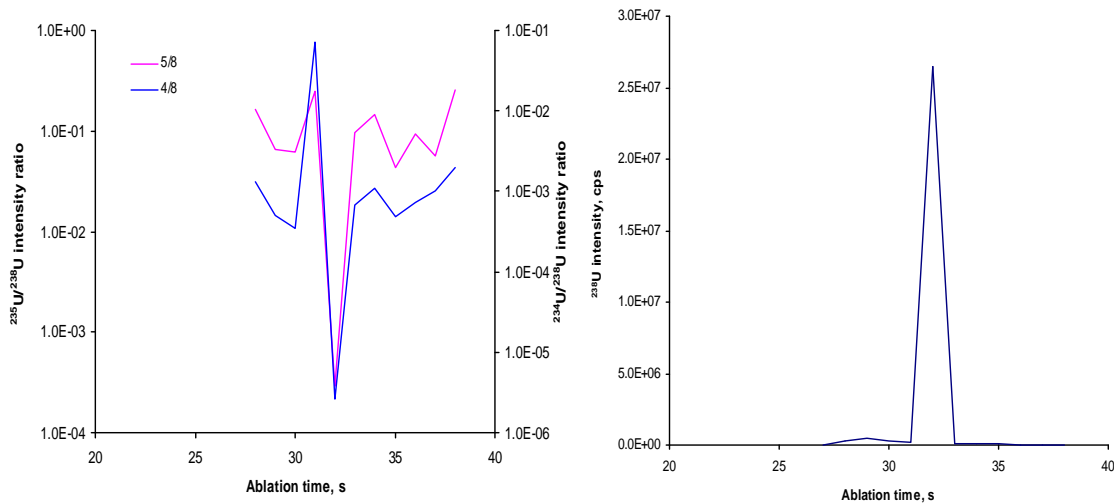
Figure 28.   Intensity for a) the ratios $^{235}U/^{238}U$ and $^{234}U/^{238}U$ and b) ^{238}U during the measurement of a fast ablated particle on the silicon wafer. In this setting ^{238}U was detected by the faraday cup L2.

4.3.2 Raster scan analysis

Raster scan analysis was performed for both silicon wafer and CA filter. Figure 29 clearly indicates that particles are removed during such a scan on the silicon planchet. The result of the ablation of this area is shown in figure 30.
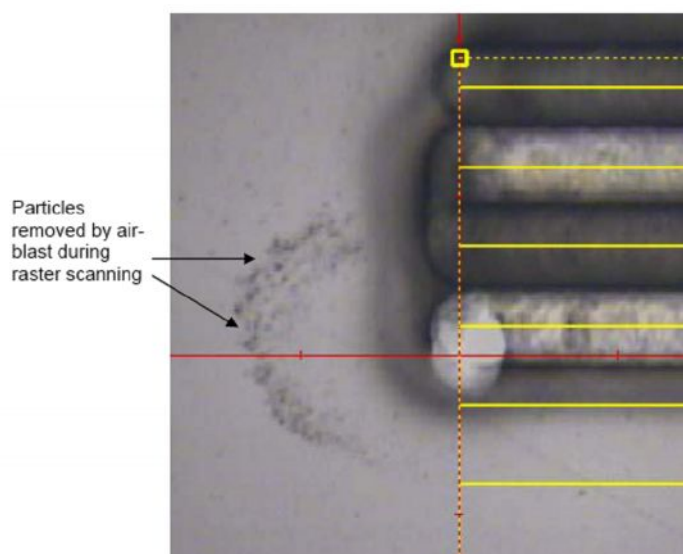
Figure 29. Dislodged particles during raster scan analysis on the silicon wafer.
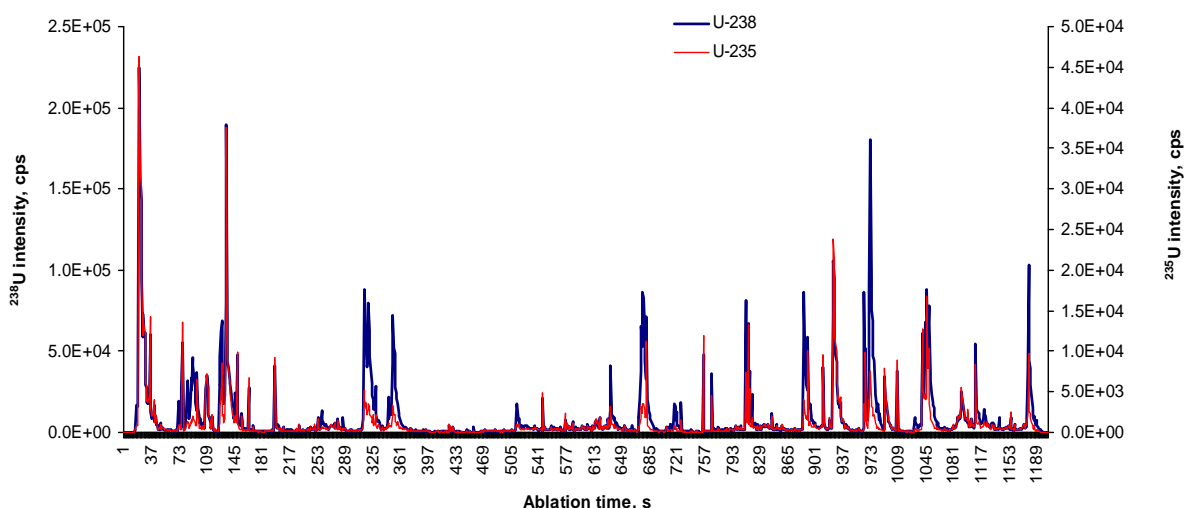
Figure 30. Intensities of ^{235}U and ^{238}U received during ablation of the raster scan area on the silicon target.

This figure indicates a high variation in isotopic ratios, a rather low sensitivity and implies that different particles were mixed during the ablation process.

On cellulose acetate on the other hand the particles seem to be affixed firmlier. The results of a raster scan performed on CA with faraday cup and ion counter detection is shown in figure 31. An image of the area after ablation is given in figure 32. Intensities are higher by a factor of more than 10 and the individual particles can be distinguished easily.

Matrix effects depend on the surface, they are significantly higher on the silicon wafer than on the CA filter, because of various other elements occurring on the silicon backing, which can

67

lead to interferences. Carbon from the CA filter does not seem to cause the same interferences as observed during single spot analysis of graphite planchets. C signals should be measured to compare both backings for further investigation.
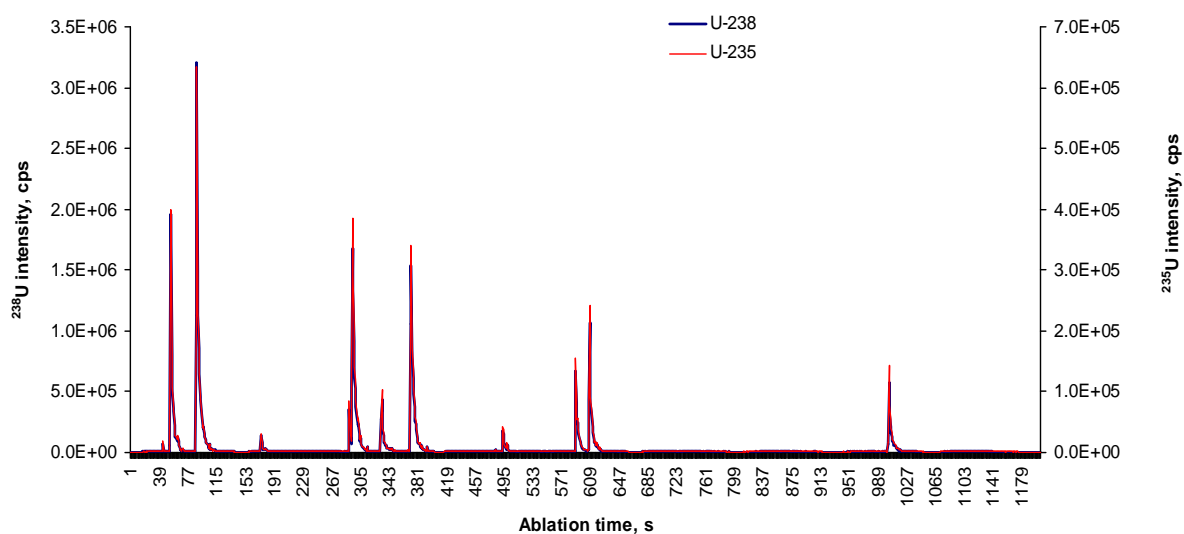
Figure 31. Intensities of ^{235}U and ^{238}U received during ablation of the raster scan area on the CA target.
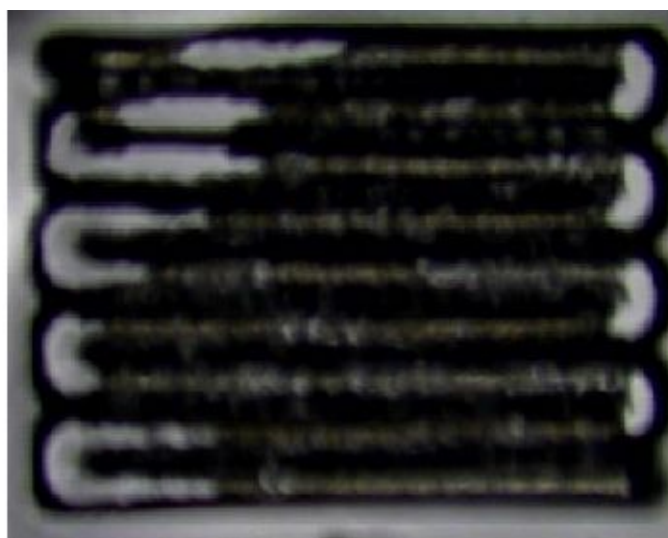
Figure 32. Ablated area of the CA target after raster scan analysis.

However, it was observed that the particles were partially dissolved by the methanol leading to a background of ^{235}U and ^{238}U intensities of 10^3 cps and 10^4 cps, respectively.

The main problem of this method is the appropriate fixing of the particles to avoid ablation in form of large packages, overburdening the ion counting multipliers and leading to wrong values at the peak maxima.

Also the change in LA parameter (different spot sizes as well as different values for the laser output were tested) did not lead to an ablation process in layers.

5 Summary and Conclusion

The investigation of human tissues could be accomplished successfully. Nonetheless, neither hair nor urine samples of the Kosovo soldier revealed remarkable uranium amounts. However, for more accurate determination of U in urine the sample preparation (especially with regard to the method blanks) should be improved. Also the variation of natural dilution of urine should be taken into account by normalization to creatinine.

In case of detection of high amounts of U it is indicated to measure isotopic ratios in addition for the determination of the source of contamination. The occurrence of natural uranium is a significant bias for the estimation of the amount of DU. Uranium is an ubiquitous element in natural environment contrary to man-made actinides like plutonium or americium and is therefore often found in humans at elevated concentrations as a result of consumption of particular mineral waters or ground water (concentrations of uranium of up to 100 ng mL^{-1} can be observed in urine of persons drinking particular mineral waters as well as in urine of e.g. inhabitants of South Korea consuming local ground water). Therefore, it is difficult to detect contamination with DU, because of the significant variations in natural background. Additional analytical problem is caused by presence of natural uranium in chemicals (acids) used for sample preparation.

Isotopic ratio measurements of U are performed preferably with multi-collector sector-field mass spectrometers.

Hair is usually a better bioindicator for past contamination of the individual with heavy metals such as U. In addition the application of LA simplifies sample preparation and offers the possibility of spatially resolved analysis. This leads to time resolved information in the example of hair. The method is limited by the more complex quantification strategies.

The determination of DU as man-made introduction of specific isotopic signatures is of importance for tracing, for e.g. in forensic sciences, but also for the evaluation of the health risk posed by the military employment of DU. The latter is a very controversial issue not only regarding the medical aspects, but also the political disputes about the 'peaceful' use of nuclear energy in context with the reutilization of nuclear waste materials.

Although it is appreciated in many publications [Bleise et al. 2003, McLaughlin 2005] that the health risk for populations in DU contaminated regions is neglectible.even thoug the long term consequences such as the possibility of increased amounts of cancer cases are not yet to be judged. Therefore long term studies are of great importance, a problem comparable to Chernobyl NPP accident.

The human thyroids from the rural areas of Belarus revealed higher lead concentrations than the samples from Minsk, although Pb contamination is usually higher in cities than at the countryside. Cancerous samples revealed the highest amount of Pb, but a lower amount of U than Minsk samples. In general Pb concentrations were significantly higher than the ones observed from U. As a consequence the isotopic analysis of Pb is more informative in these samples.

The lead used during Chernobyl NPP accident was probably collected from different sources. This can be recognized, when the soil samples collected in the vicinity from Chernobyl (KRA, RAD and MAS) were compared to an average of major production sites of former USSR. Thyroid samples from residents of Homel revealed delta values which were closer to the soil samples from the Chernobyl vicinity and therefore could be distinguished from samples from Minsk and tumor samples. However, uncertainty of the measured lead isotope ratio in soil samples was relatively large due to matrix effects, which have to be investigated in more detail.

The method used in this work for the determination of Pb isotopes can be improved for future applications: either by the advancement of the HG system or by a matrix separation prior to the analysis like for e.g. U-Pb-column-chemistry routinely employed in geology.

Further strategies for improving hydride generation for lead include the use of different oxidants (such as sodium persulfate) and acids. Another parameter influencing the plumbane generation is the reaction time and connected with that the length of the sample loop and the corresponding flow rates. Also more investigations should be adressed to the behavior of plumbane.

Although many methods have been developed by now, thereis still need for improvement. A large number of samples with complex matrices could be analysed without or with reduced interferences and the sample preparation procedures would be simplified when applying a well working Pb-hydride generation system.

The work on particle measurements revealed the potential of single particle analysis by LA-MC-ICP-MS. Becker et al. 2008 analysed 10 single uranium oxide particles of about 1 μm diameter by LA-ICP-SF-MS with a single collector instrument (ELEMENT, Thermo Electron GmbH, Bremen, Germany) on a filter area of 3 mm * 3 mm by imaging mass spectrometry. In that work only an average isotope ratio of $^{235}U/^{238}U$ was obtained demonstrating an enrichment of ^{235}U. However, the applied technique did not allow determining isotope ratios

of U isotopes in single particles. The determination of minor isotopes like ^{234}U and ^{236}U is even more difficult. No data were reported in that work. Thus, Becker et al. 2008 stress the analytical challenge arising from the up-to-date requirements of nuclear forensics.

In the present work it was proven that isotopic ratios of ^{235}U/^{238}U, ^{236}U/^{235}U and ^{234}U/^{238}U in uranium oxide particles made of CRMs could be measured by LA-MC-ICP-MS. Nonetheless, accuracy and uncertainty require further improvement. The major problem was the fixation of the particles on the backing. The graphite planchet was unsuitable as underlay for measurements with LA-ICP-MS, since particles could not be spotted with the laser ablation system and the matrix produced interferences (most probable carbon cluster ions with masses up to actinide range) leading to a poor accuracy of the measurements. The situation on the silicon wafer was superior, but still unidentified interferences were observed and particles were not fixed sufficiently. The last approach, the analysis of particles on a CA filter, revealed the best fixation. Particles were not completely removed from their places even during raster scanning. However, the ablation could still not be performed in layers in order to avoid IC saturation after the impact of large amounts of ions leading to false values for isotopic ratios.

Possible solutions of this problem are (I) enlargement of the particles by vapor deposition or coating, (II) sintering or (III) sputtering of the wafer with gold for a better fixation, (IV) solubilization of the particles with acid or (V) destruction of the ablated particles by e.g. preceding microwave induced plasma (MIP).

A potential experimental set up of the latter combined to an optical emmission spectrometer (OES) is shown in figure 33.
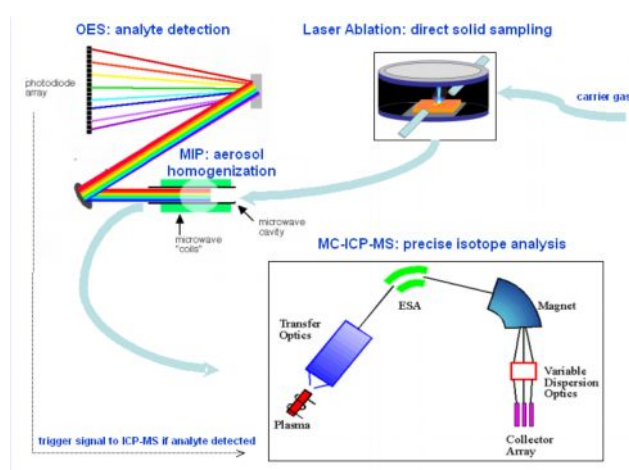
Figure 33.   Experimental setup for improved particle analysis with OES-MIP-LA-ICP-MS [Boulyga 2007b].

In addition, if particle measurements are performed by scanning a larger surface, an ablation cell could be employed similar to the one used by Feldmann et al. 2006 for blot membrane analysis (figure 34).
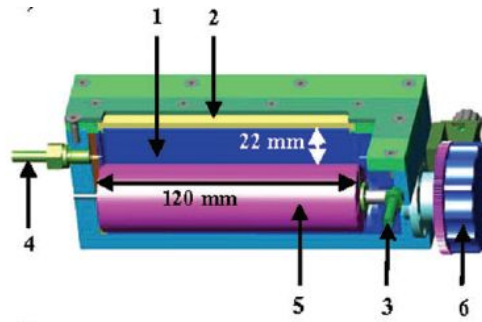
Figure 34. An ablation cell for the measurement of a whole blot membrane (1: PTFE insert, 2: quartz window, 3: gas inlet, 4: gas outlet, 5: membrane holder, 6: rotary knob) [Feldmann et al. 2006].

Another favourable issue for particle measurements would be a modified arrangement of the collector block in order to detect ^{235}U, ^{236}U and ^{238}U simultanously with the three ion counters (figure 35).
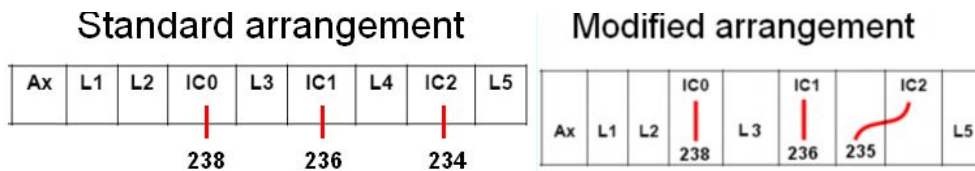
Figure 35. Collector block in a) the standard arrangement and b) the modified arrangement for U isotope measurements [Boulyga 2007b].

Summing up, the work comprise the challenging potential of a range of ICP-MS systems for quantitative (ICP-Q-MS, ICP-SF-MS) or isotope ratio (ICP-SF-MS, MC-ICP-SF-MS) analysis in nuclear forensics. In addition, the advantages of liquid introduction for bulk analysis, the advantage of hydride generation for matrix separation and laser ablation for single particle analysis could be evaluated successfully. Therefore, this work gives a unique overview of the assessment of a variety of ICP-MS instruments combined with different sample introduction systems in nuclear research.

6 Bibliographies

Agarande, M., Benzoubir, S., Neiva-Marques, A.M., Bouisset, P., 2003. Sector field inductively coupled plasma mass spectrometry, another tool for plutonium isotopes and plutonium isotope ratios determination in environmental matrices. Journal of Environmental Radioactivity 72, 169–176.

Alcaraz-Pelegrina, J. M., Martinez-Aguirre, A., 2007. U/Th dating of carbonate deposits from Constantina (Sevilla), Spain. Applied Radiation and Isotopes 65 (7), 798-804.

Arbuthnot, F., Bertell, R., Bristow, R., Diehl, P., Fahey, D., Keur, H. van der, Robicheau, D., 1999. Depleted Uranium – A post-war disaster for environment and health. Brochure from Laka Foundation, documentation and research center on nuclear energy, Ketelhuisplein 43, 1054 RD Amsterdam (The Netherlands).

Barth, S., 1998. Application of boron isotopes for tracing sources of anthropogenic contamination in groundwater. Water Research 32, 685-690.

Becker, J.S., 2003. Mass spectrometry of long-lived radionuclides. Spectrochimica Acta Part B 58, 1757-1784.

Becker, J.S., 2005. Inductively coupled plasma mass spectrometry (ICP-MS) and laser ablation ICP-MS for isotope analysis of long-lived radionuclides. International Journal of Mass Spectrometry 242, 183-195.

Becker, J.S., Sela, H., Dobrowolska, J., Zoriy, M., Becker, J.S., 2008. Recent applications on isotope ratio measurements by ICP-MS and LA-ICP-MS on biological samples and single particles. International Journal of Mass Spectrometry 270, 1-7.

Begichev, S.N., Borovoj, A.A., Burlakov, E.V., Gagarinsky, A.J., Demin, V.F., Khrulev, A.A., Khodakovsky, I.L., 1989. Radioactive Releases Due to the Chernobyl Accident. Presentation at International Seminar on Fission Product Transport Processes in Reactor Accidents, Dubrovnik (Croatia), May 1989.

Benincasa, C., Lewis, J., Perri, E., Sindona, G., Tagarelli, A., 2007. Determination of trace element in Italian virgin olive oils and their characterization according to geographical origin by statistical analysis. Analytica Chimica Acta 585 (2) 366-370.

Bentley, R.A., 2006. Strontium Isotopes from the Earth to the Archaeological Skeleton: A Review. Journal of Archaeological Method and Theory 13 (3), 135-187.

Betti, M., 2003. Civil use of depleted uranium. Journal of Environmental Radioactivity 64, 113-119.

Betti, M., 2005. Isotope ratio measurements by secondary ion mass spectrometry (SIMS) and glow discharge mass spectrometry (GDMS). International Journal of Mass Spectrometry 242, 169–182.

Betti, M., Tamborini, G., Koch, L., 1999. Use of Secondary Ion Mass Spectrometry in Nuclear Forensic Analysis for the Charakterization of Plutonium and Highly Enriched Uranium Particles. Analytical Chemistry 71, 2616-2622.

Beyer, D., Biehl, R., Pilwat, G., 1993. Normal concentration of uranium in urine. Health Physics 64 (3), 321.

Binder, H.H., 1999. Lexikon der chemischen Elemente. S. Hirzel Verlag, Stuttgart, Leipzig (Germany).

Bleise, A., Danesi, P.R., Burkart, W., 2003. Properties, use and health effects of depleted uranium (DU): a general overview. Journal of Environmental Radioactivity 64, 93-112.

Bollhöfer, A.,Rosman, K. J. R., 2001. Isotopic source signatures for atmospheric lead: The Northern Hemisphere. Geochimica et Cosmochimica Acta 65 (11), 1727-1740.

Bollhöfer, A.,Rosman, K. J. R., 2002. The temporal stability in lead isotopic signatures at selected sites in the Southern and Northern Hemispheres. Geochimica et Cosmochimica Acta 66 (8), 1375–1386.

Boulyga, S.F., 2007a. Advanced analytical techniques for elemental trace and isotope analysis (lecture slides). University of Natural Resources and Applied Life Sciences, Vienna (Austria).

Boulyga, S.F., 2007b. Performance of laser ablation inductively coupled plasma mass spectrometry (LA-ICP-MS) for actinide isotopic analysis in particles. Technical Meeting on Particle Analysis, IAEA, Vienna (Austria), 12-16. November 2007.

Boulyga, S.F., Becker, J.S., Malenchenko, A.F., Dietze, H.-J., 2000. Application of ICP-MS for Multielement Analysis in Small Sample Amounts of Pathological Thyroid Tissue. Microchimica Acta 134, 215-222.

Boulyga, S.F., Desideri, D., Meli, M.A., Testa, C., Becker, J.S., 2003. Plutonium and americium determination in mosses by laser ablation ICP-MS combined with isotope dilution technique. International Journal of Mass Spectrometry 226, 329-339.

Boulyga, S.F., Heumann, K.G., 2006. Determination of extremely low 236U/238U isotope ratios in environmental samples by sector-field inductively coupled plasma mass spectrometry using high-efficiency sample introduction. Journal of Environmental Radioactivity 88, 1-10.

Boulyga, S.F., Prohaska, T., 2008. Determining the isotopic compositions of uranium and fission products in radioactive environmental microsamples using laser ablation ICP–MS with multiple ion counters. Analytical and Bioanalytical Chemistry 390 (2), 531-539.

Brännvall, M.L, Bindler, R., Emteryd, O., Renberg, I., 2000. Four thousand years of atmospheric lead pollution in northern Europe: a summary from Swedish lake sediments. Journal of Paleolimnology 25, 421–435.

Buchmann, J. H., Sarkis, J. E. S., Rodrigues, C., 2003. Environmental monitoring used to identify nuclear signatures. Journal of Radioanalytical and Nuclear Chemistry 258 (1), 139-142.

Buzon, M.R., Simonetti, A., Creaser, R.A., 2007. Migration in the Nile Valley during the New Kingdom period: preliminary strontium isotope study. Journal of Archaeological Science 34, 1391-1401.

Cankur, O., Korkmaz, D., Ataman, O.Y., 2005. Flow injection-hydride generation-infrared spectrophotometric determination of Pb. Talanta 66, 789–793.

Carbol, P., Solatie, D., Erdmann, N., Nylén, T., Betti, M., 2003. Deposition and distribution of Chernobyl fallout fission products and actinides in a Russian soil profile. Journal of Environmental Radioactivity 68, 27–46.

Cetac 2007. Overview brochure. HGX-200 Hydride Generation & Cold Vapor System: http://www.cetac.com/nebulizers/hgx_200.asp

Chen, S., Zhang, S., Yu, H., Liu, W., Sun, M., 2002. Determination of trace lead by hydride generation-inductively coupled plasma-mass spectrometry. Analytica Chimica Acta 463, 177–188.

Ciurapinski, A., Parus, J., Donohue, D., 2000. Particle analysis for a strengthened safeguards system: Use of a scanning electron microscope equipped with EDXRF and WDXRF spectrometers. Journal of Radioanalytical and Nuclear Chemistry 251 (3), 345–352.

Crittenden, R.G., Andrew, A.S., LeFournour, M., Young, M.D., Middleton, H., Stockmann, R., 2007. Determining the geographic origin of milk in Australasia using multi-element stable isotope analysis. International Diary Journal 17, 421-428.

Dang, H.S., Pullat, V.R., Pillai, K.C., 1992. Determining the normal concentration of uranium in urine and application of the data to its biokinetics. Health Physics 62, 562-566.

Donohue, D.L., 1998. Strengthening IAEA safeguards through environmental sampling and analysis. Journal of Alloys and Compounds 271–273, 11–18.

Donohue, D.L., 2002. Strengthened Nuclear Safeguards. Analytical Chemistry 74, 28A-35A

Erdmann, N., Betti, M., Stetzer, O., Tamborini, G., Kratz, J.V., Trautmann, N., Van Geel, J., 2000. Production of monodisperse uranium oxide particles and their characterization by scanning electron microscopy and secondary ion mass spectrometry. Spectrochimica Acta Part B 55, 1565-1575.

Ezzo, J.A., Johnson, C.M., Price, T.D., 1997. Analytical perspective on prehistoric migration: A case study from east-central Arizona. Journal of Archaeological Science 24, 447–466.

Feldmann, I., Koehler, C.U., Roos, P.H., Jakubowski, N., 2006. Optimisation of a laser ablation cell for detection of hetero-elements in proteins blotted onto membranes by use of inductively coupled plasma mass spectrometry. Journal of Analytical Atomic Spectrometry 21, 1006-1015.

Fisenne, I.M., Perry, P.M., Harley, N.H., 1988. Uranium in Humans. Radiation Protection Dosimetry 24, 127-131.

Garger, E.K., Kashpur, V., Belov, G., Demchuk, V., Tschiersch, J., Wagenpfeil, F., Paretzke, H.G., Besnus, F., Holländer, W., Martinez-Serrano, J., Vintersved, I., 1997-1998. Measurement of resuspended aerosol in the Chernobyl area. Part I, II and III. Radiation and Environmental Biophysics 36-37, 139-148, 275-283, 201-208.

Gerdes, A., Zeh, A., 2006. Combined U–Pb and Hf isotope LA-(MC-)ICP-MS analyses of detrital zircons: Comparison with SHRIMP and new constraints for the provenance and age of an Armorican metasediment in Central Germany. Earth and Planetary Science Letters 249, 47–61.

Hatch, M., Ron, E., Bouville, A., Zablotska, L., Howe, G., 2005. The Chernobyl Disaster: Cancer following the Accident at the Chernobyl Nuclear Power Plant. Epidemiologic Reviews 27, 56–66.

Hill, S.J., 1999. Inductively Coupled Plasma Spectrometry and its Applications.Sheffield Academic Press, Sheffield (UK).

Hoffman, D.C., Lawrence, F.O., Mewherter, J.L., Rourke, F.M., 1971. Detection of plutonium-244 in nature. Nature, London 234, 132-134.

Hogan, J. F., Blum, J.D., 2003. Boron and lithium isotopes as groundwater tracers: a study at the Fresh Kills Landfill, Staten Island, New York, USA. Applied Geochemistry 18, 615-627.

Hoppe, K.A., Koch, P.L., 2007. Reconstructing the migration patterns of late Pleistocene mammals from northern Florida, USA. Quaternary Research 68, 347–352.

Horn, P., Michler, G., Todt, W., 1987. Die anthropogene Bleibelastung im Raum München, ermittelt aus Pb-Isotopenmessungen von Wasser- und Sedimentproben. Mitteilungen Geographischer Gesellschaft München 72.

Ivanov, V.K., Tsyb, A.F., Gorsky, A. I., Maksyutov, M. A., Rastopchin, E. M., Konogorov, A. P., Korelo, A.M., Biryukov, A. P., Matyash, V.A., 1997. Leukaemia and thyroid cancer in emergency workers of the Chernobyl accident: estimation of radiation risks (1986–1995). Radiation and Environmental Biophysics 36, 9–16.

Jung, S., Hellebrand, E., 2007. Textural, geochronological and chemical constraints from polygenetic titanite and monogenetic apatite from a mid-crustal shear zone: An integrated EPMA, SIMS, and TIMS study. Chemical Geology 241, 88–107.

Juul-Pedersen, A., Frei, R., Appel, P.W.U., Persson, M.F., Konnerup-Madsen, J., 2007. A shear zone related greenstone belt hosted gold mineralization in the Archean of West Greenland. A petrographic and combined Pb–Pb and Rb–Sr geochronological study. Ore Geology Reviews 32, 20–36.

Kashparov, V.A., Ivanov, Y.A., Zvarich, S.I., Protsak, V.P., Khomutinin, Y.V., Polyakov, V.D., Gudkov, A.N., Kurepin, A.D., Pazukhin, É.M., 1994. Model of Hot Particle Formation during the Chernobyl Acident. Radiochemistry 36 (1), 98-104.

Kashparov, V.A., Lundin, S.M., Zvarych, S.I., Yoshchenko, V.I., Levchuk, S.E., Khomutinin, Y.V., Maloshtan, I.M., Protsak, V.P., 2003. Territory contamination with the radionuclides representing the fuel component of Chernobyl fallout. The Science of the Total Environment 317, 105–119.

Kelley, J.M.,Bond, L.A., Beasley, T.M., 1999. Global distribution of Pu isotopes and 237Np. The Science of the Total Environment 237/238, 483-500.

Lariviere, D., Taylor, V.F., Evans, R.D., Cornett, R.J., 2006. Radionuclide determination in environmental samples by inductively coupled plasma mass spectrometry. Spectrochimica Acta Part B 61, 877–904.

Lee, M.H., Park, Y.J., Jee, K.Y., Kim, W.H., Clark, S.B., 2007. Study of an alpha track analysis and a fission track analysis for determining the hot particles contaminated with Pu and U isotopes. Applied Radiation and Isotopes 65, 85–91.

Lieser, K. H. (Hrsg.), 1997. Nuclear and Radiochemistry- Fundamentals and Applications. VHC Verlagsgesellschaft mbH., Weinheim (Germany).

Likhtariov, I.A., Repin, V.S., Bondarenko, O.A., Nechaev, S.J., 1995. Radiological Effects after Inhalation of highly radioactive Fuel Particles Produced by the Chernobyl Accident. Radiation Protection Dosimetry 59 (4), 247-254.

Lind, O.C., Salbu, B., Janssens, K., Proost, K., García-León, M., García-Tenorio, R., 2007. Characterization of U/Pu particles originating from the nuclear weapon accidents at Palomares, Spain, 1966 and Thule, Greenland, 1968. Science of the Total Environment 376, 294–305.

Mayer, K., Wallenius, M., Fanghänel, T., 2007. Nuclear forensic science – From cradle to maturity. Journal of Alloys and Compounds 444-445, 50-56.

McDiarmid, M.A., Keogh, J.P., Hooper, F.J., McPhaul, K., Squibb, K., Kane, R., DiPino, R., Kabat, M., Kaup, B., Anderson, L., Hoover, D., Brown, L., Hamilton, M., Jacobson-Kram, D., Burrows, B., Walsh, M., 2000. Health Effects of Depleted Uranium on Exposed Gulf War Veterans. Environmental Research Section A 82, 168-180.

McLaughlin, J.P., 2005. Public health and environmental aspects of DU. International Congress Series 1276, 137-140.

Medley, D.W., Kathren, R.L., Miller, A.G., 1995. Diurnal urinary volume and uranium output in uranium workers and unexposed controls. Health Physics 68 (5), 732-733.

Milačić, S., Petrović, D., Jovičić, D., Kovačević, R., Simić, J., 2004. Examination of the health status of populations from depleted-uranium-contaminated regions. Environmental Research 95, 2-10.

Milestone Acid Digestion Cookbook. Report Code 291. Update 1/1/1996.

Miralles, J., Véron, A.J., Radakovitch, O., Deschamps, P., Tremblay, T., Hamelin, B., 2006. Atmospheric lead fallout over the last century recorded in Gulf of Lions sediments (Mediterranean Sea). Marine Pollution Bulletin 52, 1364–1371.

Montaser, A., 1998. Inductively Coupled Plasma Mass Spectrometry. Wiley-VCH, New York (USA).

Møller, A.P., Mousseau, T.A., 2006. Biological consequences of Chernobyl: 20 years on., Trends in ecology and evolution 21 (4), 200-207.

Mukai, H., Machida, T., Tanaka, A., Vera, Y.P., Uematsu, M., 2001. Lead isotope ratios in the urban air of eastern and central Russia. Atmospheric Environment 35, 2783-2793.

National Council on Radiation Protection and Measurements, 1999. Biological Effects and Exposure Limits for 'Hot Particles'. NCRP-Report 130.

Nelms, S.M., 2005. Inductively Coupled Plasma Mass Spectrometry Handbook. Blackwell Publishing, Oxford (UK).

Nelms, S.M., Quétel, C.R., Prohaska, T., Vogel, J., Taylor, P.D.P., 2001. Evaluation of detector dead time calculation models for ICP-MS. Journal of Analytical Atomic Spectrometry 16, 333-338.

Neuburger, A., 1921. Die Technik des Altertums (2. Auflage). R. Voigtländersverlag, Leipzig (Germany).

New Wave Research, 2005. Product description of UP193 Solid-State: http://www.new-wave.com/1nwrProducts/UP193SS.htm

Nu Instruments, 2005. DSN Operators Manual V1.5, 3.

Nu Instruments, 2005a. NP Manual V2, 5; 8;

Nu Instruments, 2005b. NP High Resolution.

Oeh, U., Priest, N.D., Roth, P., Ragnarsdottir, K.V., Li, W.B., Höllriegl, V., Thirlwall, M.F., Michalke, B., Giussani, A., Schramel, P., Paretzke, H.G., 2007. Measurements of daily urinary uranium excretion in German peacekeeping personnel and residents of the Kosovo region to assess potential intakes of depleted uranium (DU). Science of the Total Environment 381, 77–87.

Orloff, K.G., Mistry, K., Charp, P., Metcalf, S., Marino,R., Shelley, T., Melaro, E., Donohoe, A.M., Jonesc, R.L., 2004. Human exposure to uranium in groundwater. Environmental Research 94, 319–326.

Parrish, R.R., Horstwood, M., Arnasonc, J.G., Cheneryd, S., Brewera, T., Lloyda, N.S., Carpentere, D.O., 2008. Depleted uranium contamination by inhalation exposure and its detection after ~20 years: Implications for human health assessment. Science of the total environment 390, 58-68.

Perelygin, V.P., Chuburkov, Y.T., 1997. Man-Made Plutonium in Environment – Possible Serious Hazard for Living Species. Radiation Measurements 28 (1-6), 385-392.

Peres, B., Barlet, N., Loiseau, G., Montet, D., 2007. Review of the current methods of analytical traceability allowing determination of the origin of foodstuffs. Food Control 18 (3), 228-235.

Petrov, P.K., Wibetoe, G., Tsalev, D.L., 2006. Comparison between hydride generation and nebulization for sample introduction for the determination of lead in plants and water samples by inductively coupled plasma mass spectrometry, using external calibration and isotope dilution. Spectrochimica Acta Part B 61, 50 – 57.

Pöllänen, R., Ketterer, M.E., Lehto, S., Hokkanen, M., Ikäheimonen, T.K., Siiskonen, T., Moring, M., Rubio Montero, M.P., Martín Sánchez, A., 2006. Multi-technique characterization of a nuclear bomb particle from the Palomares accident. Journal of Environmental Radioactivity 90, 15-28.

Preciado, H.F., Li, L.Y., Weis, D., 2007. Investigation of Past and Present Multi-metal Input along Two Highways of British Columbia, Canada, Using Lead Isotopic Signatures. Water, Air and Soil Pollution 184, 127-139.

Rosman, K.J.R., Taylor, P.D.P., 1998. Isotopic composition of the elements (Technical Report). Pure and Applied Chemistry 70 (1), 217-235.

Roth, P., Werner, E., Paretzke, H.G., 2001. A study of uranium excreted in urine - An assessment of protective measures taken by the German Army KFOR Contingent. Research report for the Federal Ministry of Defense, GSF report 3/01, GSF - National Research Center for Environment and Health, Institute of Radiation Protection, Neuherberg (Germany).

Rummel, S., Hölzl, S., Horn, P., 2007. Isotopensignaturen von Bio und Geo-Elementen in der Forensik. In Hermann, B., Saternus, K.-S. (Hrsg.). Biologische Spurenkunde, Band 1 Kriminalbiologie (pp 381-407). Springer-Verlag, Berlin Heidelberg (Germany).

Salbu, B., Krekling, T., Oughton, D.H., Østby, G., Kashparov, V.A., Brand, T.L., Day, J.P., 1994. Hot Particles in Accidental Releases From Chernobyl and Windscale Nuclear Installations. Analyst 119, 125-130.

Salt, C., Lennox, A.J., Takagaki, M., Maguire, J.A., Hosmane, N.S., 2004. Boron and gadolinium neutron capture therapy. Russian Chemical Bulletin, International Edition 53 (9), 1871-1888.

Schramel, P., Wendler, I., Roth, P., Werner, E., 1997. A method for the determination of Thorium and Uranium in urine samples by ICP-MS. Mikrochimica Acta 126, 263-266.

Sealy, J.C., Van Der Merwe, N.J., Sillen, A., Kruger, F.J., Krueger, W.H., 1991. $^{87}Sr/^{86}Sr$ as a dietary indicator in modern and archaeological bone. Journal of Archaeological Science 18, 399–416.

Sela, H., Karpas, Z., Zoriy, M., Pickhardt, C., Becker, J.S., 2007. Biomonitoring of hair samples by laser ablation inductively coupled plasma mass spectrometry (LA-ICP-MS). International Journal of Mass Spectrometry 261, 199-207.

Seltzer, M.D., 2003. Laser Ablation Inductively Coupled Plasma Mass Spectrometry Measurement of Isotope Ratios in Depleted Uranium Contaminated Soils. Applied Spectroscopy 57 (9), 1173-1177.

Simonetti, A., Heaman, L.M., Hartlaub, R.P., Creaser, R.A., MacHattie, T.G., Böhm, C., 2005. U–Pb zircon dating by laser ablation-MC-ICP-MS using a new multiple ion counting Faraday collector array. Journal of Analytical Atomic Spectrometry 20, 677–686.

Solatie, D., 2002. Development and Comparison of Analytical Methods for the Determination of Uranium and Plutonium in Spent Fuel and Environmental Samples. PhD Thesis, University of Helsinki (Finland).

Stetzer, B.O., 2001. Spaltspuranalyse von Uranoxidpartikeln. PhD Thesis, University of Mainz (Germany).

Swoboda, S., Brunner, M., Boulyga, S.F., Galler, P., Horacek, M., Prohaska, T., 2008. Identification of Marchfeld asparagus using Sr isotope ratio measurements by MC-ICP-MS. Analytical and Bioanalytical Chemistry 390 (2), 487-494.

Tamborini, G., Betti, M., Forcina V., Hiernaut, T., Giovannone, B., Koch, L., 1998. Application of secondary ion mass spectrometry to the identification of single particles of uranium and their isotopic measurement. Spectrochimica Acta Part B 53, 1289-1302.

Taylor, D.M., 1995. Environmental Plutonium in Humans. Applied Radiation and Isotopes 46 (11), 1245-1252.

Taylor, D.M., Taylor, S.K., 1997. Environmental uranium and human health. Reviews on Environmental Health 12, 147–57.

Taylor, H.J, Goldhaber, M., 1935. Detection of nuclear disintegration in a photographic emulsion. Nature, London 135, 341-248.

Thermo Electron GmbH, 2004. Product description of ELEMENT2: http://www.thermo.com/com/cda/product/detail/0,,11756,00.html?ca=element2

Tyson, J.F., Ellis, R.I., Carnrick, G., Fernandez, F., 2000. Flow injection hydride generation electrothermal absorbtion spectrometry with in-atomizer trappingfor the determination of lead in calcium supplements. Talanta 52, 403-410.

Uijt de Haag, P., Smetsers, R., Witlox, H., Krüs, H., Eisenga, A., 2000. Evaluating the risk from depleted uranium after the Boeing 747-258F crash in Amsterdam, 1992. Journal of Hazardous Materials 76, 39-58.

UNSCEAR. United Nations Scientific Committee on the Effects of Atomic Radiation, 1993. Report to the General Assembly with scientific annexes, New York (USA).

UNSCEAR. United Nations Scientific Committee on the Effects of Atomic Radiation, 2000. The 2000 report to the General Assembly with scientific annexes, New York (USA).

U.S. department of health and human services, 2007. Toxicological profile for lead. Public Health Service, Agency for Toxic Substances and Disease Registry, Atlanta (USA).

U.S. department of health and human services, 1999. Toxicological profile for uranium. Public Health Service, Agency for Toxic Substances and Disease Registry, Atlanta (USA).

USSR State Committee on the Utilization of Atomic Energy, 1986. The Accident at the Chernobyl NPP and its Consequences. Information compiled for the IAEA Post-Accident Review Meeting, Part I and II , Vienna (Austria), 25-29. August 1986.

Wallenius, M., Mayer, K., Ray, I., 2006. Nuclear forensic investigations: Two case studies. Forensic Science International 156, 55-62.

Williams, D., 2002. Cancer after nuclear fallout: lessons from the Chernobyl accident. Nature Reviews Cancer 2, 543–549.

World Health Organization, 2001. Depleted Uranium, Sources, Exposure and Health Effects. World Health Organziation. Department of Protection of the Human Environment, Geneva (Switzerland).

Yamada, M., Aono, T. 2006. U-238, Th isotopes, Pb-210 and Pu239+240 in settling particles on the continental margin of the East China Sea: Fluxes and particle transport processes. Marine Geology, 227, 1-12.

Zhao, X.L., Nadeau, M.J., Kilius, L.R., Litherland, A.E., 1994. The first detection of naturally-occurring ^{236}U with accelerator mass spectrometry. Nuclear Instruments and Methods in Physics Research Section B: Beam Interactions with Materials and Atoms 92 (1-4), 249-253.

Zheng, J., Yamada, M., 2006. Inductively coupled plasma-sector field mass spectrometry with a high-efficiency sample introduction system for the determination of Pu isotopes in settling particles at femtogram levels. Talanta 69, 1246-1253.

7 Appendix

7.1 List of Figures

7.2 List of Tables

7.3 Raw data

7.3.1 Elemental concentrations of Pb and U in thyroids and soil

Sample ID	Pb (µg g^{-1})	U (µg g^{-1})	Sample ID	Pb (µg g^{-1})	U (µg g^{-1})
85H	0.601	0.159	78p	1.913	0.127
65H	0.422	0.042	82p	1.520	0.041
78H	0.388	0.044	30p	1.304	0.056
89H	1.719	0.048	87p	0.947	0.064
75H	0.650	0.045	64p	1.986	0.049
79H	0.936	0.048	96p	0.940	0.075
93H	0.471	0.033	98p	0.724	0.078
71H	0.775	0.041	97p	1.778	0.052
37H	0.671	0.046	94p	1.053	0.097
101H	0.841	0.073	77p	0.720	0.055
100H	0.690	0.027	69p	0.661	0.061
94H	0.468	0.046	xp	0.892	0.096
72H	0.774	0.052	106p	1.126	0.076
87H	0.512	0.034	70p	2.514	0.054
68H	0.910	0.068	52p	0.938	0.092
73H	0.673	0.052	76p	1.996	0.087
77H	0.786	0.052	75p	1.511	0.067
96H	0.699	0.089	84p	1.865	0.073
67H	1.692	0.067	90p	1.807	0.076
99H	0.564	0.050	88p	0.845	0.058
66H	0.340	0.049	67p	1.179	0.068
98H	0.301	0.030	79p	2.351	0.071
76H	2.271	0.088	36M	2.836	0.072
84H	2.358	0.058	29M	0.281	0.105
74H	0.910	0.047	34M	0.364	0.161
88H	0.300	0.034	39M	0.816	0.517
91H	1.273	0.042	30M	13.430	0.182
69H	0.616	0.034	26M	0.552	0.135
92H	1.155	0.051	21M	0.607	0.109
80H	0.766	0.125	24M	0.338	0.126
97H	1.210	0.087	37M	0.583	0.087
95H	0.638	0.038	32M	0.351	0.105
86H	0.910	0.148	27M	0.782	0.084
90H	1.981	0.063	23M	0.433	0.137
80p	0.743	0.112	28M	0.851	0.130
92p	1.662	0.051	38M	0.353	0.099
99p	1.132	0.054	35M	0.362	0.132
81p	0.838	0.034	22M	0.233	0.140
1p	0.389	0.014	33M	0.204	0.082
4px	0.212	0.004	25M	0.360	0.112
4p	1.329	0.015	IAEA	24.767	4.510
5px	1.515	0.054	KRA	54.874	0.319
61p	0.843	0.049	RAD	19.243	0.856
83p	1.701	0.090	MAS	10.437	0.334

7.3.2 Pb ratios of thyroids and soil

Sample ID	Pb ratios					standard deviation				
	208/204	207/204	206/204	208/206	207/206	208/204	207/204	206/204	208/206	207/206
SRM981	36.7221	15.4711	16.8719	2.1765	0.9170	2.22E-03	9.14E-04	9.74E-04	2.86E-05	1.34E-05
KRA	38.6311	15.6262	18.4505	2.0938	0.8469	1.91E-03	6.60E-04	9.32E-04	5.44E-05	1.56E-05
RAD	38.4016	15.6289	18.3827	2.0889	0.8502	4.71E-03	1.73E-03	1.69E-03	1.42E-04	3.95E-05
MAS	38.2231	15.6054	18.2871	2.0903	0.8534	3.67E-03	1.42E-03	1.65E-03	5.36E-05	2.09E-05
IAEA	39.3173	15.7908	18.8299	2.0874	0.8383	2.37E-02	5.88E-03	3.65E-03	1.09E-03	2.29E-04
SRM981	36.7504	15.4777	16.8718	2.1782	0.9173	4.86E-03	1.98E-03	2.15E-03	6.91E-05	2.06E-05
SRM981	36.6886	15.4876	16.9360	2.1663	0.9145	7.87E-04	3.47E-04	3.58E-04	1.31E-05	5.93E-06
67p	38.0282	15.5238	18.0050	2.1125	0.8623	1.51E-02	3.95E-03	3.47E-03	7.15E-04	1.44E-04
94p	38.1209	15.6159	18.0531	2.1114	0.8650	5.60E-03	2.00E-03	1.75E-03	2.14E-04	5.06E-05
97p	37.9311	15.5607	18.0291	2.1038	0.8631	3.43E-03	1.48E-03	1.69E-03	2.77E-05	1.65E-05
98p	38.3434	15.6755	18.0528	2.1238	0.8683	5.86E-03	2.03E-03	2.18E-03	2.21E-04	4.71E-05
96p	38.0413	15.6048	18.0700	2.1052	0.8636	5.65E-03	2.56E-03	2.76E-03	4.98E-05	2.27E-05
64p	37.8690	15.5293	17.9784	2.1064	0.8638	2.40E-03	9.27E-04	1.11E-03	2.48E-05	1.27E-05
SRM981	36.6882	15.4856	16.9276	2.1673	0.9148	9.81E-04	4.31E-04	4.04E-04	2.02E-05	1.18E-05
77h	38.0397	15.5588	18.1254	2.0986	0.8584	4.03E-03	1.52E-03	1.93E-03	2.36E-05	1.09E-05
96h	38.1321	15.5399	18.2281	2.0919	0.8525	3.00E-03	1.32E-03	1.45E-03	2.38E-05	1.17E-05
67h	37.9295	15.5344	18.0665	2.0994	0.8599	1.45E-03	5.71E-04	6.90E-04	2.06E-05	1.12E-05
99h	38.1249	15.5918	18.1907	2.0960	0.8571	5.56E-03	2.08E-03	2.43E-03	3.20E-05	1.76E-05
66h	37.9943	15.5624	18.0661	2.1029	0.8614	9.27E-03	3.26E-03	3.85E-03	4.91E-05	2.37E-05
98h	37.7486	15.4538	17.9571	2.1027	0.8608	1.30E-02	5.31E-03	6.47E-03	4.76E-05	2.75E-05
SRM981	36.6911	15.4833	16.9213	2.1683	0.9150	1.75E-03	7.72E-04	7.71E-04	2.27E-05	9.76E-06
SRM981	36.6908	15.4873	16.9368	2.1664	0.9144	1.06E-03	3.91E-04	5.50E-04	1.61E-05	6.85E-06
87p	37.8927	15.5505	17.9894	2.1063	0.8643	6.86E-03	2.89E-03	3.19E-03	3.58E-05	1.44E-05
30p	37.4479	15.3757	17.7572	2.1088	0.8658	4.29E-03	1.76E-03	2.03E-03	2.47E-05	1.20E-05
82p	37.5318	15.4228	17.8358	2.1044	0.8647	8.94E-03	3.60E-03	4.42E-03	6.99E-05	3.82E-05
78p	36.1547	14.8524	17.1620	2.1070	0.8654	1.51E-02	6.06E-03	7.03E-03	8.00E-05	2.94E-05
83p	37.5895	15.4265	17.8481	2.1061	0.8645	1.20E-02	4.68E-03	5.62E-03	9.46E-05	4.50E-05
61p	37.8291	15.5592	17.9204	2.1106	0.8681	1.10E-02	4.37E-03	4.87E-03	1.18E-04	2.98E-05
SRM981	36.6894	15.4861	16.9342	2.1667	0.9145	1.63E-03	6.52E-04	5.83E-04	1.42E-05	7.21E-06
94h	37.9769	15.5130	18.1083	2.0971	0.8566	6.15E-03	2.43E-03	2.97E-03	4.22E-05	2.00E-05
100h	34.5894	14.1560	16.5002	2.0964	0.8580	3.06E-02	1.25E-02	1.46E-02	4.28E-05	2.28E-05
101h	37.9627	15.5189	18.1151	2.0959	0.8567	4.85E-03	1.85E-03	2.20E-03	3.11E-05	1.56E-05
37h	37.9348	15.5469	18.0005	2.1074	0.8637	4.74E-03	1.85E-03	2.07E-03	3.65E-05	2.40E-05
71h	37.3676	15.3174	17.7241	2.1086	0.8642	7.63E-03	3.01E-03	3.40E-03	4.03E-05	1.57E-05
93h	37.3262	15.2469	17.7485	2.1029	0.8590	1.20E-02	5.08E-03	5.65E-03	7.86E-05	2.83E-05
SRM981	36.6854	15.4860	16.9324	2.1666	0.9146	6.65E-04	2.55E-04	3.00E-04	1.14E-05	5.09E-06
67p	37.4525	15.2695	17.6183	2.1251	0.8667	1.19E-02	4.02E-03	4.72E-03	8.13E-04	1.44E-04
88p	34.5404	14.1578	16.3644	2.1099	0.8648	4.80E-02	2.04E-02	2.53E-02	3.51E-04	8.93E-05
90p	38.5797	15.6411	17.8754	2.1580	0.8750	9.38E-03	3.42E-03	3.18E-03	1.51E-04	3.91E-05
84p	38.4141	15.6199	17.8842	2.1477	0.8733	4.92E-03	1.54E-03	1.35E-03	1.72E-04	3.43E-05
75p	37.1461	15.1687	17.4604	2.1274	0.8688	6.64E-03	2.90E-03	3.30E-03	1.99E-04	4.25E-05
76p	31.7076	13.0139	15.0733	2.1036	0.8634	2.65E-02	1.08E-02	1.26E-02	6.19E-05	4.05E-05
SRM981	36.6812	15.4835	16.9296	2.1667	0.9146	7.90E-04	4.19E-04	3.71E-04	1.53E-05	5.89E-06
79h	33.0341	13.5139	15.8083	2.0898	0.8549	9.64E-03	3.94E-03	4.57E-03	1.86E-05	1.08E-05
75h	36.7537	15.0099	17.5185	2.0980	0.8568	2.26E-02	9.35E-03	1.10E-02	3.76E-05	1.60E-05
89h	37.5326	15.3598	17.8257	2.1055	0.8617	4.18E-03	1.79E-03	1.90E-03	2.12E-05	7.81E-06
78h	37.2771	15.2626	17.7521	2.0999	0.8597	6.85E-03	2.80E-03	3.20E-03	3.24E-05	3.33E-05
65h	37.8679	15.5049	18.0383	2.0992	0.8595	4.88E-03	2.05E-03	2.36E-03	3.43E-05	1.40E-05
85h	38.0998	15.5470	18.2447	2.0881	0.8521	3.55E-03	1.44E-03	1.58E-03	3.08E-05	1.22E-05
SRM981	36.6844	15.4824	16.9237	2.1676	0.9148	1.24E-03	4.71E-04	4.72E-04	1.28E-05	5.38E-06

52p	37.2400	15.2716	17.6694	2.1075	0.8643	4.92E-03	1.97E-03	2.22E-03	1.03E-04	3.09E-05
70p	37.8411	15.5403	18.0489	2.0966	0.8610	9.77E-03	3.98E-03	4.65E-03	6.09E-05	4.02E-05
106p	37.7679	15.4940	17.9281	2.1068	0.8643	5.18E-03	2.13E-03	2.38E-03	6.97E-05	3.68E-05
xxp	36.6172	14.9967	17.2301	2.1251	0.8704	7.89E-03	3.29E-03	4.19E-03	2.85E-04	7.72E-05
69p	38.5480	15.7208	18.0165	2.1398	0.8725	6.32E-03	2.67E-03	2.67E-03	1.39E-04	3.35E-05
77p	37.7515	15.4831	17.8920	2.1097	0.8653	9.73E-03	3.92E-03	4.56E-03	1.23E-04	6.41E-05
SRM981	36.6844	15.4825	16.9252	2.1674	0.9147	8.96E-04	4.01E-04	3.85E-04	1.75E-05	8.06E-06
73h	38.0962	15.5630	18.1406	2.1000	0.8579	4.53E-03	1.90E-03	2.13E-03	3.53E-05	1.68E-05
68h	35.0227	14.3044	16.6844	2.0987	0.8571	3.02E-02	1.23E-02	1.39E-02	2.18E-05	1.51E-05
87h	36.3074	14.8477	17.2969	2.0991	0.8584	2.72E-02	1.11E-02	1.30E-02	3.46E-05	1.48E-05
72h	37.5358	15.3415	17.8769	2.1000	0.8582	4.33E-03	1.88E-03	2.21E-03	3.09E-05	1.90E-05
5p	38.1396	15.6180	18.0611	2.1117	0.8647	2.27E-03	9.31E-04	9.57E-04	6.36E-05	1.49E-05
4p	37.9707	15.5635	18.0143	2.1079	0.8640	3.00E-03	1.06E-03	1.26E-03	2.99E-05	1.77E-05
SRM981	36.6900	15.4834	16.9253	2.1678	0.9148	1.26E-03	5.18E-04	5.15E-04	1.76E-05	7.44E-06
SRM981	36.7078	15.4600	16.8599	2.1772	0.9170	5.87E-04	2.48E-04	2.95E-04	2.98E-05	9.84E-06
92h	35.9629	14.7009	17.0515	2.1089	0.8622	5.58E-03	2.26E-03	2.89E-03	2.64E-04	6.95E-05
80h	38.0706	15.5407	18.0279	2.1117	0.8621	2.55E-03	1.22E-03	2.05E-03	2.22E-04	5.63E-05
97h	35.7225	14.6391	17.0062	2.1005	0.8608	3.82E-03	1.55E-03	1.57E-03	5.39E-05	2.44E-05
95h	35.5615	14.5520	16.8016	2.1165	0.8661	1.27E-02	5.26E-03	5.85E-03	7.74E-05	2.45E-05
86h	35.3400	14.4095	16.7597	2.1087	0.8598	4.17E-03	1.73E-03	1.79E-03	7.52E-05	2.31E-05
90h	37.3746	15.2995	17.6268	2.1203	0.8680	1.27E-02	5.26E-03	5.85E-03	7.74E-05	2.45E-05
SRM981	36.7574	15.4686	16.8590	2.1802	0.9175	1.15E-03	3.16E-04	5.91E-04	9.49E-05	2.35E-05
37m	36.3884	14.8750	17.1636	2.1202	0.8666	1.85E-02	7.91E-03	8.82E-03	9.70E-05	4.18E-05
32m	35.3544	14.4553	16.6497	2.1238	0.8683	1.43E-02	6.22E-03	7.65E-03	2.36E-04	5.37E-05
27m	32.8585	13.4169	15.5010	2.1195	0.8655	7.23E-03	2.99E-03	3.45E-03	1.16E-04	3.78E-05
23m	34.7341	14.2057	16.3157	2.1292	0.8708	1.72E-02	7.26E-03	8.68E-03	1.04E-04	2.58E-05
28m	36.4215	14.8591	17.1131	2.1285	0.8684	1.40E-02	5.68E-03	6.43E-03	7.26E-05	1.99E-05
38m	37.5782	15.3357	17.5866	2.1367	0.8720	1.35E-02	5.38E-03	6.21E-03	1.15E-04	4.19E-05
SRM981	36.8818	15.4906	16.8281	2.1917	0.9205	1.34E-03	3.65E-04	3.29E-04	6.63E-05	1.55E-05
35m	39.8600	15.9891	18.1694	2.1940	0.8801	7.86E-03	3.17E-03	3.08E-03	1.93E-04	4.70E-05
22m	40.4447	16.1211	18.2598	2.2153	0.8830	9.43E-03	3.53E-03	4.01E-03	2.22E-04	4.85E-05
33m	40.2068	16.0687	18.2299	2.2052	0.8815	1.14E-02	4.32E-03	4.88E-03	3.37E-04	7.16E-05
25m	40.0721	15.9936	18.4668	2.1700	0.8660	8.95E-03	2.85E-03	2.81E-03	2.58E-04	5.34E-05
30m	26.3225	15.8298	17.9485	1.4661	0.8820	2.21E-02	1.17E-03	3.60E-04	1.18E-03	4.73E-05
26m	39.2478	15.8611	17.8433	2.1994	0.8888	5.26E-03	2.23E-03	1.87E-03	1.96E-04	5.09E-05
SRM981	37.0691	15.5400	16.8339	2.2020	0.9231	1.79E-03	5.54E-04	5.10E-04	8.02E-05	1.96E-05
76h	39.4891	15.9156	18.0766	2.1848	0.8805	6.24E-03	1.54E-03	8.96E-04	2.87E-04	6.33E-05
84h	39.4263	15.9276	18.0612	2.1832	0.8820	7.79E-03	1.85E-03	7.91E-04	3.84E-04	7.62E-05
74h	39.5062	15.9532	18.2060	2.1697	0.8764	1.58E-02	4.02E-03	2.93E-03	6.69E-04	1.37E-04
88h	40.0590	16.0551	18.2322	2.1973	0.8806	1.09E-02	3.35E-03	3.79E-03	2.62E-04	5.15E-05
91h	39.5567	15.9420	18.1562	2.1787	0.8780	5.96E-03	1.54E-03	1.18E-03	2.64E-04	5.56E-05
69h	39.5144	15.9251	18.1937	2.1716	0.8752	1.12E-02	2.90E-03	2.13E-03	4.67E-04	1.01E-04
SRM981	36.8344	15.5033	16.8654	2.1840	0.9192	1.06E-03	4.02E-04	3.56E-04	4.68E-05	1.41E-05
21m	40.4833	16.1780	18.2557	2.2176	0.8862	8.99E-03	2.72E-03	2.45E-03	3.10E-04	5.51E-05
24m	37.0401	15.0140	17.2138	2.1521	0.8722	2.02E-02	7.79E-03	7.95E-03	3.03E-04	7.17E-05
36m	38.6178	15.7291	17.9619	2.1500	0.8757	6.78E-03	1.98E-03	8.29E-04	3.04E-04	7.53E-05
29m	38.7468	15.7552	18.1484	2.1349	0.8683	8.36E-03	3.59E-03	3.72E-03	2.51E-04	6.38E-05
34m	38.8888	15.8064	18.1309	2.1450	0.8718	6.08E-03	2.15E-03	2.42E-03	1.85E-04	4.47E-05
39m	38.4720	15.5585	17.7407	2.1683	0.8769	9.93E-03	2.78E-03	2.51E-03	5.63E-04	1.30E-04
SRM981	36.8385	15.5140	16.8939	2.1806	0.9183	1.34E-03	5.39E-04	4.98E-04	5.35E-05	1.59E-05
4xp	39.0455	15.8300	18.0343	2.1652	0.8778	9.45E-03	2.35E-03	9.79E-04	4.37E-04	9.43E-05
1xp	38.7820	15.8122	18.1683	2.1345	0.8703	7.83E-03	2.97E-03	3.27E-03	2.80E-04	5.59E-05
81p	39.1691	15.9106	18.1716	2.1555	0.8755	1.76E-02	5.29E-03	3.90E-03	6.68E-04	1.46E-04
99p	38.6693	15.8270	18.2203	2.1223	0.8686	1.38E-02	5.55E-03	6.38E-03	2.04E-04	6.01E-05

92p	39.0085	15.8599	18.1066	2.1545	0.8759	6.37E-03	2.17E-03	2.31E-03	2.26E-04	4.77E-05
80p	38.8809	15.9193	18.4325	2.1094	0.8637	1.89E-02	7.65E-03	8.66E-03	1.57E-04	5.90E-05
SRM981	36.8095	15.5072	16.9092	2.1769	0.9171	2.21E-03	8.39E-04	8.76E-04	4.07E-05	1.20E-05
SRM981	36.8498	15.4676	16.7925	2.1944	0.9211	1.62E-03	4.57E-04	5.48E-04	9.95E-05	2.39E-05
79p	39.7226	15.9733	18.0656	2.1992	0.8840	1.90E-02	4.72E-03	1.97E-03	8.49E-04	1.76E-04
IAEA	39.2019	15.5952	18.3659	2.1345	0.8491	9.09E-03	3.54E-03	4.38E-03	1.66E-04	4.22E-05
KRA	39.3097	15.8384	18.5440	2.1197	0.8541	6.48E-03	1.55E-03	3.53E-04	3.27E-04	7.07E-05
RAD	40.0287	16.0255	18.5019	2.1633	0.8662	3.69E-03	1.09E-03	6.53E-04	1.19E-04	3.48E-05
MAS	39.0032	15.8400	18.3733	2.1228	0.8621	1.32E-02	3.15E-03	1.00E-03	6.34E-04	1.33E-04
SRM981	36.6894	15.4684	16.8619	2.1758	0.9174	1.06E-03	3.94E-04	3.98E-04	3.03E-05	9.67E-06
KRA	38.5727	15.6299	18.4627	2.0892	0.8466	7.04E-04	2.71E-04	3.07E-04	2.08E-05	8.84E-06
RAD	38.6190	15.7201	18.4332	2.0951	0.8528	6.39E-03	1.77E-03	7.63E-04	2.83E-04	7.03E-05
MAC	38.1512	15.6100	18.2972	2.0850	0.8531	1.72E-03	7.63E-04	6.55E-04	4.57E-05	1.59E-05

7.3.3 Delta Values for thyroid and soil samples

sample ID	δ^{208}	δ^{207}	sample ID	δ^{208}	δ^{207}	sample ID	δ^{208}	δ^{207}
KRA	-38	-76	77h	-32	-62	28m	-24	-54
KRA	-40	-77	96h	-35	-68	38m	-20	-50
RAD	-40	-73	67h	-31	-60	35m	1	-44
RAD	-37	-70	99h	-33	-63	22m	11	-41
MAS	-40	-69	66h	-30	-58	33m	6	-42
MAS	-42	-70	98h	-30	-59	25m	-10	-59
67p	-25	-57	94h	-32	-63	26m	3	-34
94p	-25	-54	100h	-32	-62	21m	15	-36
97p	-29	-56	101h	-33	-63	24m	-15	-51
98p	-20	-50	37h	-27	-56	36m	-16	-47
96p	-28	-56	71h	-27	-55	29m	-22	-55
64p	-28	-55	93h	-29	-61	34m	-18	-52
87p	-28	-55	79h	-36	-65	39m	-7	-46
30p	-27	-53	75h	-32	-63			
82p	-29	-54	89h	-28	-58			
78p	-27	-54	78h	-31	-60			
83p	-28	-55	65h	-31	-60			
61p	-26	-51	85h	-36	-68			
67p	-19	-52	73h	-31	-62			
88p	-26	-54	68h	-32	-63			
90p	-4	-43	87h	-32	-62			
84p	-9	-45	72h	-31	-62			
75p	-18	-50	92h	-31	-60			
76p	-29	-56	80h	-30	-60			
52p	-28	-55	97h	-35	-61			
70p	-33	-59	95h	-28	-55			
106p	-28	-55	86h	-31	-62			
xxp	-20	-49	90h	-26	-53			
69p	-13	-46	37m	-28	-56			
77p	-27	-54	32m	-26	-54			
5p	-26	-55	27m	-28	-57			
4p	-27	-55	23m	-23	-51			

7.4   List of Abbreviations

[A]	ampere
[a]	year
[amu]	atomic mass unit
Ar	argon
B	boron
[°C]	degree celsius
CA	cellulose acetate
[cm]	centimetre
cps	counts per second
CRM	certified reference material
Cs	caesium
DSN	desolvation nebulizer system
DU	depleted uranium
EDX	energy dispersive X-ray spectroscopy
ESA	electrostatic sector analyzer
[eV]	electronvolt
FT	fission track
[g]	gram
[GBq]	gigabequerel
GLS	gas liquid separator
[Gy]	gray
HEU	highly enriched uranium
HG	hydride generation
H_2O_2	hydrogen peroxide
HF	hydrofluoric acid
HFP	hot fuel particle
hms	hours minutes seconds
HNO_3	nitric acid
HR	high resolution
[Hz]	hertz
I	iodine
IAEA	International Atomic Energy Agency
ICP-MS	inductively coupled plasma mass spectrometry
IDMS	isotope dilution mass spectrometry
In	Indium
ITU	Institute for Transuranium Elements
[J]	joule
[keV]	kiloelectronvolt
[kg]	kilogram
[km]	kilometre
[L]	litre
LA	laser ablation
LEU	low enriched uranium
Li	lithium
M	molar
[m^3]	cubicmetre
[mbar]	milibar
MC	multiple collector
[Mci]	megacurie
[min]	minute
[mL]	mililitre
[µg]	microgram
[mg]	milligram
[µl]	microlitre
[µm]	micrometre
[mm]	milimetre
MSA	magnetic sector analyzer
m/z	mass-to-charge ratio

[ng]	nanogram
[nm]	nanometre
Np	neptunium
NPP	nuclear power plant
NPT	Treaty on the Non-Proliferation of Nuclear Weapons
p.a.	pro analysi
Pb	lead
PFA	polyfluoroalkoxy
[pg]	picogram
Pu	plutonium
[Psi]	pound-force per square inch
Q	quadrupole
RF	radio frequency
RSD	relative standard deviation
Ru	ruthenium
[s]	second
SAL	safeguards analytical laboratory
SEM	scanning electron microscopy
SF	sector field
SIMS	secondary ion mass spectrometry
[t]	tonne
Th	thorium
TIMS	thermal ionization mass spectrometry
U	uranium
UO_2	uranium dioxide
[V]	volt
[W]	watt
WDX	wavelength dispersive X-ray spectroscopy
w/v	weight per volume
w/w	weight per weight
XRF	X-ray fluorescence spectroscopy